DISSERTATION

ENHANCED RECOVERY FROM ANCIENT CARBONATE RAMPS: LESSONS AND ANALOGS FROM PALEOZOIC SUCCESSIONS AND THE PERSIAN GULF

Submitted by

Ali R. Jaffri

Department of Geosciences

In partial fulfillment of the requirements

For the Degree of Doctor of Philosophy

Colorado State University

Fort Collins, Colorado

Spring 2009

COLORADO STATE UNIVERSITY

March 24, 2009

WE HEREBY RECOMMEND THAT THE DISSERTATION PREPARED UNDER OUR SUPERVISION BY ALI R. JAFFRI ENTITLED ENHANCED RECOVERY FROM ANCIENT CARBONATE RAMPS: LESSONS AND ANALOGS FROM ANCIENT PALEOZOIC SUCCESSIONS AND THE MODERN PERSIAN GULF BE ACCEPTED AS FULFILLING IN PART REQUIREMENTS FOR THE DEGREE OF DOCTOR OF PHILOSOPHY.

Committee on Graduate Work

Dr. Gamze Cavdar Yasar

Dr. John Ridley

Dr. Ellen Wohl

Dr. Sven Egenhoff, Advisor

Dr. Sally Sutton, Department Head

ABSTRACT OF DISSERTATION

ENHANCED RECOVERY FROM ANCIENT CARBONATE RAMPS: LESSONS AND ANALOGS FROM ANCIENT PALEOZOIC SUCCESSIONS AND THE MODERN PERSIAN GULF

Satellite imagery of the Persian Gulf, fieldwork in Kuwait and Abu Dhabi, and data from published sources are integrated to develop a thorough understanding of large-scale stratal architecture in carbonate ramps.

A section of this study deals with the identification of key-surfaces in homogeneous successions. An Ordovician carbonate ramp from Sweden is selected to illustrate the importance of trace fossils in identification of maximum regression surfaces. By comparing Ordovician trace fossils from Sweden with modern crab burrows in Kuwait, a sequence stratigraphic model that shows strata architecture is presented.

Oolitic facies in ancient carbonate ramps in the Devonian-Mississippian Bakken Formation that have been previously ignored or considered subtidal sheet-like deposits have been reinterpreted as coastal embayment, eolian dunes on barrier islands, and tidal channel deposits. Geometric analyses of similar environments in the modern Persian Gulf reveal that none of the oolitic facies in the Bakken Formation would be conducive to a sheet-like morphology.

This paper highlights the diversity in shapes and dimensions of modern oolitic tidal channels in the Persian Gulf. Tidal channels documented in satellite imagery are oriented parallel, perpendicular or oblique to the shoreline.

Planforms are remarkably similar to terrestrial fluvial systems, and transitions between straight, meandering, anastomosing, and braided patterns occur. Wide, straight channels form where bank materials consist of non-cohesive oolitic-skeletal sands, whereas those with prolific cyanobacterial growth along banks are prone to sinuous channels.

A section investigates the challenges that oil and gas companies face when attempting to strike a balance between appeasing authorities and exploiting hydrocarbons while maintaining sustainable development. It also recommends policies that include amendments regarding oil fields in Kurdish territory and healthy alternatives to Production Sharing Agreements which ensure the flow of oil from Iraq while maintaining sustainable development. These include exclusion of oil fields in the Kurdish territory, which constitute only 3 percent of Iraq's oil reserves, from article 5a of the Iraqi Oil and Gas Law. This study recommends the use of contracts, such as Technical Service Agreements, that satisfy both the foreign oil companies and the Iraqi populace.

Ali R. Jaffri
Department of Geosciences
Colorado State University
Fort Collins, CO 80523
Spring 2009

ACKNOWLEDGMENTS

These acknowledgements are arranged chronologically to highlight the contributions of my mentors and friends, without whom this dissertation would be incomplete.

I would like to start by thanking my adviser Dr. Sven Egenhoff. He pushed me to improve my writing style and taught me to think about sedimentary processes. He has encouraged me every step of the way throughout my tenure as a PhD student. When I decided to study recent carbonate sand bodies in the Persian Gulf, he assured me of his support.

My first summer was spent working for Chevron, where Petro Papazis introduced me to reservoir simulation and the need for geometric and dimensional data of recent lithofacies. The Saudi-PNZ team at Chevron took the time to review my methodology and helped me focus on the problems encountered while developing oil and gas fields in Saudi Arabia and Kuwait. The following semester I presented my research at the ExxonMobil's Upstream Research Company and Middle Eastern Business Unit. Conversations with Anthony Sandomierski and Ian Russell led to a focus on modern oolitic accumulations and the section on geopolitics of hydrocarbon exploitation.

Fieldwork conducted in Kuwait and the United Arab Emirates was supported by a grant from the AAPG. Wahab Sadeqi personally escorted me to the beaches near the Iraqi border in Kuwait during 130^0 Fahrenheit weather. A course on Middle Eastern Geopolitics with Dr. Gazme Cavdar was enlightening, and I am honored that she not only joined my committee but reviewed the sections on oil recovery and geopolitics in Iraq. Mayada al-Douri and Zainab al-Ward provided an Iraqi perspective on the issue. I was privileged to intern with ConocoPhillips and meet with their Iraq Team. Chuck Caughey explained the nature of oil contracts and leases, and the rationale for preferring Production Sharing Agreements.

Dr. Frank Ethridge guided me in my search for Seismic Geomorphology literature and Dr. Dennis Harry was kind enough to review my work on the subject. Dr. Sam Akande helped me prepare for my PhD Comprehensive Exams, and Zach Wessel prepared all the graphs in this manuscript. I was fortunate to have a Bakken Formation expert: Aaron VanDolah in the office next door. During my masters, I was his TA, during my PhD he was my mentor on the Bakken Formation. The willingness to help expressed by the staff at the North Dakota Geological Survey and Denver Core Research center facilitated the progress of study.

This dissertation was funded through short-term projects on the sequence stratigraphy of the Paradox Formation and the sedimentology of the Bakken and Three Forks Formations. For this I am indebted to Harry Held at Delta Petroleum and Pat Medlock at Brigham Oil and Gas.

I would like to thank John Ridley and Ellen Wohl for taking the time and reviewing my manuscript. Finally, I would like to thank Chris Cassle and Jeff Dereume for creating a pleasant working environment.

TABLE OF CONTENTS

CHAPTER 1. INTRODUCTION

1.0 Study objectives

The objective of this study is to increase our understanding of depositional processes in carbonate ramp depositional systems which produce hydrocarbons in Middle Eastern oil and gas fields. Enhanced recovery is defined as the practice of extracting hydrocarbons from the sub-surface through artificial means such as hydraulic fracturing, and water or gas injection. To allow application of these primarily engineering technologies, geologists need to develop a thorough understanding of reservoir volume, geometry, distribution, connectivity and compartmentalization. Besides these sub-surface interpretations, enhanced recovery is also contingent on local geopolitics that may hinder efficient development and production. Therefore, this study examines solutions to both subsurface geological and surficial anthropogenic problems.

The largest oil and gas fields in the world are located in the Middle East and produce from mixed (carbonate-siliciclastic-evaporite) sedimentary systems that were deposited in ramp settings (Kirkland and Evans, 1981; Klemme, 1983; Grunau, 1987; Alsharhan and Nairn, 1997). The most common reservoirs in such systems are carbonate sand bodies dominated by ooids (Druckman and Moore, 1985; Feazel, 1985; Wilson, 1985; Petta and Rapp, 1990; Chimene, 1991; Meyer et al., 1996; Saner and Sahin, 1999; Haywick et al, 2000; Cantrell et al., 2001). Although several studies on facies distribution in these systems have been published (Sarg, 1988; Clemmesen, 1985; Evans, 1995; El-Sayed, 2000; Kendall, 2000; Barth, 2002; Evans and Kirkham, 2002; LaGesse and Read, 2005; Vigorito et al., 2005), none has investigated sequence stratigraphic controls on reservoir distribution[1] in detail. Because these reservoirs are so prolific, the oil industry highly benefits from such a study.

The best modern analog for mixed sedimentary systems in a ramp setting is the modern Persian Gulf. This area has been the focus of Dr. Christopher Kendall's (University of South Carolina) research career. During this career he described facies distribution (Kendall et al., 2002), potential source rocks (Kendall et al., 2002), and sedimentary structures and bed-forms (Alsharhan and Kendall, 2003). A summary of his research is provided in a presentation that is available online (Kendall, 2009). At the end of this presentation Dr. Kendall emphasizes two scientific questions, the solution of which would vastly increase our current understanding of mixed systems. The first is the potential of carbonate mud as a source rock, which Kendall is pursuing himself (Kendall et al., 2007). The second is a detailed lithofacies analysis of mixed systems in the modern Persian Gulf with a focus on facies geometries. A past challenge with doing such a study was access to detailed aerial photographs or satellite imagery. With the availability of software programs such as Google Earth or NASA World Wind, which make satellite imagery available to the general public, this problem can now be solved. Although lithofacies maps of the Persian Gulf were created by Wagner and Van Der Togt (1973), the focus was on surficial area covered by facies and not on the geometry of individual sedimentary packages such as ebb deltas, flood deltas, tidal bars or tidal channels.

[1] Reservoir distribution here refers to shape, dimensions (geometry), connectivity and compartmentalization

Determining these bulk-geometries in three dimensions using satellite data and published material is one of four projects incorporated into this study.

The practice of sequence stratigraphic analysis in carbonates relies largely on the identification of key-surfaces (Clari et al, 1995; Sarg, 1998; Ehrenberg and Svana, 2002). However, in the absence of obvious sequence stratigraphic surfaces (hardgrounds, terra rosa, birdseye texture, or karst), the task becomes daunting. Ramp successions tend to be much finer-grained and show less well-differentiated lateral facies belts than age-equivalent carbonate platform successions. Lateral shifts of facies belts due to fluctuating sea level are therefore often not mirrored as well in ramp facies architecture as they are in carbonate platform successions. This makes it difficult to identify sequence stratigraphic key surfaces, especially in mid-ramp areas which are dominated by mostly wackestone facies (Burchette & Wright 1992). New concepts that would allow the integration of relatively monotonous mid-ramp strata into the sequence stratigraphic framework of mixed carbonate-siliciclastic-evaporite ramp successions would therefore be integral parts in fuller understanding of these systems. This study explores a new sedimentary feature that can be used to identify key surfaces. Crab-like burrows collected from the Ordovician of Scandinavia show remarkable similarity to modern crab burrows from the Persian Gulf. Data from these fossil examples, along with data from modern burrows, are integrated to check the validity of the burrows as a sequence stratigraphic tool.

Because this study is geared towards the Middle Eastern oil and gas fields, and production from these fields relies not only on sub-surface geology but geopolitics and economics (Sandrea and Buraiki, 2002; Bahgat 2007), a chapter of this study is devoted to these issues of hydrocarbon exploitation while maintaining sustainability. The current geopolitical situation in Iraq is used as a case study.

1.1 The scientific importance of mixed sedimentary systems in ancient carbonate ramp successions.

Although the penecontemporaneous deposition of carbonates, siliciclastics and evaporites is relatively uncommon, ancient associations containing these three rock types host the largest oil and gas reservoirs in the world (Fig. 1.0). This is largely due to the sealing capacity of evaporites to migrating fluids and gases. Although hydrocarbons can accumulate in ancient terrestrial settings with lacustrine carbonates or alluvial fan sands acting as reservoirs and playa evaporites acting as seal (Permian San Andres Formation, Texas), these are exceedingly rare and have not been investigated in this study, which is confined to marine settings.

1.2 Economics of Middle Eastern Oil: need for this study

The Middle East currently holds 55 % of the world's total oil reserves. With current trends in US oil consumption, and China's and India's increasing demands for energy, these reserves are the most promising, economically viable source of oil (Table 1.0). Because of a myriad of economic factors, such as increasing demand in developing countries, and decreasing global reserves, Middle Eastern oil will not diminish in importance to the United States. These factors include difficulties associated with successful exploration and development of deepwater oil fields, political instability in countries with large onshore reserves, and high success rates in Middle Eastern oil fields.

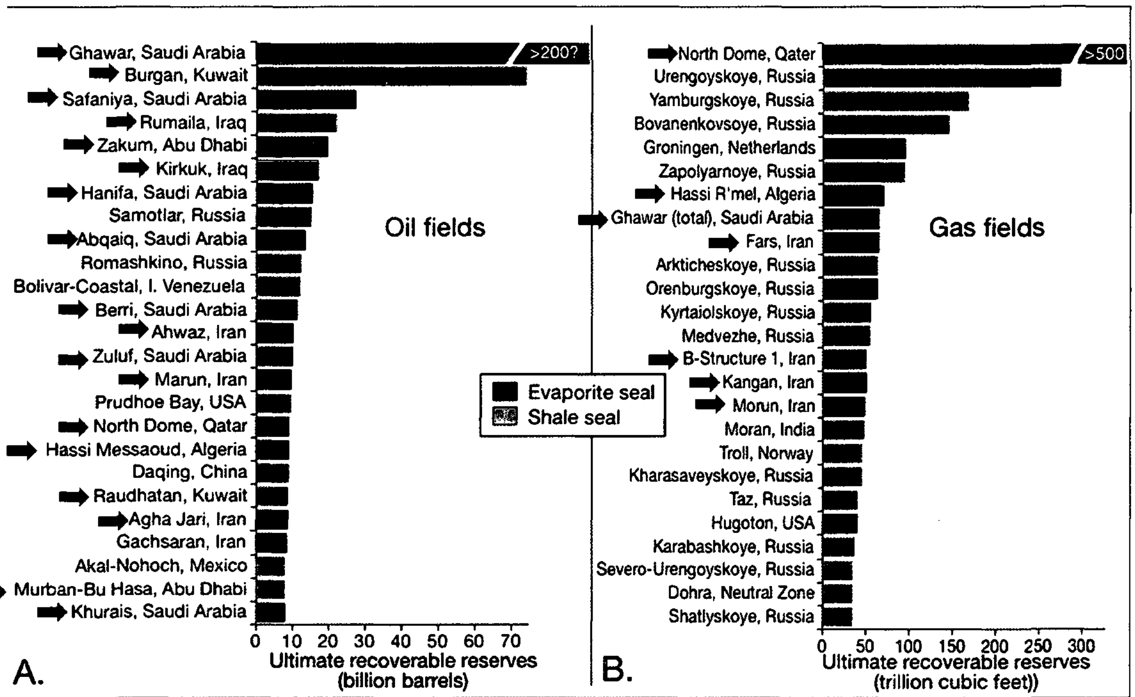

Figure 1.0. The world's largest oil and gas fields and their depositional systems. Red arrows show fields located in the Middle East. (Modified from Warren, 2006)

According to the International Energy Outlook for year 2007, the current rate of US oil consumption is 20 MBO/day with a yearly increase of 2 percent. In contrast, the current rate of US oil production is only 9 MBO/day. To compensate for this the US imports 11 MBO/day, half of which comes from the Middle East. At the current rate of consumption (and if no foreign oil is imported), the national oil reserves in Prudhoe, Alaska would be depleted in less than 2 years.

Deepwater oil reserves from the Gulf of Mexico may seem promising, but production from that region combined with that from Nigeria, Angola, Equatorial Guinea, Brazil, Borneo and elsewhere only accounts for 2 percent of the world's total oil production (Sandrea & Buraiki, 2002). This production is unlikely to increase significantly because of technical complexities involved in deepwater exploration and development. Because of seismic resolution issues (shallow gas shadow zones, sub-salt imaging), the average success rate for drilling economically viable wells in deepwater plays is around 35 % (Pettingill & Weimer, 2001). The average cost of a deepwater well is approximately $100 million (the most expensive onshore wells such as those in the Middle East cost less than $25 million to drill). The elaborate infrastructure needed for successful exploitation of these plays leads to lengthy cycle times (for example, the cycle time for the Bonga Field, Nigeria was 9 years). Cycle time refers to the time interval it takes from date of discovery of an oil field to the date of production from that field. Cycle time is inversely proportional to long-term economic gain because petrodollars earned from a field that is rapidly developed can be invested in competitive bidding for acquiring leases in prospective frontier areas elsewhere. Therefore, to gain a competitive edge over other operators, exploration and production companies strive for the shortest cycle time possible. Even if the US were to overcome the obstacles of exploration and development, production from global deepwater reserves would peak around 2010 and then decline rapidly (Sandrea & Buraiki, 2002).

An alternative to West African and Gulf of Mexico deepwater oil is that from onshore South America. Cheaper development and production costs and proximity to the US make it more economically viable. Therefore, South America has historically been a large exporter of oil to the US. However, due to recent changes in regimes, policies focusing on export of oil to the US have radically changed. In 2007 Venezuela, which is the second largest exporter of oil to the US after Saudi Arabia (10% of all US oil imports) decided to nationalize Venezuelan Oil (a complete oil embargo is impending). The politically simplest solution to the problems associated with importing foreign oil is producing oil from the continental US. Unfortunately, most US oil reserves have been exploited to depletion.

An alternative that is *en vogue* is the exploitation of unconventional oil and gas reserves within the continental US. These may serve as a last resort when global oil production declines to a point at which gas prices make such unconventional reserves economically viable. Current unconventional plays include fractured plays, fluvial systems with complex stacking patterns and shale gas systems. Complex geology makes these extremely complicated to develop and they have low returns. Gas-shales such as the Barnett Shale have porosity lower than cement and permeability in the nanodarcy range. Development is only possible

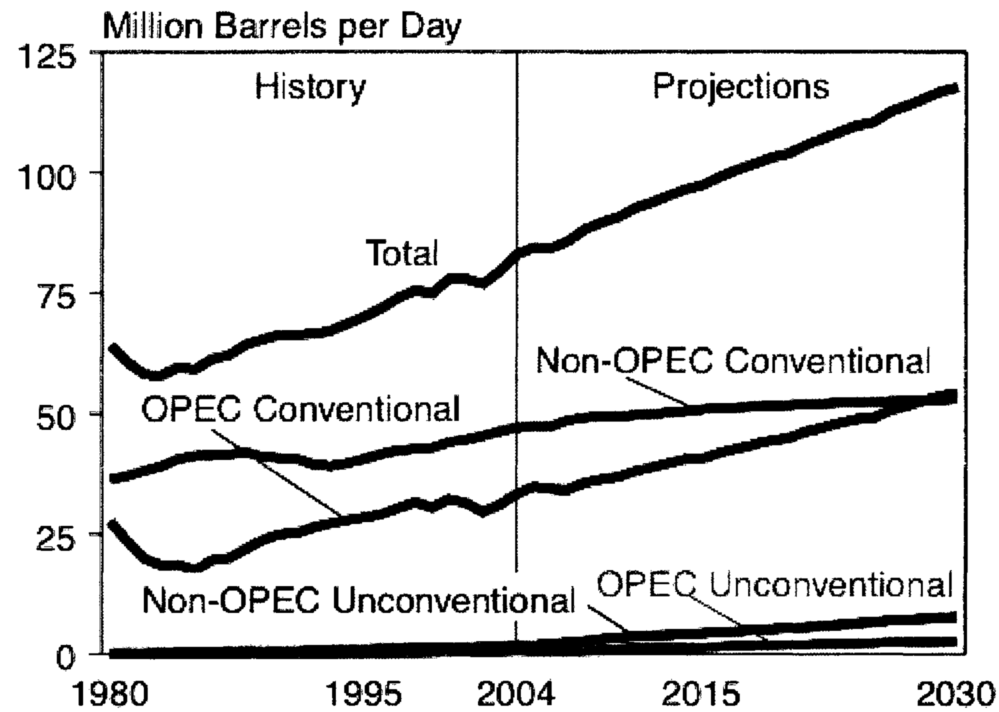

Figure 1.1 OPEC and Non-OPEC Conventional and Unconventional Liquids Production (reproduced from the EIA Energy Outlook Report, 2007)

Country	Reserves (BBL)	Largest Reservoirs
Saudi Arabia	262.3	Arab and Khuff Formations
Iran	136.3	Rus and Asmari Formations
Iraq	115.0	Khuff, Arab and Rus Formations
Kuwait	101.5	Burgan and Maudud Formations
United Arab Emirates	97.8	Hith and Asab Formations

Table 1.0 Largest oil reserves and associated formations. Data from Salameh (2003), Warren (2006), and EIA Outlook 2007

through intense hydraulic fracturing, which makes these wells marginally economical. Because of the complications associated with development of unconventional plays, their global production is an order of magnitude lower than those from conventional plays (Fig. 1.1).

1.3 Summary

By the year 2010 the US is expected to be importing 79% of its oil needs, two thirds of which will come from the Middle East (Salameh, 2003). Most giant Middle Eastern oil and gas fields (Ghawar, North Dome, Safaniya and others) are in mixed carbonate-siliciclastic-evaporite systems (Warren, 2006). The most prolific of these are the Late Paleozoic Khuff and Jurassic Arab reservoirs, which produce in Saudi Arabia (largest oil reserves in the world), Kuwait and the UAE (Pollastro, 2003). The same formations extend into Iraq and produce from the most prolific (Tikrit) oil fields there (Ehrenberg et al. 2007). Iraq has the third largest oil reserves in the world (112 billion bbl) but is currently the eleventh largest producer due to lack of development (Nadkarmi, 2007). As a result of their sheer abundance of oil, Middle Eastern fields and their strata have not been studied with reference to EOR goals. In the near future, detailed characterization of reservoirs and their relationship to surrounding sources and seals will determine continuing development in these oil and gas fields.

1.4 References

Alsharhan, A. S. and C.G.St.C, Kendall., 2003, Holocene coastal carbonates and evaporites of the southern Arabian Gulf and their ancient analogues. Earth Science Reviews, v. 61, p. 191-243.

Alsharhan, A.S, and A.E.M. Nairn., 1997, Sedimentary basins and petroleum geology of the Middle East. Amsterdam, the Netherlands, Elselvier Science, 942 p.

Bahgat, G.2007, The oil market's hard chargers-1: China expands energy mix. Seeks investment. Oil and Gas Journal, v. 105, p. 1-5.

Barth, H.J. 2002, The sabkhat of Saudi Arabia an introduction, in H. J. Barth and B. Boer (eds). Sabkha Ecosystems: Netherlands, p. 37-49.

Burchette, T.P., and V.P. Wright. 1992, Carbonate ramp depositional systems. Sedimentary Geology, v. 79, p. 3-57.

Cantrell, D. L., P.K. Swart, C. R. Handford, C.G.S.C. Kendall, and H. Westphal. 2001, Geology and production significance of dolomite, Arab-D reservoir, Ghawar Field, Saudia Arabia. Geo Arabia, v.6, p. 45-60.

Chimene, C.A. 1991, Walker Creek Field – USA, Gulf of Mexico Basin, Arkansas in E.A. Beaumont, and N.H. Foster, eds., Treatise of Petroleum Geology; Atlas of Oil and Gas Fields: Structural Traps IV – Tectonic and nontectonic fold traps: Tulsa, OK, American Association of Petroleum Geologists, p. 55-117.

Clari, P. A., F. D. Pierre, L. Martire., 1995, Discontinuities in carbonate successions: identification, interpretation and classification of some Italian examples. Sedimentary Geology, v. 100, p. 97-121.

Clemmensen, L.B., 1985, Desert plain and sabkha deposits from the Bunter Sandstone Formation (L.Triassic) at the northern margin of the German Basin. Geologische Rundschau, v. 74, p. 519-536.

Druckman, Y., and C.H. Moore., 1985, Late subsurface secondary porosity in a Jurassic grainstone reservoir, Smackover formation, Mt.Vernon Field, Southern Arkansas, in P.O. Roehl, and P. W. Choquette, eds., Carbonate Petroleum Reservoirs: New York, Springer-Verlag, p. 197-208.

Ehrenberg, S.N., Nadeau, P.H. and Aqrawi., 2007, A comparison of Khuff and Arab reservoir potential throughout the Middle East. AAPG Bulletin, v. 91, p. 275-286.

Ehrenberg, S.N., and T. A. Svana. , 2001, Use of spectral gamma-ray signature to interpret stratigraphic surfaces in carbonate strata: An example from the Finnmark carbonate platform (Carboniferous-Permian), Barents Sea. American Association of Petroleum Geologists Bulletin, v. 85, p. 295-308.

Energy Information Administration (www.eia.doe.gov)

El-Sayed, M.I. 2000, Karstic features associated with unconformity surfaces, a case study from the United Arab Emirates. Journal of Arid Environments, v. 46, p. 295-312.

Evans, G., Kirkham., 2002, Distribution of sabkhat within the Arabian Peninsula and the adjacent countries: the Abu Dhabi Sabkha, in H. J. Barth and B. Boer (eds). Sabkha Ecosystems: Netherlands, p. 7-20.

Evans, G., 1995, The Arabian Gulf: A modern carbonate-evaporite factory, a review. Cuardernos ge Geologia Iberica, v. 19, p. 61-96.

Feazel, C.T., 1985, Diagenesis of Jurassic grainstone reservoirs in the Smackover Formation, Chathom Field, Alabama, in P.O. Roehl, and P. W. Choquette, eds., Carbonate Petroleum Reservoirs: New York, Springer-Verlag, p. 357-367.

Grunau, H.R., 1987, A worldwide look at the cap-rock problem. Journal of petroleum geology, v. 103, p. 245-266.

Haywick, D.W., M.B. Hall-Brown., L. Pfeiffer., 2000, Smackover reservoir diagenesis in the Appleton Oilfield, Escambia County, Alabama (abs). American Association of Petroleum Geologists Bulletin, v. 84, p. 1680.

Kendall, A.C. 2000. Compaction in halite-cemented carbonates – the Dawson Bay Formation (Middle Devonian) of Saskatchewan, Canada. Sedimentology, v. 47, p. 151-171.

Kendall, C.G.St.C., 2009, http://strata.geol.sc.edu/

Kendall, C.G.St.C., A.S. Alsharhan., A. Cohen., 2002, The Holocene tidal flat complex of the Arabian Gulf Coast of Abu Dhabi, in H. J. Barth and B. Boer (eds). Sabkha Ecosystems: Netherlands, p. 21-35.

Kendall, C.G.St.C., G. Shinn, X. Janson. 2007, Holocene cyanobacterial mats and lime muds: links to Middle East carbonate source rock potential (abs). American Association of Petroleum Geologists Annual Convention.

Kirkland, D.W., and R. Evans., 1981, Source-rock potential of evaporitic environments. American Association of Petroleum Geologists Bulletin, v. 65, p. 181-190.

Klemme, H.D. 1983, The geologic setting of giant gas fields: Laxemburg. International Institute for Applied Systems Analysis, p. 133-160.

LaGesse, J. and Read, F. 2005, Updip sequence development on a wave- and current-dominated, mixed carbonate-siliciclastic continental shelf: Paleogene, North Carolina, eastern U.S.A. Sedimentary Geology, v. 184, p. 155-182.

Meyer, F.O., R.C. Price, I.A. Al-Ghamdi, I.M. Al-Goba, S.M. Al-Raimi, and J.C. Cole. 1996, Sequential stratigraphy of outcropping strata equivalent to Arab-D reservoir, Wadi Nisah, Saudi Arabia. GeoArabia, v. 5, p 355-384.

Nadkami, S. 2007, Indian Oil to participate in Iraq oil projects. Oil and Gas Journal Online. Article 290292.

Petta, T.J., and S.D. Rapp, 1990. Appleton Field – USA, Gulf of Mexico Basin, Alabama, in E.A. Beaumont, and N.H. Foster, eds., Treatise of Petroleum Geology; Atlas of Oil and Gas Fields: Structural Traps IV – Tectonic and nontectonic fold traps: Tulsa, OK, American Association of Petroleum Geologists, p. 299-318.

Pettingill, H.S and Weimer, P. 2001, Global deep water exploration: Past, present, and future frontiers: in R.H. Fillon, N.C. Rosen, P. Weimer, A. Lowrie, H.W. Pettingill, R. L. Phair, H.H. Roberts, and B. Van Hoorn, eds., 2001. Petroleum systems of deepwater basins: Global and Gulf of Mexico experience: GCS-SEPM Foundation Bob F. Perkins 21st Annual Research Conference, 1-22.

Salameh, M.G., 2003, Quest for middle east oil: the US versus the Asia-Pacific region, *Energy Policy*. 31. 1085–1091.

Sandrea, I., and O. Al-Buraiki., 2002, Future of deepwater, Middle East hydrocarbon supplies. Oil and Gas Journal, v. 100, p. 1-8.

Saner, S., and A. Sahin., 1999, Lithological and zonal porosity-permeability distributions in the the Arab-D reservoir, Uthmaniyah field, Saudi Arabia. American Association of Petroleum Geologists Bulletin, v. 83, p. 230-243.

Sarg, J.F., 1998, Carbonate sequence stratigraphy, in C.K. Wilgus., B.S. Hastings., C. G. St. C. Kendall., H. W. Posamentier., C. A. Ross., and J.C. Van Wagoner (eds). Sea-level changes: An integrated approach, Society of Economic Paleontologists and Mineralogists Special Publication No. 42: Tulsa, Oklahoma.

Vigorito, M., M. Murru, and L. Simone. 2005, Architectural patterns in a multistory mixed carbonate-siliciclastic submarine channel, Porto Torres Basin, Miocene, Sardinia, Italy. Sedimentary Geology, v. 186, p. 213-236.

Warren, John, K., 2006, Evaporites: Sediments, Resources, and Hydrocarbons, Springer: Berlin. P. 1-943.

Wagner, C.W., C. Van Der Togt. 1973, Holocene sediment types and their distribution in the southern Persian Gulf, in B.H. Purser (ed)., The Persian Gulf: New York, Springer Verlag, p. 123-155.

Wilson, A.O. 1985, Depositional and diagenetic facies in the Jurassic Arab-C and –D reservoirs, Qatif field, Saudi Arabia, in P.O. Roehl, and P. W. Choquette, eds., Carbonate Petroleum Reservoirs: New York, Springer-Verlag, p. 319-340.

CHAPTER 2. HOW TO FIND AN ORDOVICIAN BEACH – CRAB-LIKE BURROWS FROM EARLY PALEOZOIC SCANDINAVIA AND THEIR USE TO DETECT MAXIMUM SEA-LEVEL LOWSTANDS

Abstract

A hitherto unknown ichnospecies of *Skolithos* from the Upper Ordovician Dalby Formation of Sweden is proposed here as a new tool for recognizing sequence boundaries in carbonate ramp successions. The lebensspuren occur as three-dimensionally preserved decimeter-scale radial mounds on bedding planes and associated bowl-shaped unbranched shallow burrows in skeletal wackestones. Modern bubbler crab burrows of the order Scopimerinae from the Persian Gulf, which are remarkably similar in size, depth, morphology, and facies associations, provide a modern analog for the Ordovician lebensspuren. Modern bubbler crab (Genera *Scopimera* and *Dotilla*) burrows are restricted to the intertidal zone and their lebensspuren preservation is contingent upon subaerial exposure. A similar depositional setting and preservation mechanism is suggested for their ancient counterparts. These conditions render the *Skolithos* from Sweden as a powerful tool for recognition of subaerial unconformities (sequence boundaries) in the geologic record of Scandinavia and potentially elsewhere through large parts of geological history.

2.0 Introduction

Sequence stratigraphy and facies distribution of carbonate and mixed carbonate-siliciclastic ramp systems has been the focus of much research since the introduction of the ramp concept by Ahr (1973). One reason is that many important hydrocarbon reservoirs occur in these successions, especially in the Middle East (e.g., van Buchem et al., 2002). As outlined for carbonate ramp systems by Burchette and Wright (1992) and Wright and Burchette (1998), sequence stratigraphy relies on facies trends within the succession and the recognition of distinctive key surfaces to confidently reconstruct base level fluctuations (e.g., Read, 1998). However, in highly bioturbated ramp successions, especially those with low accumulation rates and strongly mud-dominated facies, both distinct small-scale lithological changes as well as key surfaces are often partially or completely destroyed by burrowing organisms. In such stacks of relatively homogenized ramp deposits where most original facies trends have been obliterated, additional criteria have to be explored to detect surfaces and intervals that reflect base level changes.

Here we present a specific, hitherto undescribed Ordovician ichnofossil that very closely resembles recent traces from the beach area in the Persian Gulf region. This study discusses the formation and preservation of these structures and their relevance as an indicator of a specific environment. It is proposed that the structures can be used to define one sequence stratigraphic key surface, the maximum regressive surface (MRS; Catuneanu, 2006; Helland-Hansen and

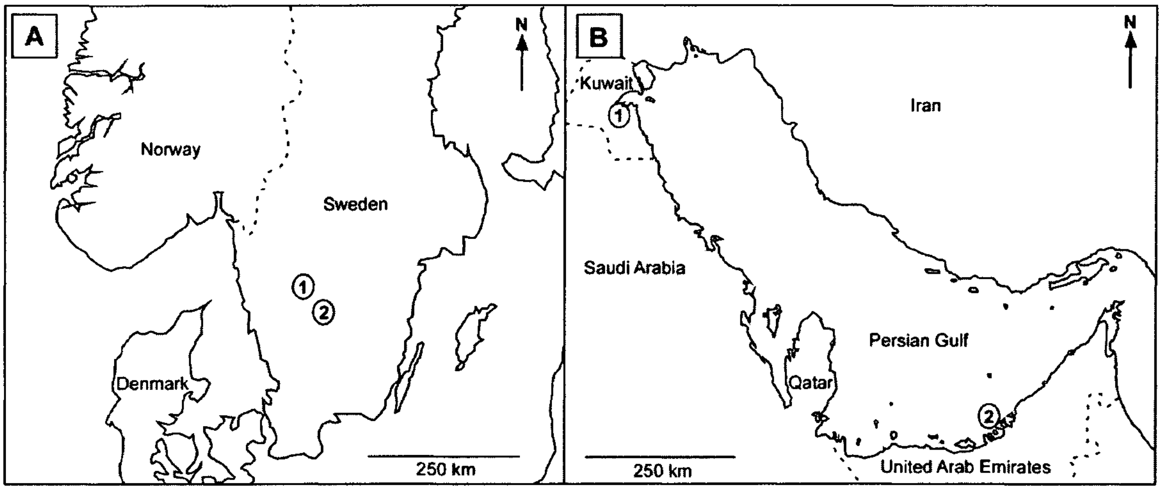

Figure 2.0. A) Study area in Sweden showing the localities of Kinnekulle (1) and Skövde (2) where Ordovician lebensspuren were collected. B) Map of Persian Gulf showing the tidal flats of Al-Jahra (1) along Kuwait Bay and the beaches along Abu Dhabi (2) in the United Arab Emirates where burrows of bubbler crabs were observed and documented.

Martinsen, 1996), in otherwise relatively monotonous-appearing carbonate ramp successions. Furthermore, this structure shows that a behavioral mechanism observed today in bubbler crabs had already been evolved by an unknown predecessor in Ordovician times which occupied the same ecological niche. Although the systematic position of this enigmatic organism remains unclear, these structures are a remarkably good example for parallelism in behavioral evolution within two likely completely unrelated animal groups.

2.1 Sedimentology and geological setting

2.1.0 The Ordovician Dalby Formation of Sweden

In the Early Palaeozoic, Scandinavia formed part of the Baltica plate. This microcontinent was located in the southern hemisphere between ~70° and 35°S during the Late Cambrian, but successively moved northwards into the tropics by the end-Ordovician (Cocks and Torsvik, 2002). Large parts of Baltica were covered by an epicontinental sea during this time (Lindström, 1971) with southern Sweden situated on its eastern flank (present orientation). Throughout the Ordovician, a carbonate ramp (Egenhoff, 2004) inclined to the west characterized the Baltic states and Scandinavia. The overall condensed succession shows mostly fine-grained carbonates in nearshore areas which gradually transition into shales towards deep shelf and basinal settings (Jaanusson, 1976).

The newly described ichnofossils occur in the Upper Ordovician Dalby Formation in the Gullhögen Quarry in Skövde, southern Sweden (Fig. 2.0). This unit shows a thickness of 11.9 m (Jaanusson, 1982) and has traditionally been divided into two members, the lower measuring 5.6 m (Jaanusson, 1982; our measurements deviate by 0.1 m from Jaanusson's original ones, thereby defining the boundary between the two members at 5.7 m, see Fig. 2.1), and the upper 6.3 m. The boundary of the Dalby Formation with the underlying Ryd Limestone is gradational and in places characterized by chamosite ooids and large invertebrate fossils, e.g. nautiloids, with stromatolitic overgrowth (Jan Johansson in Jaanusson, 1982). However, these stromatolites also occur in other stratigraphic levels within the Dalby Formation (Holmer, 1989). The upper contact of the Dalby Formation is defined by a distinct 1.1 m thick bentonite bed (Jaanusson, 1982). The Dalby Formation shows gray colors only (Jaanusson, 1982). This makes it easy to distinguish from the underlying Ryd Limestone, which is characterized by intercalations of gray and red nodular beds

(Jaanusson, 1982). The lower member of the Dalby Formation consists of nearly exclusively carbonate beds some centimeters to several decimeters thick. A single 2 cm thick shale layer, which was not recognized by Jaanusson (1982), is intercalated close to the base of the unit. The facies of the lower member consists predominantly of packstones and some wackestones. The upper member, in contrast, is characterized by several centimeters to decimeter-thick carbonate beds with abundant, mostly centimeter-thick shale intercalations (Jaanusson, 1982). The carbonate facies consists exclusively of wacke- and mudstones. Carbonate grains in the Dalby Formation comprise predominantly trilobite and brachiopod debris, some echinoderms, *Echinophaerites*, and nautiloids. Additionally, chamosite ooids occur close to the base of the unit. The facies is bioturbated throughout (bioturbation index about 3 to 4 following Taylor and Goldring, 1993) and therefore does not preserve any sedimentary structures. The facies of the Dalby Formation indicates deposition in a tranquil to moderately tranquil environment on a carbonate ramp (cf. Burchette and Wright, 1992). The lower member of the Dalby Formation featuring predominantly packstones likely represents an inner- to mid-ramp setting based on the abundance of grains. It is assumed that much of the packstones were originally deposited as distinct grain-rich layers, likely as event beds, over- and underlain by wackestones and mudstones representing carbonate background sedimentation. However, bioturbation destroyed all small-scale facies trends recognition and differentiation of inner and mid-ramp facies belts will remain difficult.

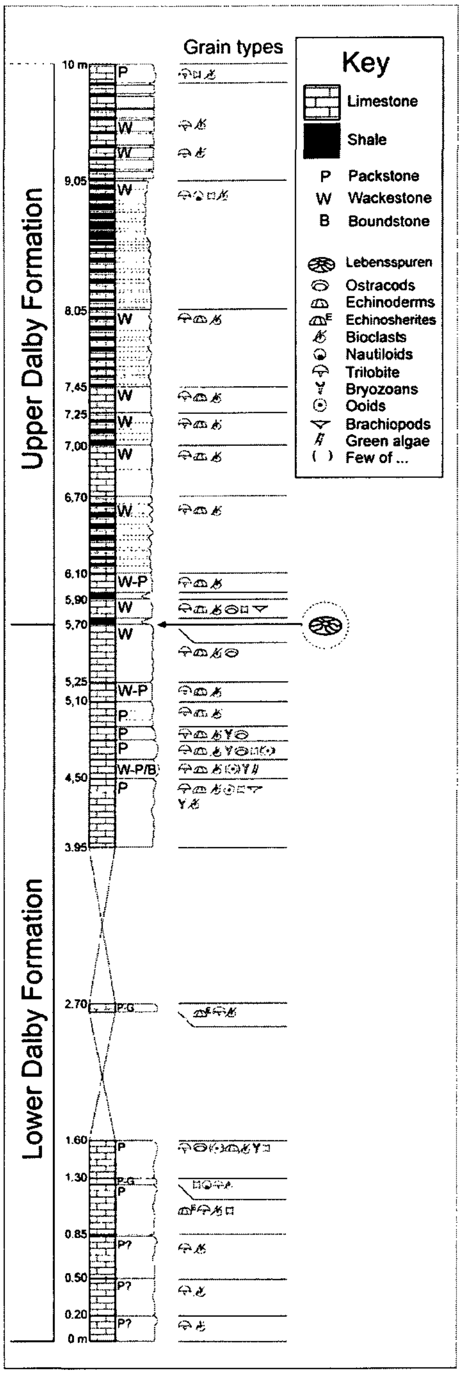

Figure 2.1. Detailed sedimentological log through the Dalby Formation in the Gullhögen Quarry in Skövde, southern Sweden. The unit has been subdivided into a lower part that is carbonate-dominated, and an upper part that shows carbonate-shale intercalations. The lebensspuren occur right at the boundary between the two sub-units at 5.7 m.

In the case of the lower member, grain-rich beds must have been so frequent that, even though they have been mixed in with mud-rich layers, the resulting facies is still grain-supported. Coarse-grained layers must have been significantly scarcer in the upper Dalby Formation even before it was bioturbated, as reflected in the predominance of wackestones. The general fining-upward trend within the Dalby Formation therefore shows a deepening from an inner-/mid- to an outer ramp and basin setting below the reach of storm waves. The increasing water depth with lower energy conditions also facilitated the preservation of volcanic ash beds (bentonites) at the upper boundary of the unit. In a shallow inner- to mid-ramp environment they would likely have been reworked.

As the lebensspuren occur exactly at the boundary between the Lower and the Upper Dalby Formation (Fig. 2.1), they separate underlying shallow subtidal wacke- to packstones from overlying mud- to wackestones and shales. Along the surface they define, a significant backstepping of facies belts during a transgression occurred, indicated by the deposition of low-energy outer ramp fine-grained carbonates and shales directly on top of higher-energy and relatively grain-rich inner ramp facies.

2.1.1 Sedimentology of Scopimera habitats

The burrows of genus *Scopimera* occur along the margins of the Indian Ocean in Western Australia, along peninsular India and in the Persian Gulf. The crabs do not show a preference within unconsolidated soft substrates and are found in mud-rich tidal flats of peninsular India (Chakrabarti, 1972), sand-rich beaches of the United Arab Emirates (Alsharhan and Kendall, 2003) and evaporite-rich sabkha environments of Kuwait. The present study investigated these burrows at two locations along the coastlines of Kuwait and the United Arab Emirates.

The sabkhas of Kuwait develop on sheets of eolian, medium-grained quartz sand (Al-Hurban and Gharib, 2004). Two main sabkha types can be distinguished along the periphery of Kuwait Bay. The first type in the northwestern part of the bay interfingers with alluvial fan deposits originating from canyons within the Jal-Az-Zor escarpment (Al-Hurban and Hersi, 2008). The supratidal portion of this sabkha is characterized by small sand dunes that migrate onto a wide gypsiferous deflation surface (Saleh et al., 1999). The intertidal zone is characterized by gypsum-encrusted cyanobacterial mats, which display crenulated and flat textures in the sense of Kendall and Skipwith (1968). These mats also show oscillation ripples closer to the surf-zone. The subtidal portion of the sabkha consists of quartz-rich skeletal sands. Crab burrows are common in the intertidal zone and were observed on patches of quartz-rich sand where cyanobacterial mats were absent (Fig. 2.2C). Burrows tend to be isolated and associated mounds can be 20-30 cm in diameter. Feeding pellets 2-3 mm in diameter and composed of fine-grained quartz sand are arranged in a radial pattern around the burrow opening. The second type of sabkha has developed The second type of sabkha has developed along the southern margin of the Kuwait Bay near the town of Al-Jahra (Fig. 2.0). This sabkha is mud-rich because longshore currents transport the fine-grained sediment from the Shat-al-along the southern margin of the Kuwait Bay near the town of Al-Jahra (Fig. 2.0).

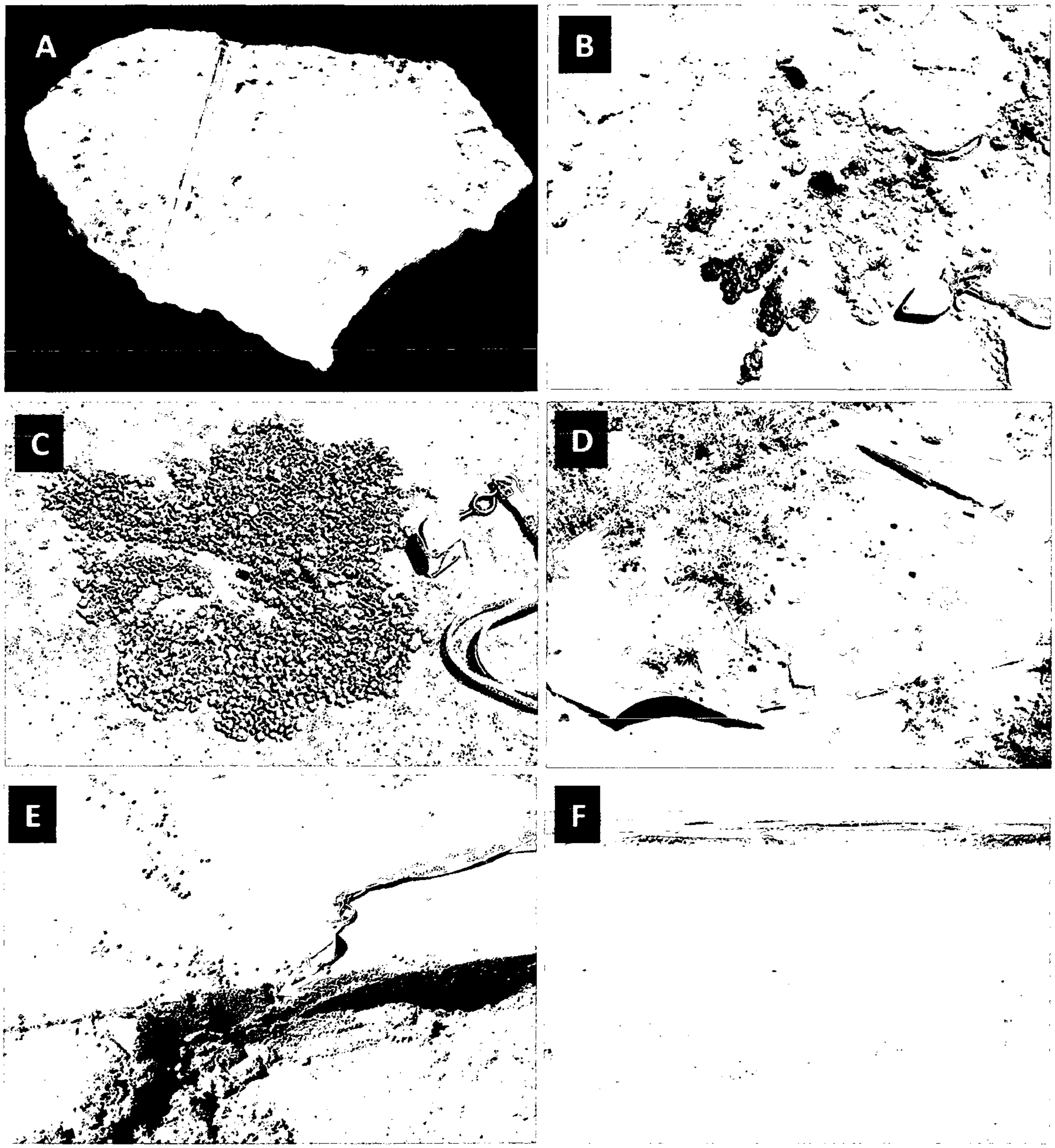

Figure 2.2. A) Ordovician lebensspuren from the Dalby Formation (scale bar is 15.0 cm) B) Modern bubbler-crab burrows on the tidal flats of Kuwait. Note the occurrence of desiccation cracks around the burrow mound. C) Polygonal Bubbler crab burrow, Kuwait Bay; D) Shallow Bubbler crab burrows on a rusty metal sheet; E) Trench through shallow bubbler-crab burrows (arrows); F) Cluster of bubbler crab burrows in the intertidal zone along Kuwait Bay.

Arab Delta in Iraq to deposit it in this area (Saleh et al., 1999). The supratidal portion of this sabkha is a vast coastal plain dominated by halophytes (Boulos and Aldosari, 1994). This coastal plain consists of a cohesive, sun-baked, mud-rich matrix that is covered by a thin veneer of wind-blown quartz sand. Remnants of abandoned dessicated *Scopimera* burrows get more common in a seaward direction. The intertidal zone contains shallow (< 1 meter) tidal channels and inter-channel bars. Tidal range along this coastline is approximately 4 meters (Al-Zamel et al., 2007). The margins of these bars contain gravel-pebble-sized shell hash of bivalves. The tops of these bars show low-amplitude current ripples (Hunter, 1977) on an eolian deposit of fine quartz sand and broken ooids. Tidal channels are filled with aragonitic ooid-rich sand that shows current ripples. This sand is coated with a fine calcareous organic-rich mud film that is 1-2 mm thick. Small (1-2 meters across) tidal pools developed in the intertidal zone contain green algae. Groves of halophytes form reed beds in the intertidal zone. The algae, along with the organic-rich calcareous mud film, attract cerithid gastropods that leave grazing traces in the soft wet mud. The intertidal zone also contains abundant *Scopimera* crab burrows (Fig. 2.2F). Elongate, tabular fecal pellets of the crabs about 1-2 cm in length are littered amongst grazing pathways of gastropods. Crab burrows occur in this intertidal zone only as clusters in tidal channels. Clusters forming on channel beds normally contain 10-15 burrows, whereas those in reed beds can have up to 30 burrows. There are also distinct differences in morphology between burrows formed on channel beds and those formed on reed beds. Burrows on channel beds tend to have narrower openings(1-2 cm), have associated mounds that are widely spaced, and have larger radii (20-30 cm) with very little relief (1-2 cm). Burrows in reed beds, in contrast, tend to have wider openings (3-4 cm), associated mounds which are very tightly spaced with small radii (10-15 cm) and high relief (4-5 cm). Trenches cut through the burrows revealed the depth of the burrows (Fig. 2.2E). Although there is variation within the depth of burrows between 2 – 5 cm (size variation in crabs due to age and sexual dimorphism), none of the burrows exceeded depths of 5 cm. Burrows also showed a slight tilt and were not perfectly vertical. However, due to lack of cohesion in sediment, trenches collapsed, and the exact angle of tilt could not be measured. Figure 3D shows a cluster of crab burrows constructed on a rusty steel sheet, and demonstrates the extremely shallow nature of the burrows. In the interidal zone the feeding pellets along the burrows are made of extremely wet clay, which causes the pellets to disintegrate, leaving a lumpy-reticulated texture around each burrow (Fig. 2.2B). Water-saturated pellets in the intertidal zone are extremely fragile, and crumbled when any attempts to take samples was made. Modern *Scopimera* burrows from previous seasons are preserved along the coastal plain south of Kuwait Bay. Although *Scopimera* preferentially inhabit burrows in the upper tidal flat (Koga, 1995), abandoned burrows on the coastal plain are common. Crabs that inhabited the coastal plain during winter left behind these burrows. During winters, coastal plains along the Persian Gulf are inundated with storm tides that can occasionally flood vast areas (Barth and Steinkohl, 2004). The addition of moisture to coastal plain sediments triggers algal growth, and attracts *Scopimera* and other grazers.

As spring approaches, and the shoreline recedes, crabs abandon their burrows and follow the tides. In the summer, temperatures can exceed 50 degrees Celsius and the sun bakes the mud of the coastal plain into a firm pavement. Burrows and pellets composed of clay dehydrate and cement. Those composed of coarser sand desiccate, crumble and are obliterated by weathering. During the following winter, storm tides once again cause a seasonal transgression and a thin veneer of organic-rich carbonate mud is deposited on the hardened dry surface of the coastal plain. Algae bloom in tidal pools and their filaments bind sediment. A new generation of *Scopimera* arrives and constructs burrows in this new sediment, and complete the cycle of burrow construction, abandonment, hardening, burial, and re-construction.

The Abu Dhabi beach investigated is not associated with a coastal sabkha and lines the margins of a large tidal channel. The beach along the banks of this channel consists of skeletal sand and ooids and shows current ripples, and bubbler crab burrows. These burrows are similar in dimensions and morphology to the burrows seen in the gypsiferous sabkha in Kuwait. However, the feeding pellets associated with these burrows are composed of coarse-grained sand. When moisture is removed from these pellets, they lose cohesion and crumble.

2.2 Ordovician ichnofossils from the Dalby Formation

2.2.0 Description

The host lithology of the Ordovician ichnofossils is best described as a chaotic mélange of skeletal fragments showing random orientation with no evidence of imbrication. A thin (1-2 mm) green mudstone film coats skeletal wackestones with dominant micrite, sparry calcite infill of fractures and skeletal cavities. Fractures start at the contact between the skeletal wackestone and the green mudstone and cut downwards across sedimentary fabric (Fig. 2.3A). The fractures are irregular, in-filled with calcite spar cement, and taper before terminating. All the fractures terminate at the same depth of 2 cm. Skeletal grains consist of echinoderm fragments, trilobite sclerites, brachiopod shell fragments, gastropod shell fragments, with minor components of cephalopods and ostracods. These skeletal wackestone are characterized by mostly diffuse bio-turbation with some distinct *Thalassinoides* and *Planolites* ichnofossils (Fig. 2.3C). These trace fossils have a random orientation and bioturbation index varies from 4-5. Coating the highly bioturbated skeletal wackestones is a thin (2-5 mm) film of green-grey calcareous mud. This mud film seems to fill in depressions within the micro-topography on top each structure (Fig. 2.3B). The film reaches a maximum thickness of 1-2 cm in the central dome region of each structure. Burrows, grains, Calcite-spar-filled fractures, and matrix truncate sharply against this fine mud.

Diagenetic hematite and pyrolusite stain the structures and may give a pseudo-cryptalgal lamination pattern when observed in hand sample. In thin sections the pyrolusite can be traced as branching upwards and forming bulbous patterns that resemble stromatolitic growth. The pyrolusite growth cuts across grain boundaries and burrow traces. No microbial laminae were found in the structures.

The ichnofossils are preserved as three-dimensional concave lenses that cover areas on bedding planes (Fig. 2.2A). Each ichnofossil is characterized by a central dome, and a reticulated pattern that radiates out from this central dome. Internally, this dome contains a bowl-like depression 2.5 cm in diameter and 1.0-1.5 cm in depth, filled with carbonate mudstone (Fig. 2.3A). The radii of individual structures vary from 5-8 centimeters. Shape and surface pattern of these ichnofossils appears to be size-dependent. Some of the smaller structures (< 6 cm) tend to be circular with a lack of surface patterns. Larger structures (>6 cm) are polygonal with a distinct short and long axis. Larger structures also tend to have a well-developed reticulated radial surface pattern. The thicknesses of these structures vary from 1-2 centimeters at the periphery to 4-5 centimeters at the central dome.

2.2.1 Interpretation

The structures are interpreted to represent a previously undescribed type of trace fossil. They occur in heavily bioturbated wackestones of the carbonate facies of the lower member of the Dalby Formation. The structures occur very close to each other, covering entire bedding planes. This reflects the ubiquity of the producing organism in this specific environment, which makes it likely to find more of these structures in suitable locations.

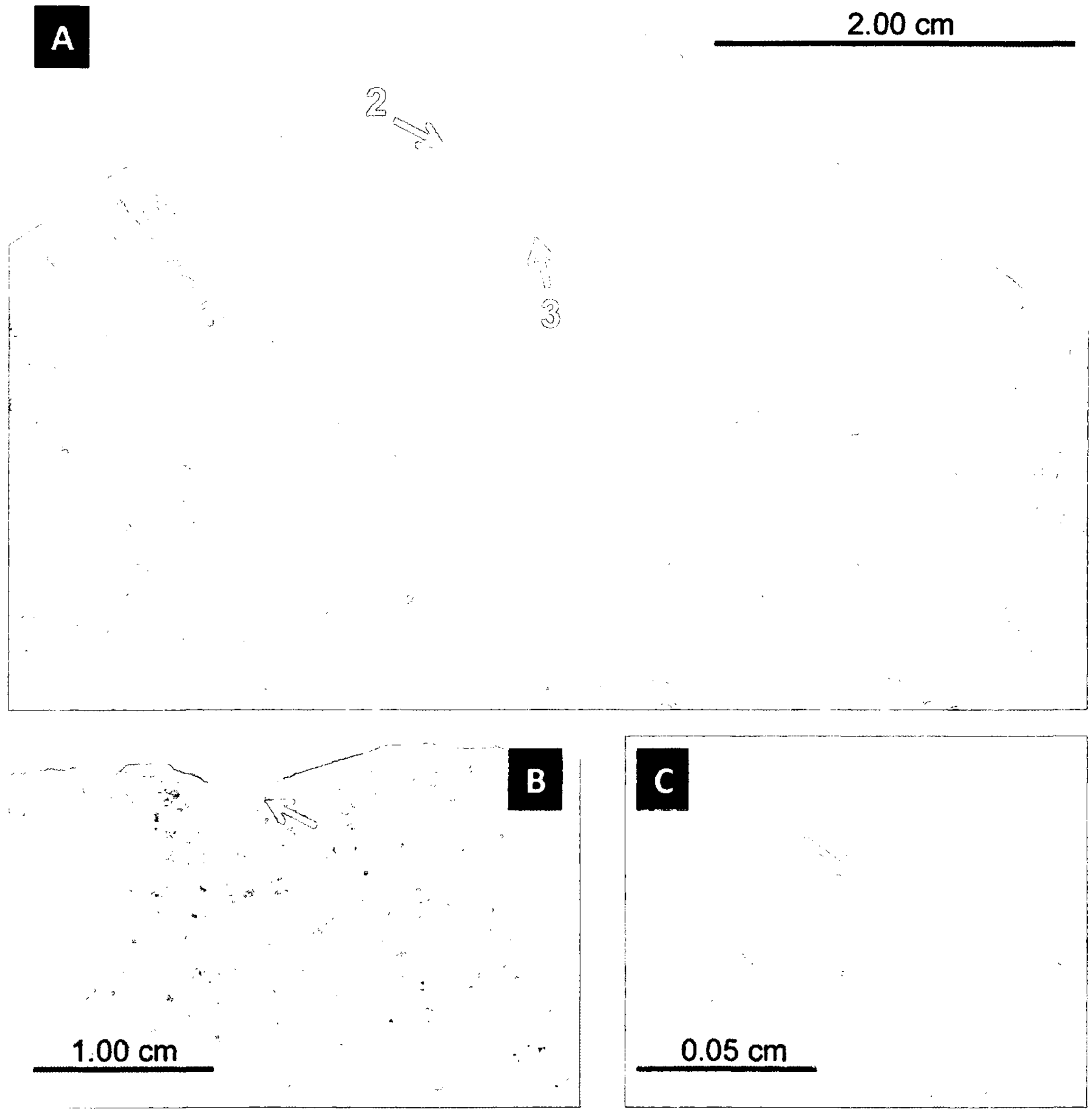

Figure 2.3. Photomicrographs of Ordovician lebensspuren from the Skövde locality, the top showing the original relief of the structures; (A) cross-section through central dome with lighter colored carbonate wackestones (w) showing a centimeter-size depression at the top now infilled by slightly darker carbonate mudstones (m); note spar-filled desiccation cracks that terminate against the upper surface of the lebensspuren (1); both the mud- and wackestones show bioturbation (2), but none of them crosses the fine line that separates the wacke- from the mudstones (3); B) Green mudstone infill of grooves C) *Planolites* isp. in dome interior

Although their outer form resembles algal structures such as low-relief stromatolites to a certain extent, the petrographic analysis of 14 thin sections from a number of these structures did not detect algal filaments/cryptalgal laminae or biological fabrics. This suggests that the structures were not produced by microbial activity, but rather by a burrowing organism that used surface and near-surface sediment. The sediment forming the slopes of the mounds was likely at least in part derived from digging out the central depression. This explains why there is no difference between the surrounding lithology and the sediment forming the slopes.

It is likely that the organism producing the ichnofossils maintained them by keeping the central hole open in which it was likely living. The infill of finer-grained carbonate into the central depression therefore postdates the active phase of these structures and reflects tranquil sedimentary conditions, much more tranquil than during the deposition of the host carbonate. Evidence for such low-energy conditions is a thin film of greenish-grey mud which coats the underlying coarser grained wackestones of the structures. The abrupt grain size change (coarse-sand-sized skeletal clasts in micrite matrix) and lithology (skeletal wackestone vs. mudstone) may represent separate depositional events. Because the mud seems to in-fill minute irregularities within the surface of the structure, and because there is erosional truncation between mud in the central dome and surrounding skeletal wackestones, this contact is interpreted as a stratal discontinuity. Vertical, irregular fractures that terminate against this contact are interpreted as dessication cracks. The thinning of fractures with depth is typical of dessication crack expansion during sediment dehydration. The calcite-spar in-fill may have precipitated during pre-burial flushing of meteoric waters.

The knobby surface characterizing the sediment sloping away from the central hole indicates that carbonate particles were originally unevenly distributed over this surface. The smooth shape of the knobs, however, resembles originally roundish soft sediment aggregates which have been only slightly modified by minor wave action (e.g., Chakrabarti, 1972). The organism inhabiting the structure therefore likely produced pellet-like sedimentary pebbles which it deposited in the direct vicinity of the central hole.

The roundish soft sediment aggregates have probably been derived in part from digging the hole. However, estimating the amount of sediment that could have been derived from digging out an only centimeters-deep central hole and the amount of sediment forming the slopes, it seems necessary that additional sediment was added to the slopes that was derived from elsewhere. This is also indicated by the fact that larger structures do not show deeper central holes than smaller structures.

The bowl-like depression with curved edges observed in these Ordovician lebensspuren, as well as the fact that they consist exclusively of a vertical component, are typical features which Alpert (1974) used to define the *Skolithos* ichnogenus. Following the crab-burrow classification scheme of Frey et al. (1984, Table 2, pg 342), these Ordovician lebensspuren are also best classified as *Skolithos*.

2.3 Discussion

2.3.0 Formation and preservation of crab burrows and lebensspuren

The modern crab burrows found along the beaches of UAE and Kuwait are used here as an analog to understand the formation and preservation processes of the Ordovician lebensspuren from the Dalby Formation. Modern bubbler crabs (Scopimerinae) inhabit burrows during the high-tide where a trapped bubble of air allows them to breathe until the beach is exposed during low-tide (Maitland, 1986). During low-tide these crabs will emerge to sift beach sediment for organic particles and will regurgitate pseudofecal pellets of sifted substrate and arrange them in a radial pattern around their burrows. Modern habitats of Bubbler Crabs along the coastlines of the Persian Gulf are inundated at high tides during winter storms (Barth and Steinkohl, 2004). As the survival of the crabs depends on episodic water supply, these periodically flooded sabkhas allow bubbler crabs to extend their range landwards. During spring, the flood waters evaporate and the abandoned burrows of bubbler crabs are subaerially exposed. Weathering during this period of exposure tends to destroy most burrow pellets composed of sand. However, clay-rich pellets and burrows are cemented and harden. During the succeeding winter, these burrows are then coated with a layer of fine calcareous mud, and more crabs will colonize the flooded sabkha. In such a scenario, annual cycles of burrows would be stacked. However, in rare instances, e.g. during large storm events, the intertidal zone is pushed several meters inland (Warren, 2006). Burrows constructed during that period are not inundated by next year's winter storm events. These burrows and associated pellets would only be buried during a relative sea-level rise. In such an instance, there would be a single layer of well preserved burrows with an overlying transgressive mud.

Our observations in the Recent indicate that the position of the burrows relative to the waterline during winter dictates whether burrows are preserved or reworked. Consequently, it is likely that the Ordovician lebensspuren also represent burrows constructed close to the extreme high-water line which were subsequently exposed and therefore could harden and be preserved. Pellets composed of fine-grained material held together much better in the recent, while sandy pellets were easily destroyed by weathering; therefore, the mud-rich nature of the Ordovician intertidal sediments also favored preservation. As large parts of the Ordovician succession in Sweden and adjacent Estonia are characterized by fine-grained carbonates with some assumed exposure surfaces (Harris et al., 2004), it seems likely that more of these structures may appear and can aid in refining Ordovician relative sea-level fluctuations for the Baltica plate. Although so far the Ordovician lebensspuren have been found exclusively in Sweden, this may be an effect of a sampling bias. The ichnofossils are most visually striking in plan view, but are not readily apparent in cross section. Therefore, their occurrence elsewhere in two-dimensional outcrops may have been overlooked or attributed to other ichnofossils within the *Skolithos* group. However, our field work in Sweden also revealed their presence within the same unit in the Kinnekulle locality (Fig. 2.1), indicating that they may be relatively frequent in the Ordovician succession of Scandinavia in the right facies. Closer inspection of Ordovician ramp successions along the sea-land interface of Baltica and along other coastal areas of the Iapetus Ocean may reveal the presence of similar ichnofacies.

2.3.1 *Intertidal versus subtidal origin of the lebensspuren*

As discussed above, pellets produced by recent bubbler crabs form exclusively in the upper intertidal environment (Chakrabarti, 1972), and these pellets are too fragile to withstand reworking by strong waves reaching high up on the beach. The sandy pellets cannot be produced in the subtidal realm, as grains are held together by a thin watery film, which is only possible under subaerial conditions. Fecal pellets composed of fine-grained carbonate sediment are reported from subtidal environments all over the world (see compilation in Flügel, 2004), so the structures described here could potentially also have formed in a quiet subaqueous setting.

In contrast to fecal pellets which are more strongly compressed due to digestive processes, the pellets produced by bubbler crabs are formed by their mouth parts outside the organism (Gherardi and Russo, 2002), but such loose sediment does not stick together under water. In subtidal environments, the sediment would have to be swallowed by the organism to produce stable pellets. The striking similarity between the ancient and the recent structures, however, suggests a similar formation mechanism, which makes it more likely that the pellets constituting part of the Ordovician structure have also been formed under subaerial conditions. Were these lebensspuren of subtidal origin, then they should be much more frequent in the Swedish succession and commonly preserved, especially on hardgrounds marking flooding surfaces, which are ubiquitous in the Swedish succession (Jaanusson, 1961). However, the supratidal lebensspuren are restricted to local occurrences along two specific bedding planes in the Dalby Formation and are not known from elsewhere so far. This distribution pattern fits much better with structures located in the upper intertidal zone. This represents a narrow facies belt rather than a subtidal occurrence which would – especially in a ramp environment with low gradient – show a broad geographical distribution. The dessication cracks cutting through the lebensspuren also strongly support an intertidal rather than a subtidal formation of the structures as they indicate subaerial exposure prior to the deposition of the overlying transgressive mudstones.

2.3.2 *Ethological aspects*

The recent bubbler crab burrows appear to be the closest modern analog for the Ordovician ichnofossils from the Dalby Formation. The burrows have strikingly similar morphology, dimensions, lithology and internal structure. On the basis of these similarities in ethology of the burrow-makers, and the environment of deposition, it seems likely that the Ordovician burrows were constructed by an organism that showed similar behavioral patterns as modern bubbler crabs. However, in the Ordovician, no group closely linked to modern bubbler crabs had evolved. It seems therefore plausible that the same behavior was developed by two non-related animal groups independently to thrive in the intertidal realm during different periods in earth history.

Unfortunately, the producer of these burrows is unknown and the knowledge on organisms living in intertidal environments in the Paleozoic is strongly limited. Thus, it is quite challenging to speculate on the origination of these trace fossils, especially when we see that the colonization of the intertidal and subaerial environment only started during the Lower Paleozoic. The first animal group exploring the terrestrial landscape was most probably the arthropods. Initial terrestialization occurred in the early Paleozoic by myriapods and chelicerates (Jeram et al., 1990; Edgecombe, 1998; Pisani et al., 2004), but arthropods may have been able to colonize brackish waters in the Lower Cambrian (Mángano and Droser, 2004). This step in expansion of ecospace utilisation towards completely terrestrial life styles must have been predated by intertidal to supratidal life styles. It does not necessarily require a colonialization of brackish water environments first, but could be explained through tidal and intertidal, normal marine environments leading to truly terrestrial life styles.

Even though trace fossils are common, tier complexity increased considerably in the early Paleozoic, demonstrating the metazoan colonization of the marine infaunal habitat (eg. Droser and Botjjer, 1989; Mángano and Droser, 2004), the producer of these traces is rarely preserved. Cherns et al. (2006) described a peculiar circumstance, in which trilobites of the genus *Asaphus* produced the trace fossil *Thalassinoides* in the Holen Limestone of Jämtland, possibly developing an infaunal life style to avoid predation. *Thalassinoides* is generally attributed to decapod crustaceans, the paleontological record of which reaches back until the Devonian, but the trace maker of the earlier *Thalassinoides* traces is still a mystery (Myrow, 1995).

Arthropod trackways have been found in eolian sandstones of basal Ordovician age in SE Ontario (MacNaughton et al., 2002), prior to the appearance of body fossils of truly terrestrial forms. This shows an origination of a terrestrial life style at least in the Lower Ordovician. As terrestrialisation increased, competition in the subtidal environments led to more organisms testing an infaunal life style and even proceeding to invade intertidal and supratidal beach environments. The presence of arthropods as the only land-living predators in terrestrial to intertidal environments may have caused the producers of the *lebensspuren* from the Dalby Formation to "go underground" to avoid predation from these organisms.

It is most probable that the trace makers actually are arthropods, but there might have been other soft-bodied organisms able to produce comparable traces. One unknown in the timing of terrestrialization of organisms remains, respiration. Modern bubbler crabs breathe through special organs, the tympana, at their legs (Maitland, 1986). It is much more likely that the Ordovician organism was still using gills than highly evolved respiratory tympana. This may explain why the central hole in the Ordovician burrows is much wider than in the recent counterparts. Whereas a narrow hole represents much better protection for the bubbler crabs and also helps to contain a pocket of air within them (Maitland, 1986), the larger hole in the Ordovician burrow could store more water which provided the organism a longer-lasting supply for breathing. However, the lebensspuren from the Dalby Formation show a gentle relief and are slightly elevated above ground, and it may only have contained water at its very bottom. The relatively steep walls of the central depression further indicate that the organism maintained this burrow open as otherwise, especially in an intertidal environment, the sidewall would have collapsed and the depression infilled with sediment. However, it could well be that the original hole was slightly deeper, and some sediment from the side walls filled in the lower portion. In this case, there should have been water in the hole for the producing organisms to breathe, as well as a deeper hole would have produced better protection from possible predators.

As the originator of the lebensspuren is likely to be of arthropod origin it seems reasonable to search for an answer to the respiratory problem by closely looking at the most old-fashioned relative of the early arthropods. An animal group with survivors that have not significantly changed since the Carboniferous with ancestors dating back as early as the Cambrian are Xiphosurids (Shuster and Babcock, 2008). The recent form belonging to this order, *Limulus polyphemus* or horseshoe crab, is a marine organism that leaves the ocean for mating and buries its eggs in beaches along the Atlantic coast between Maine and Mexico (e.g., Dunlap, 1999). During this phase, the horseshoe crabs can stay in the subaerial realm for hours and even days and continue breathing as long as their gills stay moist (Dunlap, 1999). Horseshoe crabs use book gills which allow such expeditions into the subaerial realm. Although Early Paleozoic trilobites did not yet develop such powerful respiratory organs they possessed filaments on their outer legs that in many ways resemble book gills (Australian Museum, 2002). It may therefore be possible that these earlier type of gills may have allowed some trilobites to leave the marine habitat for short periods of time, analog to modern horseshoe crabs. It is therefore plausible that the originators of the Ordovician lebensspuren did not necessarily have to develop a new breathing technique, but just used the type of gills they already had to initiate the step out of the subtidal into the intertidal habitat. In case these earlier forms of gills allowed at least in part what book gills do for the horseshoe crabs today, the organism producing the Ordovician lebensspuren did not necessarily need to create a large hole in the ground to accumulate water to be able to breathe. The central depression in the lebensspuren, even though slightly elevated from the original sedimentary surface and not necessarily entirely filled with marine water, could have supplied sufficient moisture to allow organisms to continue breathing through their gills.

2.3.3 Importance of the Ordovician lebensspuren for sequence stratigraphic interpretations

Carbonate ramp successions are often heavily bioturbated, and show only subtle vertical grain-size trends and a lack of preserved sedimentary structures (Borkhataria et al., 2006; Calvet and Tucker, 1988). These characteristics make a sequence stratigraphic analysis challenging as the analysis relies primarily on occurrences of bounding surfaces and stacking patterns (Van Wagoner et al., 1988; Handford and Loucks, 1993; Sarg, 1988) which – depending on the degree of bioturbation – may not be well defined in carbonate ramp strata. One way to overcome this problem is to use the bioturbation, which reflects changing environments, to determine relative sea-level changes (MacEachern et al., 1991; Pemberton et al., 2000). Ichnofossils have been used widely in sequence stratigraphy, and are especially appropriate for the identification of flooding surfaces (MacEachern et al., 1991). Evidence from ichnofossils is applicable to a large variety of depositional environments including siliciclastic shelves *(MacEachern et al., 1998), carbonate platforms (Clari et al., 1995), and also* carbonate ramps (Rodriguez-Tovar et al., 2007). Most of the intertidal traces grouped into the *Skolithos* ichnofacies are found in sandy substrates, whereas very little is known about lebensspuren from carbonate mud-dominated beach settings such as the lebensspuren from the Dalby Formation.

The lebensspuren represent an intertidal environment and separate underlying shallow subtidal deposits from overlying deep subtidal deposits (Fig. 2.2). The fact that they indicate the facies closest to land in this marine succession is crucial for sedimentological and sequence stratigraphic interpretations. The surface with these ichnofossils defines the turning point of the relative sea-level curve from regression to transgression, first subaerially exposing the lebensspuren during a sea-level fall, and subsequently flooding them during the initial sea-level rise. Their occurrence in a succession pinpoints the exact position of the coastline during the formation of these ichnofossils. The lebensspuren are therefore valuable for very detailed paleogeographic reconstructions. The preservation of the Ordovician lebensspuren in an upper-intertidal environment is contingent upon short term subaerial exposure, indicated by the occurrence of desiccation cracks that formed on the surface of these lebensspuren.

Because of this short-term subaerial exposure, unique for the Dalby Formation, the surface with the lebensspuren is correlated with the basinward limit of the subaerial unconformity (Fig. 2.4). The use of subaerial unconformities as a powerful correlation tool has been highlighted by several workers (Vail and Todd, 1981; Posamentier and Vail, 1988) and will not be discussed in detail here. The subaerial unconformity along the basin margin has been correlated to the Maximum Regressive Surface (MRS) which occurs in the basin center (Fig. 2.4). Helland-Hansen and Martinsen (1996) have interpreted the MRS as the point of maximum curvature at which the rate of base-level rise outpaces rates of sedimentation in a basin. The lebensspuren from the Dalby Formation described here help recognize and correlate the MRS and subaerial unconformity through the intertidal zone as they separate strata deposited during regression from overlying transgressive sediments. Although carbonate ramp successions that are largely homogenized by bioturbation such as the Dalby Formation may not show distinct coarsening-upwards and fining-upwards trends, the lebensspuren mark the contact between progradation and retrogradation of strata within this Ordovician section.

Burrows produced by crabs of the genus *Scopimera*, which are here interpreted to be the modern analogs of the Ordovician lebensspuren, are ubiquitous and occur along the margins of both the Pacific and the Indian

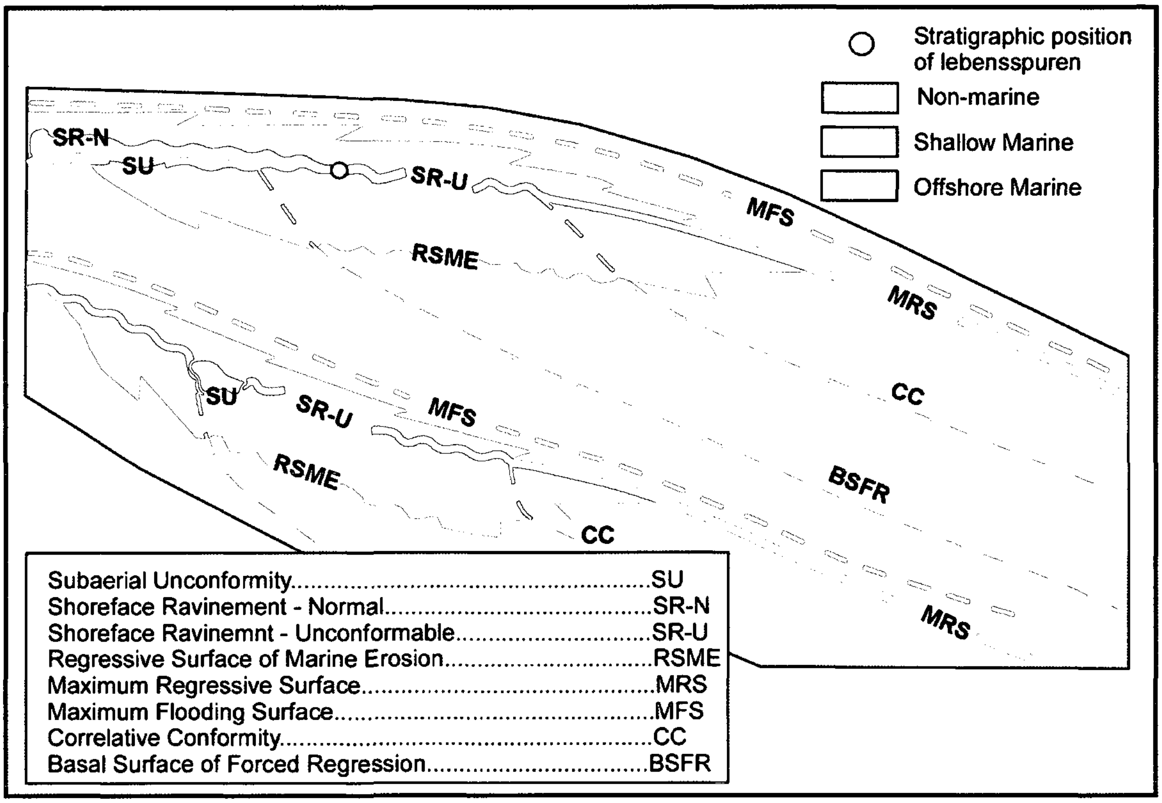

Figure 2.4. Blue dot shows stratigraphic position of the lebensspuren in the sequence stratigraphic framework of Hunt and Tucker (1992).

Oceans from Japan and Australia to the Persian Gulf (Maitland, 1986; Henmi et al., 1993). It may therefore well be that the makers of the Ordovician lebensspuren had a similar geographic range, which would make them a valuable regional correlation tool.

2.4 Conclusions

Ordovician lebensspuren from the Dalby Formation have an oval to roundish shape in plane view and consist of an irregular, bulbous surface with a central, shallow, carbonate mud-filled depression. They closely resemble modern bubbler crab burrows in the Persian Gulf region in morphology, size, and facies associations. It is therefore likely that the Ordovician lebensspuren have been produced by an organism showing similar behavioral patterns as modern bubbler crabs even though crabs had not evolved by the Ordovician.

The modern burrows are preserved only in the uppermost intertidal setting, which allows the burrows to harden and therefore withstand subsequent erosion. A similar depositional environment and preservation mechanism is envisioned for the Ordovician structures. They can thus be used as indicators for an intertidal setting in ancient successions.

In the Dalby Formation, the Ordovician lebensspuren define a surface which clearly indicates an increase in relative sea-level after formation of the structures and marks the turning point from regression below to transgression above. As the structures indicate intertidal conditions, their presence shows that the area under study was exposed, and therefore the surface represents a subaerial unconformity, correlative to the maximum regressive surface (MRS). If the makers of the Ordovician lebensspuren occupied a geographic range similar to modern bubbler crabs, they should be common in other successions throughout Ordovician and post-Ordovician geological history. This makes them very valuable indicators of recognizing one of the sequence stratigraphic key surfaces.

2.5 Acknowledgements

We wish to thank to John Ridley and Ellen Wohl for reviewing the manuscript and Wahab Sadeqi for providing logistical help while conducting fieldwork in Kuwait. This work would not have been possible without funding from the AAPG Grants in Aid Program and a grant from the International Association of Sedimentologists.

2.6 References

Ahr, W.M., 1973, The carbonate ramp: an alternative to the shelf model Transactions, Gulf Coast Association of Geological Societies, v. 23, p. 221-225.

Al-Hurban, A., and Gharib, I., 2004, Geomorphological and sedimentological characteristics of coastal and inland sabkhas, Southern Kuwait: Journal of Arid Environments, v. 58, p. 59-85,

Al-Hurban, A.E., and Hersi, A.A., 2008, Sedimentomorphic mapping of Jal Az-Zor escarpment, northern Kuwait, using GIS methods: Kuwait Journal of Science & Engineering, v. 35, p. 93-126.

Al-Zamel, A., Al-Sarawi, M., and Khader, S., 2007, Coastal geomorphology, hydrodynamics, and biolithofacies in the intertidal and subtidal areas of Umm Al-Namil Island, Kuwait Bay, Kuwait: Journal of Coastal Research, v. 23, p. 501

Alpert, S. P., 1974, Systematic review of the genus Skolithos: Journal of Paleontology, v. 48, p. 661-669

Alsharhan, A.S., and Kendall, C.G.S.C., 2003, Holocene coastal carbonates and evaporites of the southern Arabian Gulf and their ancient analogues: Earth Science Reviews v. 61, p. 191-243.

Barth, H.J., and Steinkohl, F., 2004, Origin of winter precipitation in the central coastal lowlands of Saudi Arabia: Journal of Arid Environments, v. 57, p. 101-115

Borkataria, R., Aigner, T., and Pipping, K.J.C.P., 2006, An unusual, muddy, epeiric carbonate reservoir; the lower Muschelkalk (Middle Triassic) of the Netherlands: American Association of Petroleum Geologists Bulletin, v. 90, p. 61-89.

Boulos, L., and Aldosari, M., 1994, Checklist of the flora of Kuwait: Journal of the University of Kuwait-Science, v. 21, p. 203-217.

Burchette, T.P., and Wright, V.P., 1992, Carbonate ramp depositional systems: Sedimentary Geology, v. 79, p. 3-57.

Calvet, F., and Tucker, M., 1988, Outer ramp carbonate cycles in the Upper Muschelkalk, Catalan basin, N.E. Spain: Sedimentary Geololgy, v. 57, p. 185-198.

Carl N. Shuster, Jr. and Loren E. Babcock., 2008, "Xiphosurida", in AccessScience@McGraw-Hill, http://www.accessscience.com

Catuneanu, O., 2006, Principles of sequence stratigraphy: Amsterdam, Elsevier, 375 p.

Chakrabarti, A., 1972, Beach structures produced by crab pellets: Sedimentology, v. 18, p. 129-134.

Cherns, L., Wheeley, J.R. & Karis, L. 2006. Tunneling trilobites: habitual infaunalism in an Ordovician carbonate seafloor: Geology, v. 34, 657-660.

Clari, P.A., Delapierre, F., and Martire, L., 1995, Discontinuities in carbonate successions: Identification, interpretation and classification of some Italian examples: Sedimentary Geology, v. 100, p. 97-121.

Cocks, L.R.M., and Torsvik, T.H., 2002, Earth geography from 500 to 400 million years ago: a faunal and palaeomagnetic review: Journal of the Geological Society, v. 159, p. 631-644.

Droser, M.L. & Bottjer, D.J. 1989. Ordovician increase in extent and depth of bioturbation: Implications for understanding early Paleozoic ecospace utilization: Geology, v. 17, 850-852.

Dunlap, J. (1999): Extraordinary horseshoes crabs. 48 pp., Lerner Publications.
Australian Museum (2002): www.austmus.gov.au/palaeontology/research/ trilobites 02. htm

Edgecombe, G.D. 1998. Devonian terrestrial arthropods from Gondwana: Nature , v. 394, 172-175.

Egenhoff, S.O., 2004, The Ordovician succession on Baltica—carbonate ramp or epicontinental sea? The 26th Nordic Winter meeting, Uppsala, Abstract Volume, Geologiska Föreningens i Stockholm Förhandlingar, v. 126, p. 160–161.

Flugel, E., 2004, Microfacies of carbonate rocks, Analysis, interpretation and application: Heidelberg, Springer, 976 p.

Frey, R.W., Curran, H.A., and Pemberton, S.G., 1984, Tracemaking activities of crabs and their environmental significance – the ichnogenus Psilonichnus: Journal of Paleontology, v. 58, p. 333-350.

Gherardi, F., and Russo, S., 2001, Burrowing activity in the sand-bubbler crab, Dotilla fenestrata (Crustacea, Ocypodidae), inhabiting a mangrove swamp in Kenya: Journal of Zoology, v. 253, p. 211-223.

Handford, C.R., and Loucks, R.G., 1993, Carbonate depositional sequences and system tracks - responses of carbonate platforms to relative sea-level changes, *in* Loucks, R.G., and Sarg, J.F., eds., Carbonate sequence stratigraphy: Tulsa, American Association of Petroleum Geologists, Memoir 57, p. 3-42.

Harris, M.T., Sheehan, P.M., Ainsaar, L., Hints, L., Mannik, P., Nolvak, J., and Rubel, M., 2004, Upper Ordovician sequences of western Estonia: Palaeogeography Palaeoclimatology Palaeoecology, v. 210, p. 135-148.

Hellandhansen, W., and Martinsen, O., 1996, Shoreline trajectories and sequences: Description of variable depositional-dip scenarios: Journal of Sedimentary Research, v. 66, p. 670-688

Henmi, Y., Koga, T., and Murai, M., 1993, Mating-behavior of the Sand Bubbler Crab *Scopimera-globosa*: Journal of Crustacean Biology, v. 13, p. 736-744.

Holmer, L.E., 1989, Middle Ordovician phosphatic inarticulate brachiopods from Västergötland and Dalarna, Sweden: Fossils and Strata, v. 26, p. 1-172.

Hunt, D., and Tucker, M., 1992, Stranded parasequences and the forced regressive wedge tract: deposition during base level fall: Sedimentary Geology, v. 816, p. 1-9.

Hunter, R.E., 1977, Basic types of stratification in small eolian dunes: Sedimentology, v. 24, p. 361-387.

Jaanusson, V., 1961, Discontinuity surfaces in Limestones: Bulletin of the Geological Institutions of the University of Uppsala, v. XL, p. 221-241.

Jaanusson, V., 1982, Ordovician in Västergötland, *in* Bruton, D.L., and Williams, S.H., eds., Fourth International Symposium on the Ordovician System: Oslo, Norway, Univ. Oslo, p. 164-183.

Jeram, A.J., Seldon, P.A. & Edwards, D. 1990. Land animals in the Silurian: Arachnids and Myriapods from Shropshire, England. Science: v. 250, 658-661.

Kendall, C.G.S., and Skipwith, P.A., 1968, Recent algal mats of a Persian Gulf lagoon: Journal of Sedimentary Petrology, v. 38, p. 1040

Koga, T., 1995, Movements between microhabitats depending on reproduction and life-history in the Sand-Bubbler Crab *Scopimera-globosa*: Marine Ecology-Progress Series, v. 117, p. 65-74.

Lindström, M., 1971, Vom Anfang, Hochstand und Ende eines Epikontinentalmeeres: Geologische Rundschau, v. 60, p. 419-438.

Maceachern, J.A., Pemberton, S.G., Raychaudhari, I., and Vossler, S., 1991, Application of the *Glossifungites* Ichnofacies to the recognition of sequence stratigraphic boundaries – Examples of the Western Canada sedimentary basin. Alberta, Canada: American Association of Petroleum Geologists Bulletin, v. 75, p. 626-626.

Maceachern, J.A., Zaitlin, B.A., and Pemberton, S.G., 1998, High-resolution sequence stratigraphy of early transgressive deposits, Viking formation, Joffre field, Alberta, Canada: Aapg Bulletin-American Association of Petroleum Geologists, v. 82, p. 729-756.

MacNaughton, R.B., Cole, J.M., Dalrymple, R.W., Braddy, S.J., Briggs, D.E.G. & Lukie, T.D. 2002. First steps on land: Arthropod trackways in Cambrian-Ordovician eolian sandstone, southeastern Ontario, Canada: Geology, v. 30, 391-394.

Maitland, D.P., 1986, Crabs that breathe air with their legs – *Scopimera* and *Dotilla*: Nature, v. 319, p. 493-495.

Mangano, M. G. & Droser, M. L. 2004. The ichnologic record of the Ordovician radiation. *In* Webby, R.B., Paris, F., Droser, M.L. & Percival, I.G., eds.. The great Ordovician Biodiversification Event. Columbia University Press, New York, p. 369-379.

Myrow, P. M. 1995. *Thalassinoides* and the enigma of early Paleozoic open-framework burrow systems: Palaios, v. 10, 58-74.

Pemberton, S.G., Maceachern, J.A., Gingras, M.K., and Zhang, J.P., 2000, Significance of ichnofossils to genetic stratigraphy - Examples from the Cretaceous of Alberta, Canada: Science in China Series D-Earth Sciences, v. 43, p. 541-560.

Pisani, D., Poling, L.L., Lyons-Weller, M. & Hedges, S.B. 2004. BMC Biology 2, 1-2. doi: 10.1186/1741-7007-2-1.

Posamentier, H.W., and Vail, P.R., 1988, Eustatic controls on clastic deposition II – sequence and system tracts models, *in* Wilgus, C.K., Hastings, B.S., Kendall, C.G.S.C., Posamentier, H.W., Ross, C.A., and Van Wagoner, J.C., eds., Sea-level changes - an integrated approach: Tulsa, Society of Economic Paleontologists and Mineralogists, Special Publication 42, p. 125-154.

Read, J.F., 1998, Phanerozoic carbonate ramps from greenhouse, transitional and ice-house worlds: clues from field and modelling studies, *in* Wright, V.P., and Burchette, T.P., eds., Carbonate ramps: London, Geological Society, Special Publication 149, p. 104-135.

Rodriguez-Tovar, F.J., Perez-Valera, F., and Perez-Lopez, A., 2007, Ichnological analysis in high-resolution sequence stratigraphy: The Glossifungites ichnofacies in Triassic successions from the Betic Cordillera (southern Spain): Sedimentary Geology, v. 198, p. 293-307.

Saleh, A., Al-Ruwaih, F., Al-Reda, A., and Gunatilaka, A., 1999, A reconnaissance study of a elastic coastal sabkha in Northern Kuwait, Arabian Gulf: Journal of Arid Environments, v. 43, p. 1-19.

Sarg, J.F., 1988, Carbonate sequence stratigraphy, *in* Wilgus, C.K., Hastings, B.S., Kendall, C.G.S.C., Posamentier, H.W., Ross, C.A., and Van Wagoner, J.C., eds., Sea-level changes: An integrated approach: Tulsa, Society of Economic Paleontologists and Mineralogists, Special Publication 42, p. 125-154.

Taylor, A.M., Goldring, R., 1993, Description and analysis of bioturbation and ichnofacies: Journal of the Geological Society, v.150, p. 141-148.

Vail, P.R., and Todd, R.G., 1981, Cause of the northern North-Sea Jurassic unconformities: Aapg Bulletin-American Association of Petroleum Geologists, v. 65, p. 1003-1003.

Van Buchem, F.S.P., Razin, P., P., H., Philip, J.P., Oterdoorn, W.H., and Philip, J., 2002, Stratigraphic organisation of carbonate ramps and organic-rich intrashelf basins: Natih Formation (Middle Cretaceous) of northern Oman American Association of Petroleum Geologists Bulletin, v. 86 p. 21-53.

Van Wagoner, J.C., Posamentier, H.W., Mitchum, R.M., Vail, P.R., Sarg, J.F., Loutit, T.S., and Hardenbol, J., 1988, An overview of the fundamentals of sequence stratigraphy and key definitions, *in* Wilgus, C.K., Hastings, B.S., Kendall, C.G.S.C., Posamentier, H.W., Ross, C.A., and Van Wagoner, J.C., eds., Sea-level changes: an integrated approach: Special Publication, Society of Economic Paleontologists and Mineralogists, p. 39-45.

Warren, J.K., 2006, Evaporites Sediments, resources and hydrocrabons: Heidelberg, Springer, 1036 p.

Wright, V.P., and Burchette, T.P., 1998, Carbonate ramps: an introduction, *in* Wright, V.P., and Burchette, T.P., eds., Carbonate ramps: London, Geological Society, p. 1-5.

CHAPTER 3. OOLITIC FACIES IN THE MISSISSIPPIAN BAKKEN FORMATION OF THE WILLISTON BASIN AND THEIR ANALOGS FROM THE MODERN PERSIAN GULF

Abstract

Layer-cake models are frequently applied to the stratigraphically complex Devonian-Mississippian Bakken Formation of North Dakota. Due to inherent complications in depositional style caused by sea-level changes, facies would be more likely to have low-lateral continuity. This phenomenon is best characterized in the oolitic facies of the Middle Bakken Member, which occur in 21 of the 40 cores analyzed during this study. These facies are interpreted as ancient coastal embayment, barrier-island, and tidal channel deposits. Similar environments prevail along the proximal edge of a carbonate ramp in the modern Persian Gulf. Using satellite imagery, 1400 km of coastline along this ramp were mapped to collect geometric and dimensional data. Different facies have characteristic geometry, orientation, and dimensions. Integration of core and thin section analyses of the Bakken Formation and satellite images from the recent Persian Gulf allow a thorough understanding of sedimentary processes and reservoir architecture. Future horizontal well planning should consider the issues of lateral continuity and compartmentalization in these stacked, ribbon-like reservoirs.

3.0 Introduction

The Devonian-Mississippian Bakken Formation is one of the most important reservoirs in the continental US (Pollastro, 2008). Recently the United

States Geological Survey revised their reserve estimates for the Bakken Formation of the Williston Basin in North Dakota to 3.65 billion barrels of oil, with the vast majority stored in the Middle Bakken Member. The primary target for hydrocarbon extraction from this unit is the Middle Bakken "dolomite", especially the oolitic sandstone in the upper part of the Middle Member. However, both the sedimentology and stratigraphy of this unit are not well understood (cf. Pitman et al. 2001) and therefore a detailed depositional model is lacking. Industry widely applies models developed for isolated platforms to the ramp morphology of the Bakken Formation. However, facies models developed for high relief shelves and isolated platforms should not be applied to ramps due to differences in relief and associated sedimentary processes (Purser, 1973). This hampers prediction of reservoir geometries in the Middle Bakken, and can lead to inaccurate reservoir simulation models.

Here, we present a detailed depositional model for the oolitic facies that occur in the Middle Bakken based on 40 cores from North Dakota and Montana and data from modern ooid accumulations in the Persian Gulf. The current investigation not only creates a comprehensive depositional model for the Bakken Formation, but also increases our understanding of ancient oolites in ramp settings.

3.1 Geological and Stratigraphic Settings

3.1.0 Bakken Formation

The Bakken Formation was deposited in a shallow epeiric sea in the Williston Basin during the Early Mississippian (Gerhard et al., 1982). The Williston Basin represents an intracratonic sedimentary basin and covers an area of 250,000km^2 over parts of the U.S. and Canada (Kent and Christopher, 1994; LeFever, 1991; Gerhard et al., 1982). Strata comprising Devonian and Mississippian time have been extensively studied as they contain some of the most prolific hydrocarbon reservoirs in the Williston Basin (Pollastro, et al., 2008). The initial transgression of the Late Devonian epeiric-sea inundated the earlier continental strata of the Williston Basin and the sedimentation of the Bakken Formation ensued. The Bakken can attain a maximum thickness of 26 meters and is found only in the subsurface (Webster, 1982; Dumonceaux, 1984; Smith and Bustin, 1996).

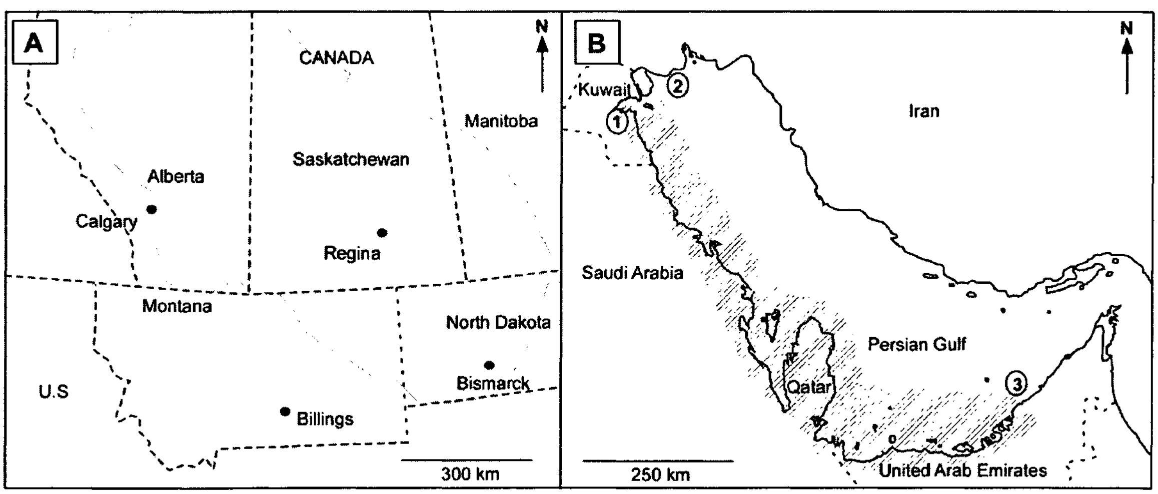

Figure 3.0. A) Shaded area shows the position of the Williston Basin B) Map of Persian Gulf showing the locality where modern ooid samples were collected (1) and the locations of the Shat al-Arab Delta (2) and the town of Mina Jebel Ali (3). Stippled lines indicate area which was surveyed using satellite images.

3.1.1 Persian Gulf

The Persian Gulf contains a warm (40-50^{0}C), shallow (<100m), epeiric sea that developed its present configuration during the Late Tertiary (Purser and Seibold, 1973; Kassler, 1973).The Persian Gulf represents a foreland basin associated with the uplift of the Zagros fold and thrust belt and covers an area of 226,600 km^2 (Purser and Seibold, 1973). The basin is asymmetrical and forms.a shallow tectonic depression about 1000 km long along the Zagros mountain front (Kassler, 1973). The primary source of terrigeneous clastic sediment in the basin is the Shat al-Arab delta in the northern part of the Persian Gulf. The majority of recent sediment in the basin includes lime muds in the outer ramp, and coarse oolitic, peloidal, and skeletal sand accumulations along the middle and inner ramp (Wagner and Van Der Togt, 1973). For a comprehensive treatment of Persian Gulf geology, readers are referred to Purser (1973).

3.2 Previous work on the Persian Gulf

During the period 1961-1968 a consortium of 31 authors from the Imperial College of London, the Kiel University and the Shell Research Group carried out extensive research in the Persian Gulf to document geology, geomorphology and environmental factors that control carbonate precipitation in ramp settings. This research resulted in a monograph (Purser, 1973), which is the most comprehensive account of Persian Gulf geology. Sections of this monograph focus on recent carbonate facies (Wagner and Van Der Togt, 1973), recent depositional environments of Qatar (Shinn, 1973), and modern oolitic

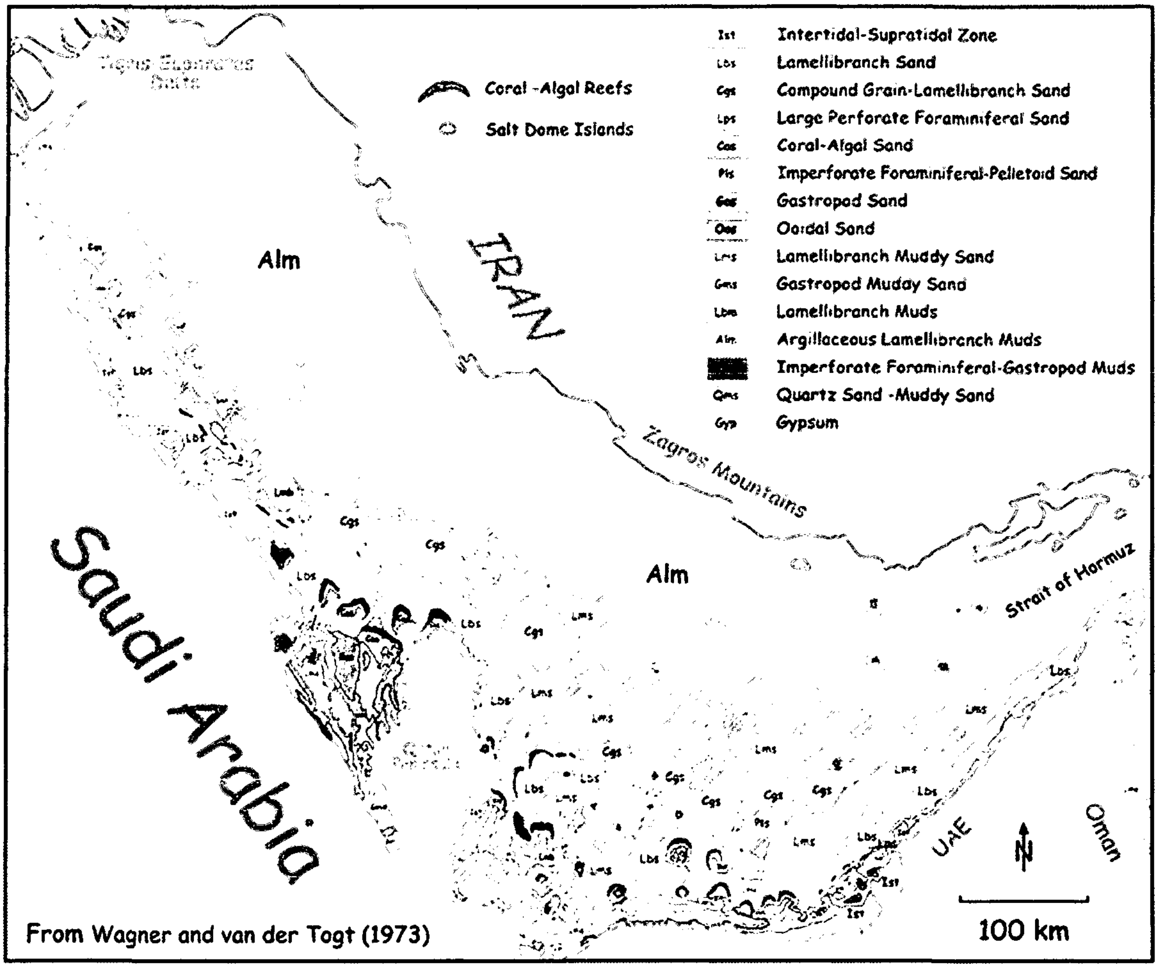

Figure 3.1.Modern facies map of the Persian Gulf showing locations of oolitic sand accumulations. Reproduced from Wilkinson (2004)

accumulations throughout the Persian Gulf (Loreau and Purser, 1973). Detailed bathymetry and lithofacies maps were created as part of this consortium and these were used to locate, identify and map the features described in the present study (Fig. 3.1). Loreau and Purser (1973) defined and documented several oolitic accumulations such as coastal embayments, ebb deltas, beaches, and eolianites. These accumulations were sampled through dredging from boats and the diagnostic sedimentary features of these environments were recorded. Although the work done by Loreau and Purser (1973) is still the definitive publication on ooids from the Persian Gulf, they made very few inferences on the geometry and dimensions of ooid accumulations. Therefore, a detailed investigation of geometrical and dimensional properties of these sediment bodies was conducted by the author of this paper.

3.3 Methodology

This study integrates information from 40 cores from wells penetrating the Middle Bakken at the U.S. Geological Survey core research center in Denver, and the North Dakota Geological Survey core library in Grand Forks. Oolitic facies within the cores are described in high-resolution, noting contacts, sedimentary structures and bedforms, and vertical stacking patterns. Plugs taken from representative facies are used to make thin sections. Microfacies analyses of these samples allow comparison with morphology and internal structure of modern ooids from the Persian Gulf. The criteria for comparison include grain packing, size, sorting, cortical thickness, symmetry, nuclei, texture, associated fauna, boring, shape, and lamination.

Satellite images of the modern Persian Gulf were acquired from NASA Visible Earth, NASA World Wind and Google Earth. Google Earth 4.2 allows measurement of geomorphic features on the computer screen with a measuring tool. This map tool can not only be used to measure lengths but can calculate the area of polygons drawn on satellite images. Software engineers at Google's New York City office were contacted to determine the accuracy of this measuring tool. Measurements using this tool are accurate to within one meter if the image is displayed in map view mode (Oral communication with Alexander Vogenthaler at Google New York). Accuracy is higher for features in areas with low topographic relief. Since all the coastal features measured were in areas with dips as low as one degree or less, the tool had high accuracy.

The modern coastline along the Persian Gulf was analyzed for ooid accumulations between the Shat-Al-Arab Delta in Iraq and the town of Mina Jebel Ali in the United Arab Emirates (Fig. 3.0). The selection criteria included 1) high resolution satellite coverage, 2) accessibility for fieldwork, and 3) pristine condition of coastline. The Shat-Al-Arab area lies at the border of Kuwait and Iraq and due to security concerns this delta was not visited. Mina Jebel Ali is a town between the emirates of Abu Dhabi and Dubai. The coastline east of Mina Jebel Ali has been drastically changed due to the construction of the Burj al-Arab, Palm and World Islands. Oolitic accumulations were recognized based on facies maps illustrated in Wagner and Van Der Togt (1973). Several of the locations were also sampled by Loreau and Purser (1973) and (Kendall, 2009). The data of these authors were also incorporated into this study.

Field locations include the coastline in northern Kuwait Bay, and the coastline of Abu Dhabi (Fig. 3.0). During field work, oolitic accumulations that were mapped on satellite images were described for lithology, sedimentary structures, thickness (where possible), body fossils and trace fossils. Shallow trenches were excavated to observe bedforms and samples were collected to create petrographic slides.

After field validation of lithofacies was complete, a database containing dimensional and geometrical data from modern oolitic accumulations within the Persian Gulf was created. Shapes recorded from each accumulation were then compared to determine if a generalized shape could be assigned to each accumulation type.

3.4 Sedimentology

Out of 40 cores that were readily available for public viewing at core facilities in the USGS in Denver and the North Dakota Geological Survey in Grand Forks at the time of publication, 21 contain oolitic facies. Three distinct oolitic lithofacies are defined in this study.

3.4.0 Facies A

Description

This facies has only been observed in the Texaco Incorporated 5-1 Thompson Unit Well in Billings County, North Dakota at a depth of 11,058 feet/3350 meters. The facies consists of a grey-brown, well cemented, low-angle (<25 degrees) trough cross-stratified ooid grainstone with a thickness of 15-20 cm (Fig. 3.1B). The facies makes a sharp, irregular, wavy contact with an underlying bioturbated siltstone. The upper contact is marked by a sharp scour of an overlying wavy bedded siltstone into the oolitic grainstone (Fig. 3.2A).

Petrographic analysis of this facies reveals that over 90% of the facies is composed of ooids, whereas minor amounts of botryoidal grains are also present

(Fig. 3.2C). The sample is grain-supported with drusy calcite cement infilling inter-granular pores. Present-day inter-crystalline porosity is less than 2% (Fig. 3.2C). Botryoidal grains in the sample are sub-rounded to elongate and show aggregates of 2-3 small ooids enveloped in a single radial coat (Fig. 3.2D). Symmetric, radial, ooids with 2-4 thick (1/3 radius length) cortical lamellae make up most of the sample. Fe-Mn pigments were observed in some ooids at the contact of lamellae. In certain ooids these pigments appear to coalesce to form a distinct darker layer between lamellae (Fig. 3.2E). The outer surface of the cortex in most ooids appears to be pitted, giving it an irregular appearance. Nuclei ofooids are dominated by skeletal fragments with minor quartz grains. Twenty ooids which showed transects through their nuclei were selected for measurement. A transect through the nucleus represents a close approximation to their original diameter. Although most ooids in the sample are symmetrical, those showing slight asymmetry were measured along their longitudinal axis. A histogram (Fig. 3.3) for these measurements of ooid diameter revealed two distinct populations. The first population showed a diameter range between 600-1100 µm, whereas the second demonstrates a diameter range between164-480 µm. Aggregates of pyrite 1-3 cm in length can be observed in core. No bioturbation or skeletal fragments were observed in this facies

Interpretation

The bimodal distribution of ooid size within the samples is characteristic of coastal embayments and of beaches (Purser and Loreau, 1973). In such

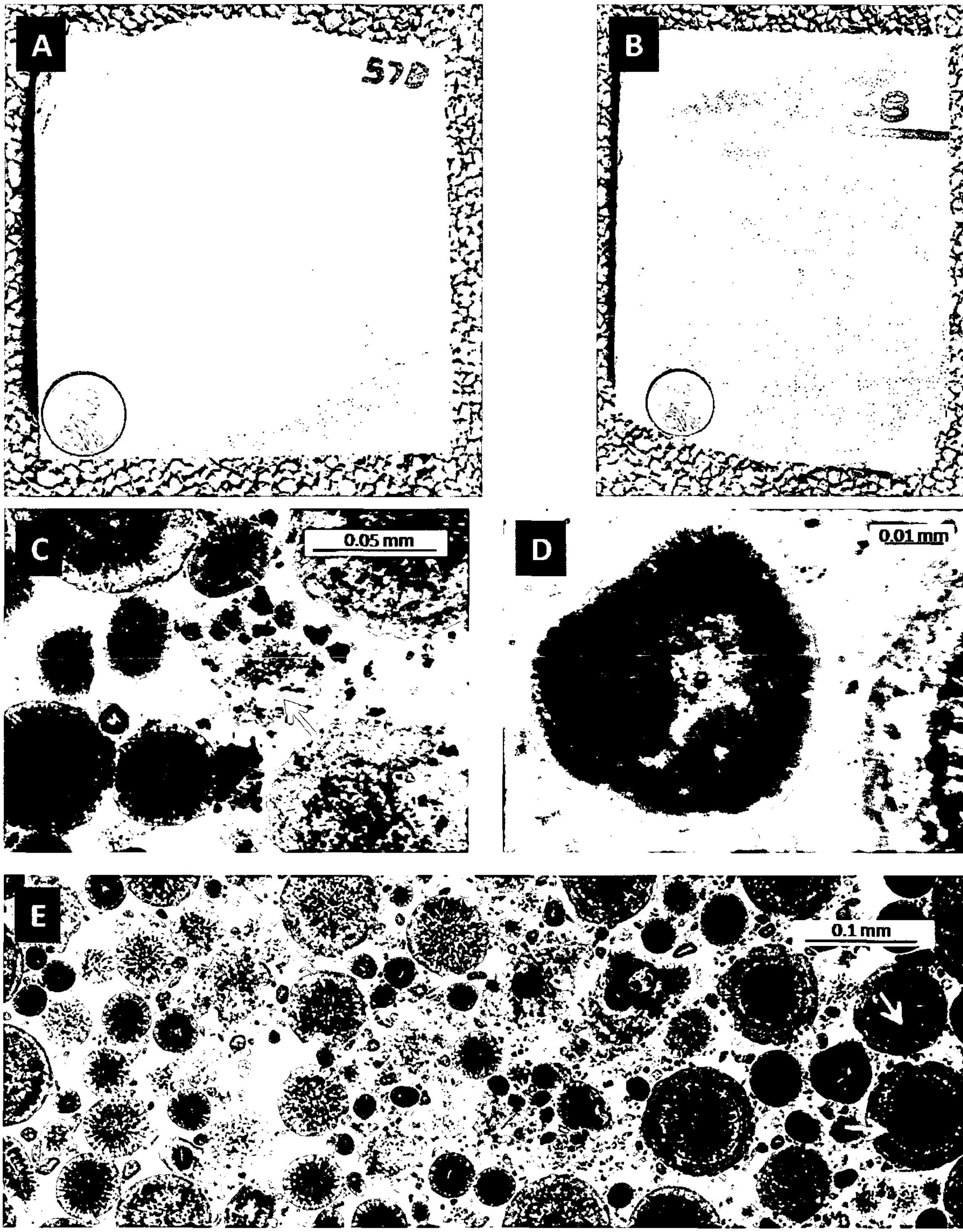

Figure 3.2. A) Scour surface between siltstone and top of ooid grainstone (Depth 11057 ft) B) Trough cross-beds in ooid grainstone (11058 feet) C) Intercrystalline porosity D) Botryoidal grain E) Note the pitting and irregularity of ooid surface, red-arrows indicate dark organic insoluble patches and layers

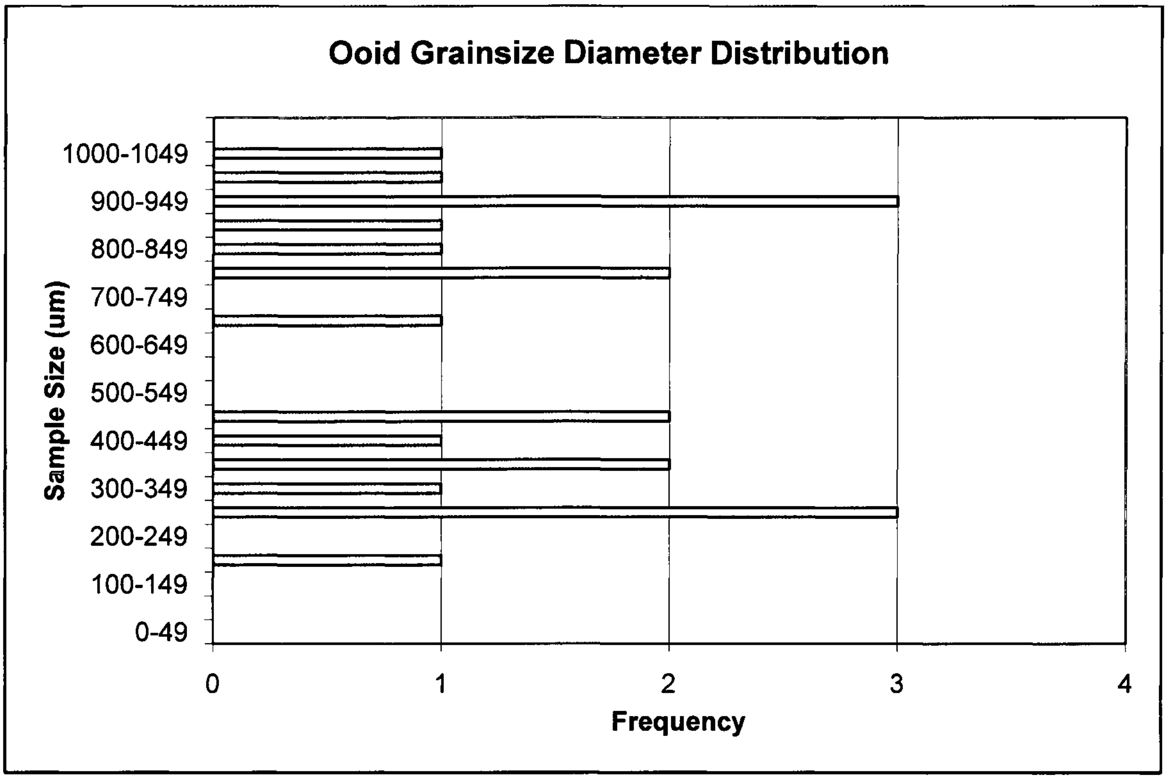

Figure 3.3. Histogram of measurements of ooid diameter in thin-section. Two distinct populations can be observed.

form in more quiescent conditions and are smaller (Sumner and Grotzinger, 1993).Movement of smaller ooids from ridge tops into topographic lows allows the mixing of the two sizes and causes a bimodal distribution. The symmetry of ooids and their pitted surface within this facies also suggest formation within an area of constant high-energy agitation (Richter, 1983). The ooids in the sample have a radial texture unlike tangential aragonitic ooids formed in modern coastal embayments and beaches. This may have been caused by the influx of meteoric waters into the sediment during early marine vadose diagenesis. Cantrell (2006) proposes that this feature forms where meteoric waters leach aragonitic ooids and create intra-granular porosity. This porosity tends to follow a radial pattern.

During conversion of aragonite to calcite these pores are in-filled with equant calcite cement enriched in iron, strontium, and manganese. These minerals impart a darker coloration and create a pseudo-radial pattern in ooids. During the leaching process, acid insoluble organics are left behind and form patches or rings between cortical lamellae. This process explains the accumulation of Fe-Mn between cortical lamellae observed in thin sections of Facies A. The presence of

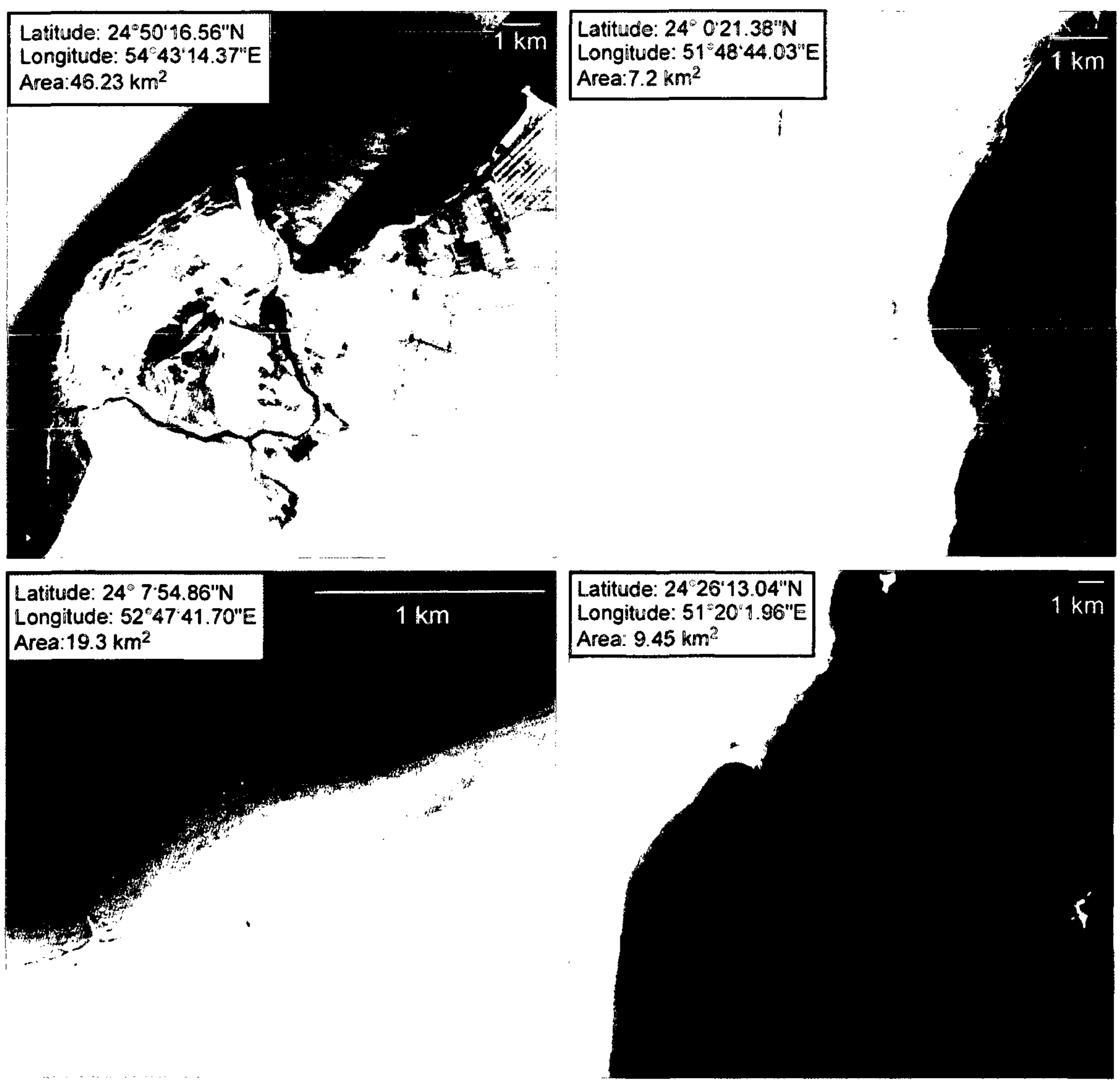

Figure 3.4. Modern coastal embayments along the western margins of the Persian Gulf (images from Google earth). Area and geographic coordinates of each coastal embayment are provided in the in-set.

botryoidal grains suggests periods of stability which would allow the binding and cementation of ooids (Fluegel, 2004). They also indicate areas with water circulation which tends to winnow fine grained particles and hence areas where sediment is mobilized (Wanless, 1981). The presence of drusy calcite cement in the facies is a sign of near-surface meteoric diagenesis (Fluegel, 2004). Satellite imagery of modern coastal embayments along the western margins of the Persian Gulf shows longitudinal shore-parallel accumulations of ooids. The area of these accumulations varies between 7 and 46 square kilometers (Fig. 3.4). Internally, these embayments are characterized by a network of shore parallel-oblique ridges and runnels (Kendall, 2008). One such embayment in the United Arab Emirates was studied in detail by Loreau and Purser (1973). Pure oolitic sands occur as a series of ridges of amplitudes of 1 m. Ooids form and accumulate in these embayments from a combination between coastal winds (*shamals*) and powerful longshore currents. However, the rarity of this facies within the Bakken Formation may be due to a lack of strong coastal winds along the paleoshoreline.

3.4.1 Facies B

Description

This facies is composed of three sub-facies and characterized by well-sorted, ooid-rich, fine-grained quartz sandstones and occurred in 19 of the 40 Bakken Formation cores analyzed in this study. The majority of these cores come from wells located in counties in northwestern North Dakota (Fig. 3.5). Because of its diagnostic well-log signature, and its 'clean' appearance on Gamma Ray Logs, this facies has been targeted as the primary reservoir within the Middle Bakken interval. This facies can be up to 6 meters in thickness and tends to form a sharp erosional contact with underlying siltstones (Fig. 3.6A) and sharp to gradational contacts with overlying facies. No trace fossils or large (>1 mm) skeletal fragments characterize these sediments and ooids tend to be broken and fragmented (Fig. 3.8). Soft sediment deformation is common in this facies and includes subtle gravity faulting, slump structures and convoluted bedding (Fig. 3.7D).

Interpretation

The presence of 1-30% broken ooids (Fig. 3.8), the absence of any type of bioturbation structures, and excellent sorting of the quartz sand as well as a maximum size of skeletal grains not more than 1 mm all suggest an eolian environment for the deposition of this facies (cf. Glennie 1970). The broken ooids, however, represent the main argument to interpret this facies as eolian rather than water-lain (Dodd et al. 1993). In subaqueous settings, the higher viscosity of water compared to air smooths grain to grain collisions, thereby prev--enting the breaking of individual ooids. In the medium air, in contrast, the lack of the cushioning effect of water tends to promote collisions of greater intensity which lead to chipping and breaking of ooids. Furthermore, the association of the ooids with large amounts of non-coated grains such as terrigenous quartz and feldspar is difficult to envision forming in a subaqueous setting. In tropical shallow-water environments such as the one characterizing Upper Devonian to Lower Mississippian sedimentation in the Williston Basin, high-energy facies leads to calcareous coatings around any form of nuclei (Donahue, 1969; Frishman and Behrens, 1969; Kahle, 1974; Fabricius, 1977; Davies et al., 1978; Simone, 1981). The absence of such coatings on the quartz, feldspar and skeletal grains therefore suggest that these have not been subjected to longer-term subaqueous transport, but may rather have accumulated in a subaerial environment. This is also indicated by the absence of any type of marginal borings in the skeletal grains, characteristic for a slow degradation process of carbonate particles in the shallow-water subtidal realm (Wanless and Tedesco, 1993). It is therefore likely that the ooids and skeletal grains have both been transported from their subaqueous origins into the subaerial environments, where they mixed with quartz and feldspar sands, all of them undergoing eolian sorting and transport processes. This process is common at the interface of eolian and aquatic settings in the modern Persian Gulf (Loreau and Purser, 1973). The Khor-al-Bazm lagoon near Abu Dhabi in the United Arab Emirates provides a natural laboratory where this process can be studied (Kendall, 1969a). Large barrier islands are separated by tidal channels where ooids form and accumulate (Loreau and Purser, 1973). During low tide, channel levees rich in ooids dessicate in exceedingly high temperatures (>50^0 C). Wind blows these low density ooids onto adjacent barrier islands.

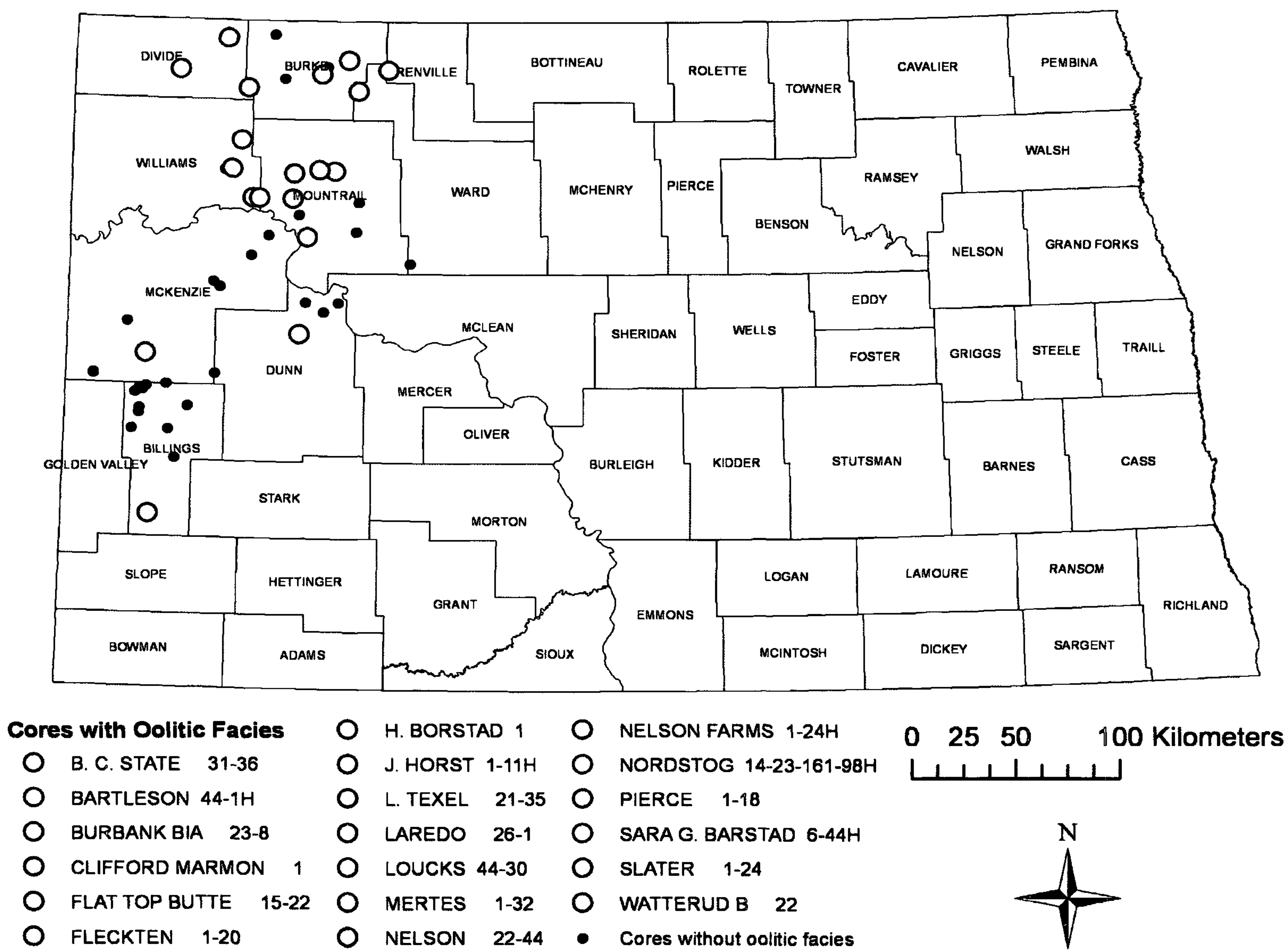

Figure 3.5. Map of North Dakota showing locations of analyzed cores.

Both gravity faulting and slump structures have been observed on the slip faces of both modern and ancient dunes (Gripp, 1961; Harms, 1969). Reineck and Singh (1975) suggest that besides the normal processes of avalanching on dune faces, moisture plays an important role in formation of deformation structures in modern eolian sand dunes. Based on the predominance of broken ooids and eolian transport bedforms, the interpreted environment of deposition for this facies is coastal dunes on a barrier island complex.

Based on eolian deposit classification and sedimentary processes defined in Hunter (1977), this facies is divided into 3 sub-facies which can be easily identified in core samples.

3.4.1.0 Subfacies B1: Traction Deposits

Description

This facies consists of grey-white, well indurated, dolomitic, fine-grained, ooid-rich quartz sandstones showing several types of ripples and cross stratification. Trough cross-stratified sandstones are composed of 1.3-1.7 cm thick laminae of darker colored, well-sorted broken ooids and crinoid fragments 2.5-2.0 φ in size, separated by 1-2 mm thick laminae of lighter colored quartz grains 3.5-3.0 φ in size (Fig. 3.6B). The beds are inclined at an angle of approximately 28 degrees with respect to the underlying reactivation surface and sharp contacts separate individual laminae.

Foreset cross-laminated sandstones have a cross-set thickness of 6 cm, laminae of broken ooids, crinoids and quartz grains dipping at an angle of approximately 12 degrees. Individual laminae are 1-2mm in thickness. Figure 3.7A shows a homogeneous, planar, solitary cross set between subcritical climbing translatent stratification and overlying apparently massive bedding in the sense of Allen (1963).

Truncated ripple-foreset cross-laminated sandstones show subcritical climbing ripple sets which attain a thickness of 1.2 cm. Dark ripple laminae are composed of broken ooids and crinoids whereas lighter laminae are predominantly quartz grains. The depositional dip of the ripples is approximately 8 degrees (Fig. 3.7C). Diagenetic overprint of pyrite can be observed in this facies.

Subcritical climbing translatent stratified sandstones are characterized by 1-2 mm thick laminae of white quartz grains interlaminated with broken ooids and skeletal grains. Subtle reverse faulting can be observed in this facies in the B.C. State 36-31 H well.

Interpretation

Based on the distinct interlamination of oolitic-skeletal clasts with thin laminae of quartz grains, and sharp contacts between laminae, this lithofacies is interpreted as eolian traction deposits in the sense of Hunter (1977).

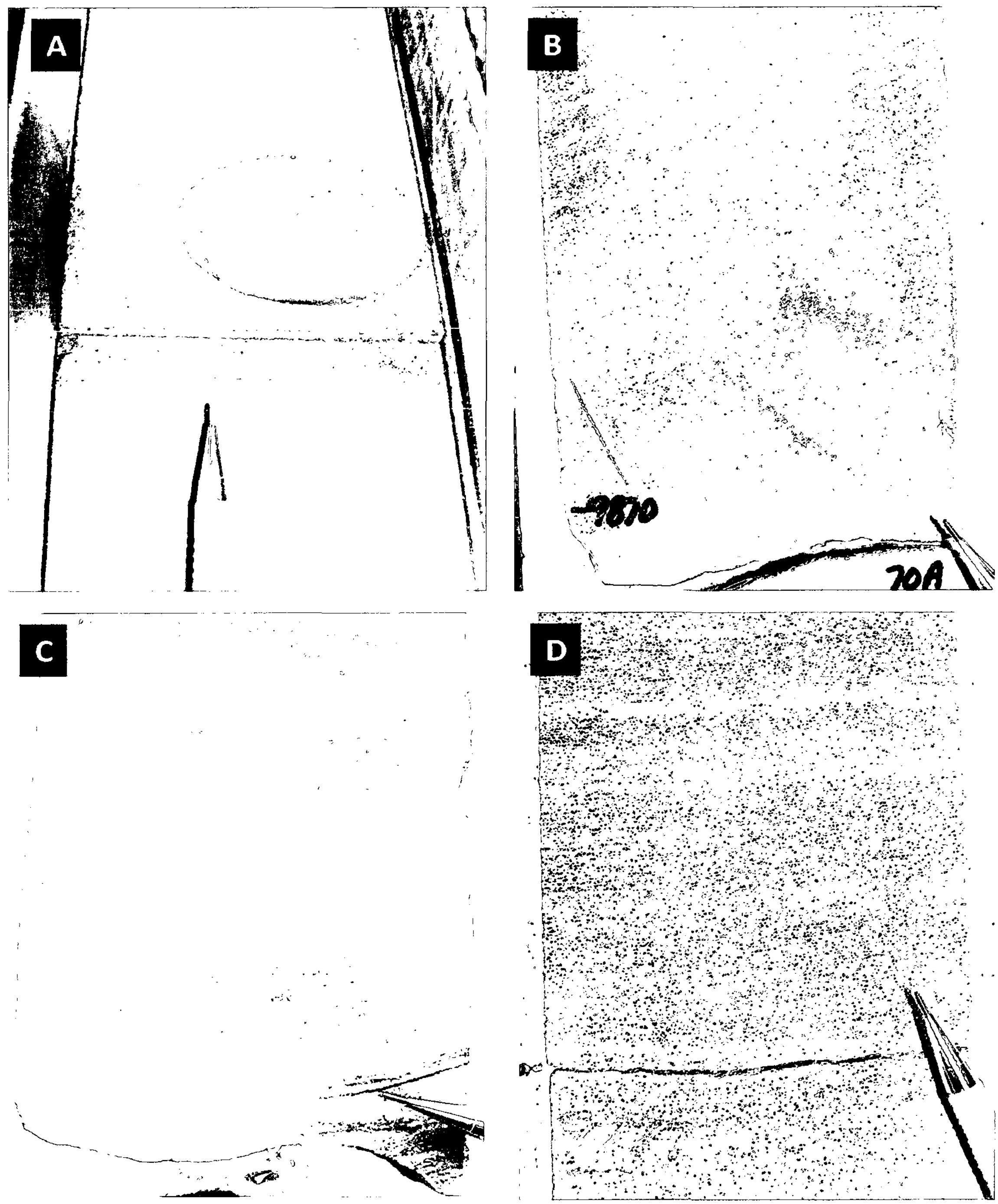

Figure 3.6. A) Sharp erosional contact at the base of sandstone (Ansbro Loucks: 7657 feet) B) Trough cross stratification C) Sandflow cross stratification D) Climbing translatent stratification

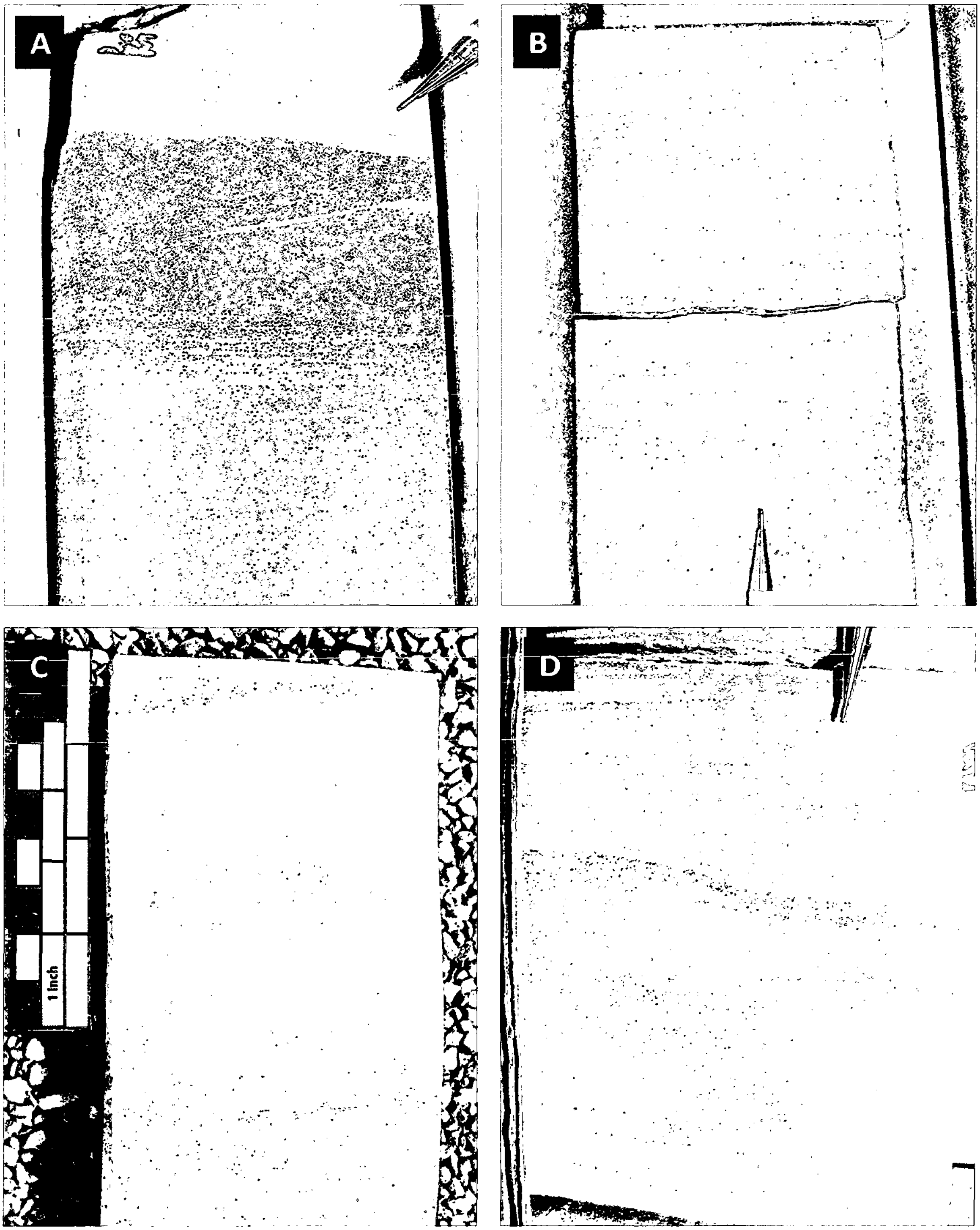

Figure 3.7. A) Foreset cross lamination B) Grainfall lamination C) Truncated ripple cross lamination D) Slump structures (Photo C reproduced from North Dakota Geological Survey web-page)

The alternation between quartz and carbonate grains can be produced in one of two ways. Bagnold (1941) suggested that the segregation of grain sizes occurs through differential transport during periodic episodes of wind activity. Smaller grains outpace larger ones, creating alternating laminae of different sized grains. Sharp (1963, 1966) proposed that the grain size segregation is produced by the interstitial settling of finer grains through a framework of larger grains. The steep dip of the cross-laminae indicates proximity to the dune crest (McKee and Tibbitts, 1964; McKee, 1966).

Planar foreset cross-lamination in well sorted sandstones can occur in eolian environments where sand is carried in suspension (Reineck and Singh, 1975). Therefore, the environment of deposition for this facies was probably along the slip face of eolian dunes.

3.4.1.1 Subfacies B2: Grainflow Deposits

Description

This sub-facies consists of sandflow cross-stratified, ooid-rich quartz sandstones. A distinct sand trough 3 cm in depth is filled with lighter colored sand and occurs between darker sub-parallel laminae that are 3-5 mm in thickness (Fig. 3.6C). The lower contact of the sand-filled trough is irregular and concave-up and is lined with darker ooid-skeletal grains, whereas the upper contact appears to be sharp and horizontal. The fill of the sand trough lacks lamination. Skeletal fragments in this facies are dominated by crinoids, whereas ooids are either broken or fragmentary.

Interpretation

The presence of sandflow cross-stratification, absence of bioturbation and skeletal fragments in well sorted fine-grained arenites suggests that this facies was deposited in an eolian environment. Sandflow cross-stratification forms during slump degeneration along lee faces of modern eolian sand dunes (Hunter, 1977). The morphology of the sand trough and its fill shows a cross section through a sand tongue (Fig. 3.6C, 3.9). Therefore, this facies represents avalanche deposits along the slip-face of an eolian dune.

3.4.1.2 Subfacies B3: Grainfall Deposits

Description

This facies consists of grainfall laminated ooid-rich sandstones with laminae that are normally graded with lighter colored quartz grains on the bottom grading into darker coarser broken ooids and crinoids towards the top. Individual laminae are approximately 1.5 cm thick and show dips around 3 degrees. Reactivation surfaces are common within cross sets (Fig. 3.6B).

Interpretation

Grainfall lamination occurs in zones of flow separation along the lee face of dunes (Hunter, 1977). It is produced by the settling of suspended grains on smooth depositional surfaces. In recent dunes depositional dip angles tend to be steep (20-28 degrees), but preservation of these is rare due to destruction by sand flows shortly after deposition. Therefore, most preserved grainfall laminated deposits tend to have lower dip angles (McKee et al, 1971). The normal grading associated within laminae may have been caused by fluctuations in transporting power (Otto, 1938). The presence of several reactivation surfaces supports the idea of fluctuating energy levels in the system during deposition.

Discussion

Eolian dune fields are distributed on the coast as well as barrier islands in the Persian Gulf (Kukal and Saadallah, 1973; Alsharhan and Kendall, 2003). Although these dunes consist mainly of miliolid and quartz sand (Shinn, 1973), those forming on barrier islands adjacent to tidal channels contain ooids (Loreau and Purser, 1973). Dodd et al. (1993) provided guidelines for distinguishing

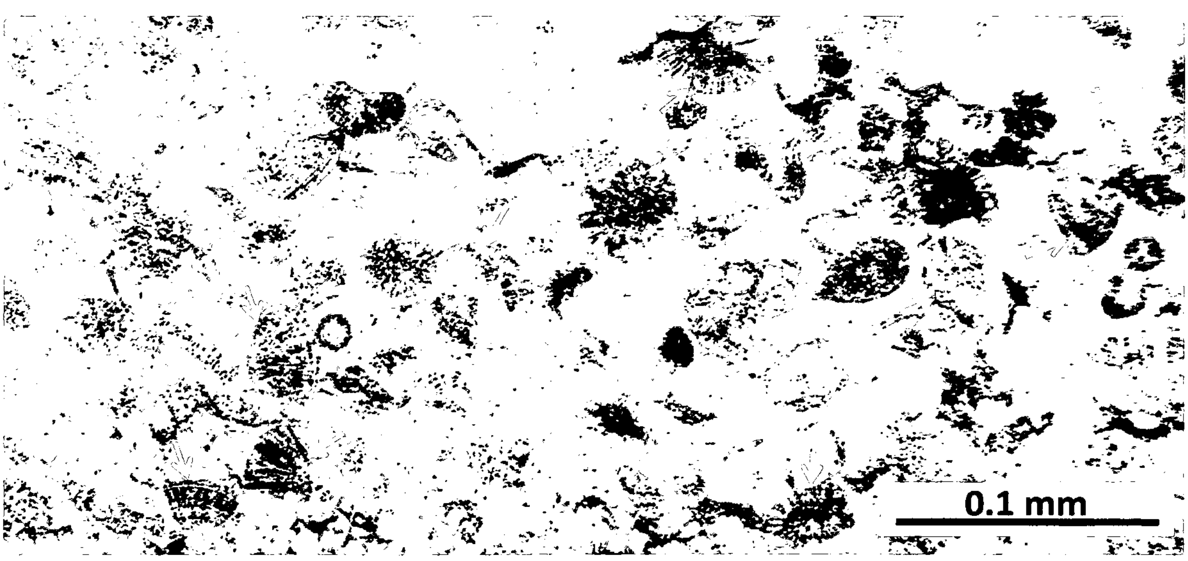

Figure 3.8. Photomicrograph of a Facies B sample from Clarion Resources Slater-1-24 (depth = 7928 feet). Red arrows point towards broken ooids.

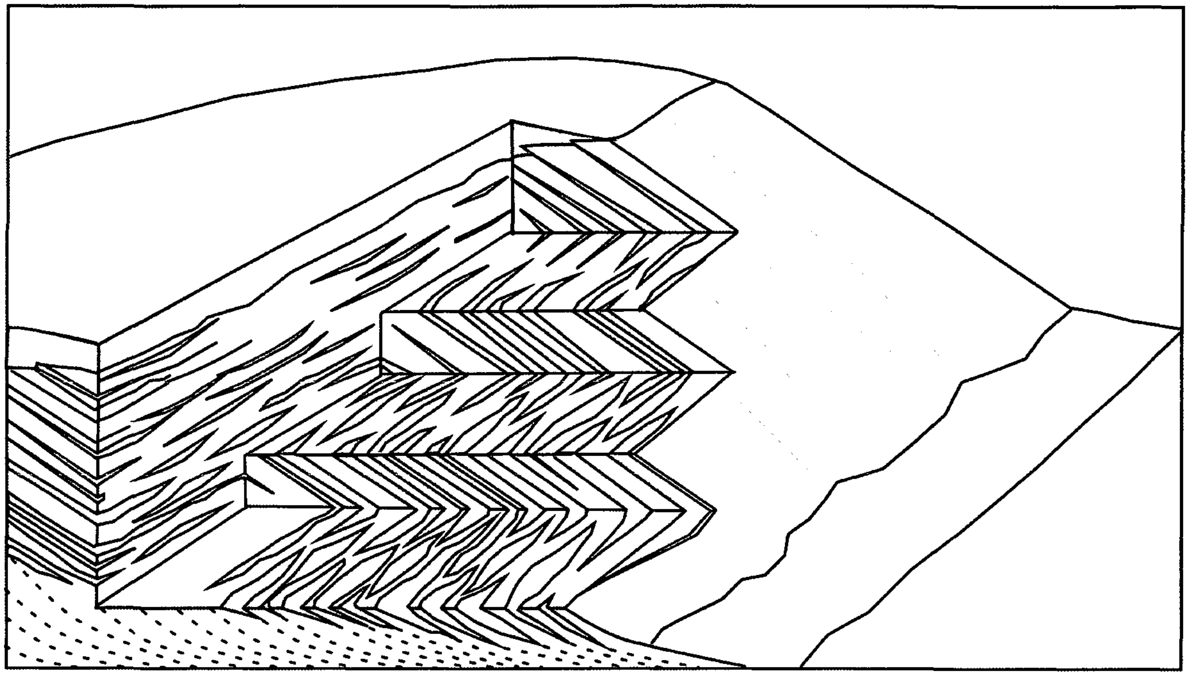

Figure 3.9. Schematic block diagram showing structure of simple cone-shaped sandflow cross-strata in a small dune (1 m high). Sandflow cross-strata are in grey. (Modified from Hunter, 1977)

eolian from marine ooid accumulations in ancient strata. Facies B was investigated in detail in order to compare interpreted eolianites from the Bakken with diagnostic characteristics of modern settings provided in Dodd et al. (1993). The eolianites of the Bakken Formation contain abundant quartz, broken ooids, diverse grain assemblage, are poorly sorted, and show a marked absence of large grains, all of which are diagnostic of eolianites (Dodd et al., 1993). Figure (3.10A, 3.10B) compares thin section scans from a subaqueous ooid grainstone of Facies A and the eolian Facies B. Unlike the homogeneous subaqueous grainstone, the eolianites show distinct laminae at the thin-section scale. Inverse grading of the eolianites is attributed to eolian processes in climbing translatent strata (Hunter, 1977). Inverse grading of this particular type is not observed in marine grainstone, therefore the presence of lamination at a thin section scale is another feature of eolianites (Dodd et al., 1993). There is a possibility that complete ooids were transported to an eolian environment where grain collisions in air cause ooids to shatter, and these ooids were then transported back to a subaqueous realm. However, as demonstrated by Esteban and Pray (1983), broken grains will develop subsequent coats once submerged in calcite-rich marine water. A rare condition occurs in tidal channels along the modern coast of Kuwait along Kadmah Bay where uncoated quartz grains occur with ooids (Fig. 3.10C). This mixing occurs during low-tide in the summers when oolitic tidal channels and bars are exposed to high (>50^0 C) temperatures (Al-Zaidan et al., 2006, Al-Zamel et al., 2007). The tops of bars dessicate and wind transports quartz sand from nearby coppice dunes on the bars, and current ripples form (Al-Hurban and Hersi, 2008). Thin-sections were collected from the tops of these bars during low-tide and compared with the interpreted eolianites from Bakken Formation. Unlike the Bakken eolianites, these samples still contain a majority of ooids (>80%) with rare (<3%) uncoated quartz grains. Most quartz grains in the sample show a superficial micritic coat (Fig. 3.10D). None of the ooids in the modern samples from Kuwait are broken and only show abrasion on the outermost cortical lamella. Therefore, it is highly improbable that the broken ooids and associated quartz grains of Facies B were deposited in a subaqueous setting.

The modern eolianites of the Persian Gulf develop in an arid environment (Shinn, 1973). As the Williston Basin was near the Equator during the deposition of the Bakken Formation, the paleoclimate was likely humid tropical (Blakey, 2007).However, coastal eolian deposits are known from modern temperate and tropical environments as well (McLaren, 2004). Therefore, even if the climate was different between the modern Persian Gulf and the Williston Basin during the Early Mississippian, it would not affect the physical processes needed for eolianite formation.

Thin beds of eolian sandstone Facies B can be intercalated with or show a gradational contact to clearly subtidal, bioturbated siltstones within the Middle Bakken Member, nicely shown in the Texakota Inc well H. Borstad No. 1 core (Fig. 3.11). Although this close association of marine and eolian facies seems to call into question the purely wind-lain interpretation of the Facies B sandstones, this facies combination may well be the result of storm reworking. Sedgwick and Davis (2003) documented similar alternating mud-free coarse sands and marine sediment in cores from the west coast of Florida. These cores were collected from barrier islands along a storm-dominated coastline, and the interbedded marine and barrier island sediments record washover events. Washover fans are also common on barrier islands in the Persian Gulf along the coast of Saudi Arabia (Fig. 3.12). It is therefore likely that these sand-shale intercalations in Facies B of the Middle Bakken Formation represent washover events across barrier islands. This interpretation is further supported by the fact that the marine siltstone associated with the reworked eolianite sands shows hummocky cross-stratification, which indicates storms (Aigner 1985).

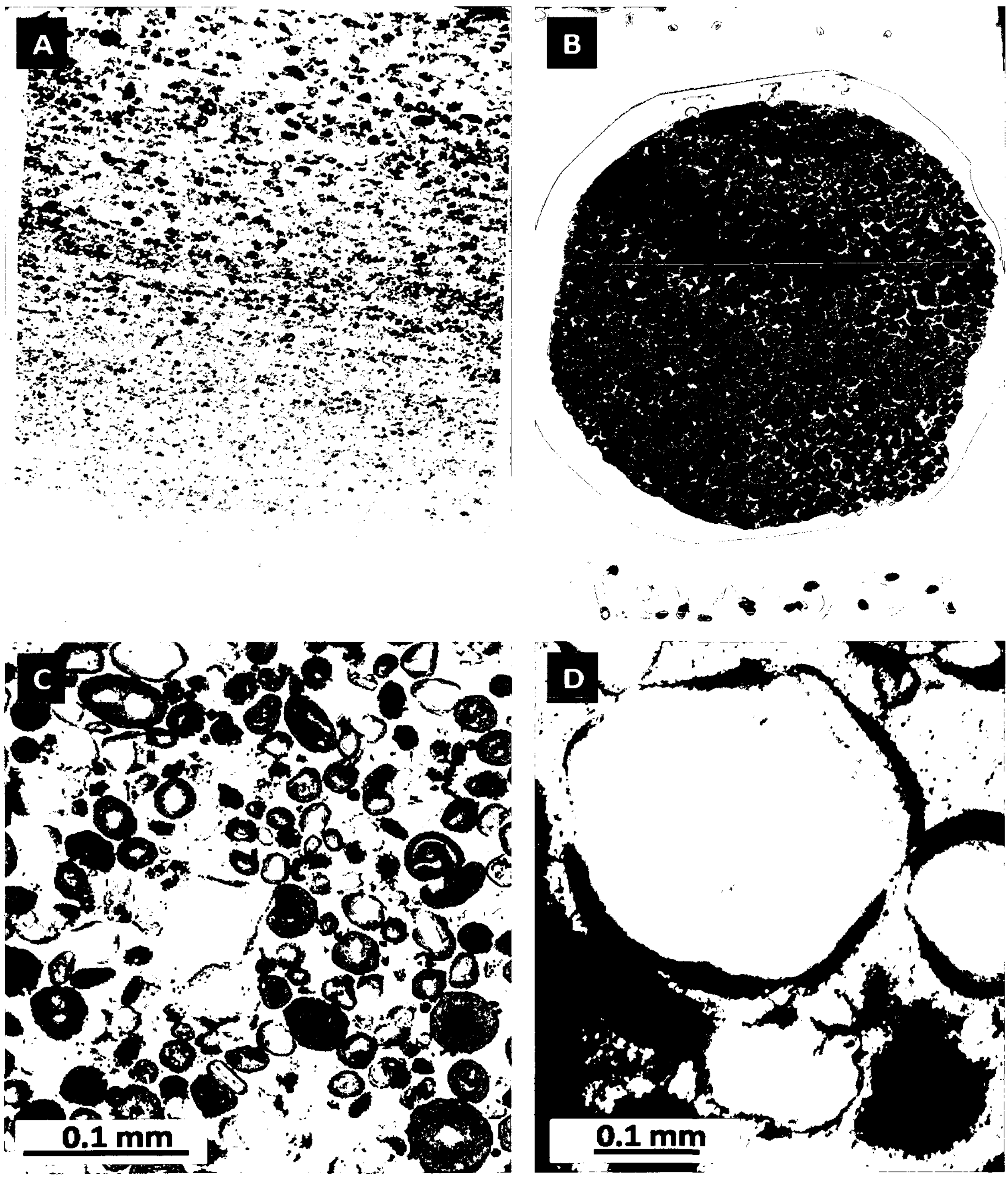

Figure 3.10. A) Laminated Eolianite of Facies B, note the distinct inverse grading B) Sub-aqueous non-laminated Facies A C) Recent ooids from Kuwait showing several quartz grains D) A close-up view of a Quartz grain with superficial coat from Kuwait.

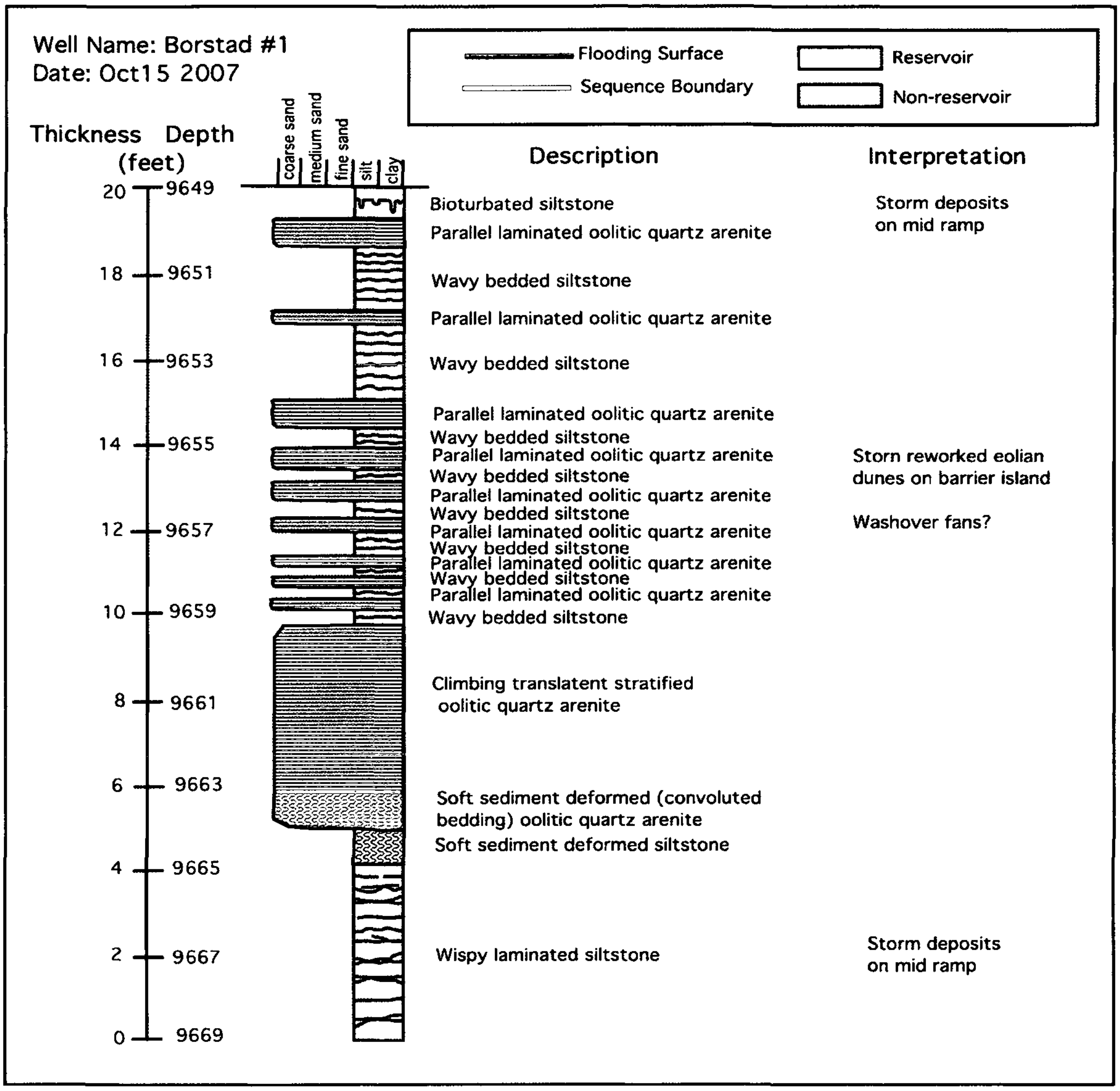

Figure 3.11. Note the sandstone-sitlstone intercalations at the top pf the section. Texakota In Borstad No 1 (Depth 9669-9649 feet/2930-2923 m).

Figure 3.12. Washover fans on a barrier island along the coast of Saudi Arabia. The island is covered with halophytes growing on eolian dunes.

3.4.2 Facies C

Description

This facies is a brown, well-indurated, trough cross-stratified, ooid dolograinstone and was only observed in the Tenneco Oil Company Graham USA 15-1 well between depths of 10,375 feet/3144 m and 10,373 feet/3143 m. The facies is characterized by a sharp base and forms a scour surface with underlying dolowackestones of the Devonian Three Forks Formation (Fig.

3.13B). The upper contact is also sharp with an overlying skeletal wackestone of the Bakken Formation (Fig. 3.13B). A collection of poorly sorted angular to sub-angular 1-2 cm sized black shale and pyritized clasts rests on top of the scour surface. Three subtle small-scale (<30 cm) trough cross-sets cut parallel to depositional dip can observed (Fig. 3.13A). Isolated shells of gastropods occur at the base of cross strata sets. The facies appears to be homogeneous in core, and individual cross-strata set laminae are visible due to undulating contacts lined with dark recrystallized calcareous algae. Recrystallization by calcite cement has obliterated the original internal structure, which makes the taxonomic affinity of algae unclear. However, the overall discoidal to tubular shape suggest that they are marine green algae (Chlorophyta). Ooids make up 60 percent of the facies and display a recurring pattern in lamination along with algal and skeletal fragments (Fig. 3.13C). Individual laminae are approximately 1 cm thick and boundaries are lined with imbricated fragments of green algae which make up 30 percent of the grains.

The sedimentary fabric is grain-supported and individual laminae have subtle normal grading of oolitic and skeletal grains. Partially mimetic dolomitization in this facies has left ooid ghosts, but destroyed their internal structure. The external morphology of ooid ghosts shows complete, symmetric ooids of varying sizes and well developed cortical lamellae. Skeletal grains make up 10 percent of the grains and include imbricated crinoidal fragments. There are three distinct lamination patterns. The first includes only very large (1-2 mm) ooids, skeletal grains, and algal fragments showing moderate sorting, and poor packing. The second pattern shows primarily tightly-packed ooids of varying sizes in normal graded lamina. The third shows very small (<1mm) and large ooids with poorly developed normal grading. These 3 distinct patterns are cyclic throughout the facies (Fig. 3.13C).

Interpretation

The scour surface and associated lag at the base of the facies, along with an increase in grain size, is interpreted as a rapid change towards higher energy conditions from low energy conditions prevalent in underlying dolowackestones. The absence of the Lower Bakken Shale and incision of this facies into the underlying Three Forks Formation reflects a significant depositional hiatus. The angular shale clasts in the gravel lag at the base may well have been derived from the erosion of the now absent Lower Bakken Shale. The presence of small-scale trough cross strata sets indicates deposition from a lower-flow regime current (Simons et al., 1965; Simons and Richardson, 1966; Allen 1968). The arrangement of these facies and erosional structures showing a basal scour surface, lined with lag deposits and overlain by megaripples, reflects a significant decrease in energy during deposition. The ooids and algal clasts that make up the sedimentary structures have formed in a shallow-water, high-energy marine environment. Although core data are largely one-dimensional and therefore do not allow the integration of sediment geometries, the combination of facies and sedimentary structures suggests that this succession likely represents a channel fill (Allen, 1965; Williams and Rust, 1969; Allen, 1982; Bridge and Tye, 2000), likely from a tidal environment. This is in agreement with data from the recent Persian Gulf where ooids accumulate in tidal channels (see Chapter 4), and green algae and sea grass locally stabilize the ooid dunes during quiescent periods (Evans et al., 1973). When the dunes are reactivated, the green algae will be eroded and incorporated along bedding planes in the ooid dunes; sea grass, however, is a Cenozoic plant that was not present in Paleozoic marine environments (cf. Wright and Azeredo, 2006). The fact that this type of succession is only rarely observed in the Middle Bakken is another argument supporting the tidal channel interpretation. Volumetrically, tidal channels make up only a very small portion of a succession, especially in the Bakken where most of the succession is subtidal. Therefore, the chance of penetrating a tidal channel within the Middle Bakken has to be considered extremely low, which explains the presence of just a single core exhibiting this facies. Internally, this tidal channel fill shows the combination of a variety of processes which are reflected in the three types of grain arrangement that characterize individual laminae. Channel mesoforms such as dunes are controlled by boundary layer thickness or flow depth (Bridge, 2003). Therefore, an empirical relationship exists between the thickness of cross-strata sets and the depth of the channel in which they form. Leclair and Bridge (2001) developed a series of mathematical equations that express this relationship for medium-scale (>0.3 m) cross strata. The equations can be modified and applied to small-scale cross strata in tidal channel cross-st-

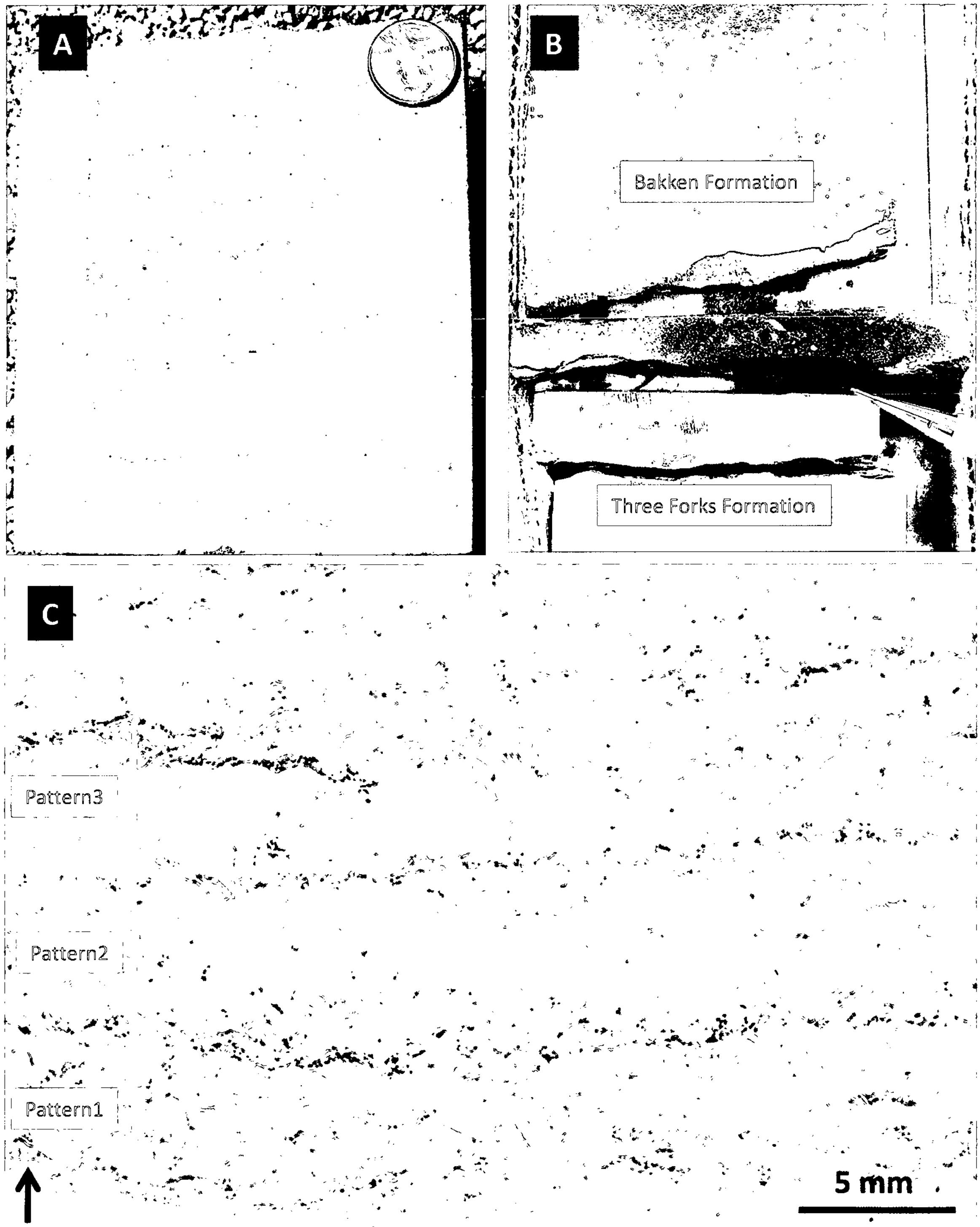

Figure 3.13. A) Trough cross-strata in core B) Scour surface and lag at base of facies C) Thin-section scan showing algal fragments (arrows) and lamination patterns

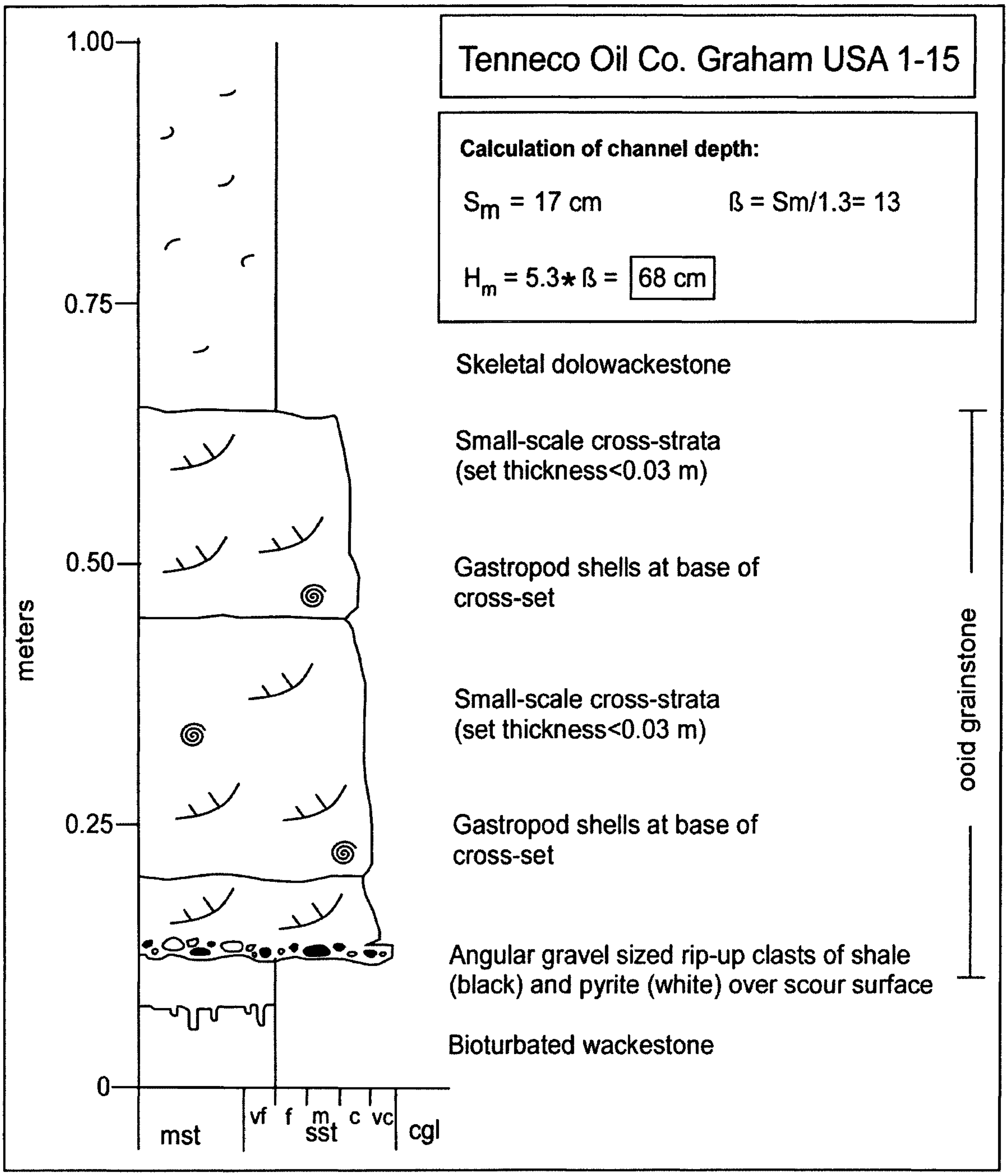

Figure 3.14. Sedimentological log of facies C showing cross-strata set thickness and channel depth calculation.

-rata (Written communication, Bridge, 2009). The cross-strata set thicknesses of this facies were used to calculate channel depth using these equations (Fig. 3.14). A channel depth of 0.63 meters was obtained for a channel at high tide, which is a value common for modern ooid-filled tidal channels in the UAE and Qatar (Loreau and Purser, 1973; Shinn, 1973).

3.5 Discussion

Layer-cake models are commonly applied to the stratigraphy of the Bakken Formation (Sperr, 1990; Canter et al., 2009). Following this overly simplistic approach would predict laterally continuous sheet-like sediment bodies across the Williston Basin. There are two levels of complexity associated with the stratigraphy of the Bakken Formation that restrict the usage of layer-cake models: (1) Analyses of cores from the Bakken Formation reveal abnormal facies associations, flooding surfaces, and scouring into the underlying Three Forks Formation (Fig. 3.13B). Although the creation of a detailed sequence stratigraphic model was not the aim of this study, the presence of key sequence stratigraphic surfaces implies relative sea-level changes during the sedimentation of the Bakken Formation. Sea-level changes can produce a variety of stratal stacking patterns, none of which can be characterized as layer-cake (Hunt and Tucker 1992; Posamentier and Morris, 2000; Plint and Nummedal 2000). (2) Oolitic facies occur in only 21 of 40 cores studied. The absence of oolitic facies in some cores exemplifies the discontinuous nature of lithofacies within the Bakken Formation. The distribution of oolitic facies within the Bakken does not render a clearly predictable pattern. Oolitic facies were documented in cores from wells that are close to the margins as well as in the interior of the basin. Depositional environments interpreted for oolitic facies in the Middle Bakken Member do not show sheet-like geometries in equivalent modern ramp settings (Table 3.0).

Most operators target Facies B for hydrocarbon exploitation through horizontal drilling. The most likely environment of deposition for this facies was dune fields on barrier islands. Barrier islands occur primarily in transgressive strata and form distinct retrograding sand packages (Rampino and Sanders, 1981). Cattaneo and Steel (2003) provided several models of sand-body architecture in transgressive deposits. The examples they cite show a large variation and complexity in the spatial arrangement of these deposits. Similar geometries should be expected for the transgressive ooid-rich sandstones of the Middle Bakken Member. Future horizontal well planning should consider the issues of lateral continuity and compartmentalization in these eolianites.

Barrier islands on attached shelves along the western Atlantic and in the Gulf of Mexico tend to form shore-parallel longitudinal sand bodies (Sanders and Kumar, 1975; Davis et al., 2003; Sedgwick and Davis, 2003). However, barrier island complexes on low relief ramps such as the Persian Gulf tend to form distinct blocky or T-shaped islands (Kendall, 1969b; Alsharhan, 2003; Kendall, 2008). Because deposition of the Bakken Formation occurred in a shallow epeiric sea, sand-body geometries should resemble those of the Persian Gulf. Therefore, horizontal drilling into these packages should target these bodies in a shore-perpendicular direction, after detailed mapping of retrograding parasequences.

Bakken Oolitic Facies	Description	Thickness (m)	Modern Analogs	Geometry	Orientation	Dimensions
Facies A	Trough cross-stratified ooid grainstone with sharp upper and lower contacts. Bimodal, radial, symmetric, ooid distribution.	0.20	Coastal Embayments	Ribbons	Shore parallel	Area Min: 7.2 km^2 Max: 46.23 km^2 Avg: 20.54 km^2 Length Min: 14 km Max: 31 km Avg: 23 km Width Min: 0.62 km Max: 3.0 km Avg: 1.35 km
Facies B	Ooid-rich, fine grained quartz sandstones showing traction, grainfall, and grainflow. Abundant broken ooids.	4.0-6.0	Eolian dunes on barrier islands	Variable	Shore perpendicular	Area Min: 2.3 km^2 Max: 296 km^2 Stacking Retrogradational parasequences
Facies C	Trough cross-stratified ooid grainstone with erosional scour and rip-up clasts. Polymorphic radial ooids with algal fragments.	1.0	Tidal Channels	Ribbons	Variable	Sinuosity Min: 1.0 Max: 1.63 km Length Min: <1km Max: 24 km Width Min: 0.5 m Max: 430 m Depth Min: 0.30 m Max: 5 m

Table 3.0. Summary of oolitic facies based on Bakken Formation core analysis and modern Persian Gulf.

3.6 Conclusions

Layer-cake stratigraphy models have been repeatedly applied to the Mississippian Bakken Formation in North Dakota (Sperr, 1990; Canter et al., 2009). These models lack the detail required for successful exploitation of hydrocarbons from reservoirs within the Middle Bakken Member. This paper focuses on the oolitic facies within this formation, including the 'Middle Bakken Dolomite.'

1. Oolitic facies include deposition in coastal embayments in the sense of Loreau and Purser (1973), eolian dunes on barrier islands, and tidal channels. Coastal Embayments form elongate, shore-parallel sand bodies that range in width from 0.62-3 km (avg = 1.35 km) and lengths between 14-31 km (avg = 23 km) along the proximal end of a carbonate ramp in the Persian Gulf. Preserved porosity in the Middle Bakken Member from comparable facies amounts to around 2 percent.

Barrier islands in the Persian Gulf are uncommon and form mainly along the Trucial Coast. Here they form a series of blocky, T-shaped islands and are covered with eolian dunes (Kendall, 1969a; Alsharhan and Kendall, 2003; Kendall, 2008). These islands show a broad range in area (2.3-296 km^2). Due to the transgressive nature of these deposits, best practice would be mapping parasequences which contain these barrier island sandstones. Porosity of facies B from thin sections in the Middle Bakken Member averages around 3 percent. This is due to extensive dolomitization which tends to plug pores.

Tidal channels in the Persian Gulf show widths between 0.50 m in Kuwait and 430 meters along the Saudi coast. The maximum recorded length of channels is along the Trucial Coast, which can run up to 25 km from the coastline to terminal ebb deltas. Planform geometry of tidal channels can be described as meandering, braided, anastomosing and straight depending on whether channels (see Chapter 4) are observed during high or low tide and scale of observation. Channels documented in this study are oriented perpendicular, parallel or oblique to the shoreline. Extensive mimetic dolomitization has destroyed macroscopically visible porosity in observed thin sections of this facies.

2. The primary objective of this study was to highlight the heterogeneity in Bakken Formation stratigraphy though examples of oolitic facies. However, it should be noted that oolitic facies only occurred in 21 of 40 cores analyzed in this study. The stacking of these sandstones along with a detailed investigation of paleobathymmetry diagnostic ichnofossils could lead to a high-resolution sequence stratigraphic model. The development of such a model should be the primary concern of all oil and gas companies interested in hydrocarbon exploitation from the Bakken Formation.

3.7 Acknowledgements

This project was inspired through thoughtful discussions with Pat Medlock and the staff at Brigham Oil and Gas. We thank Brigham Oil and gas for contributing funding for the doctoral dissertation of which this paper is a part. We also wish to express our deepest gratitude to the staff at the North Dakota Geological Survey Core Lab and USGS Core Research Center in Denver. We would like to thank Julie LeFever and Joshua Hicks in particular. Fieldwork in Kuwait would not have been possible without logistical help provided by Wahab Sadeqi. An earlier version of this manuscript was improved from helpful reviews by John Ridley and Ellen Wohl. John Bridge was kind enough to provide equations that related cross-strata set thickness to channel depth.

3.8 References

Aigner, T., 1985, Storm depositional systems; dynamic stratigraphy in modern and ancient shallow-marine sequences Lecture notes in earth sciences: Federal Republic of Germany, Springer Verlag : Berlin, Federal Republic of Germany, p.174.

Al-Hurban, A. E., and Hersi, A. A., 2008, Sedimentomorphic mapping of Az-Zor escarpment, northern Kuwait, using GIS methods: Kuwait Journal of Science & Engineering, v. 35, p. 93-126.

Allen, J. R. L., 1963, The classification of cross-stratified units, with notes on their origin, Sedimentology: International, Blackwell: Oxford-Boston, International, p. 93-114.

-, 1965, A review of the origin and characteristics of recent alluvial sediments, Sedimentology: International, Blackwell: Oxford-Boston, International, p. 91-191.

-, 1968, Current Ripples: Their Relation to Patterns of Water and Sediment Motion: Amsterdam, Holland, North-Holland Publishing Co., 433 p.

-, 1982, Sedimentary structures, their character and physical basis; I: Netherlands, Elsevier Sci. Publ. Co.: Amsterdam, Netherlands.

Alsharhan, A. S., and Kendall, C. G. S. C., 2003, Holocene coastal carbonates and evaporites of the southern Arabian Gulf and their ancient analogues, Earth-Science Reviews: Netherlands, Elsevier : Amsterdam, Netherlands, p. 191-243.

Al-Zaidan, A. S. Y., Kennedy, H., Jones, D. A., and Al-Mohanna, S. Y., 2006, Role microbial mates in Sulaibikhat Bay (Kuwait) mudflat food webs: evidence from delta C-13 analysis: Marine Ecology- Progress Series, v. 308, p. 27-36.

Al-Zamel, A., Al-Sawari, M., and Khader, S., 2007, Coastal geomorphology, hydrodynamics, biolithofacies in the intertidal and subtidal areas of Umm Al-Namil Island, Kuwait Bay, Kuwait, Arabian Gulf: Arab Gulf Journal of Scientific Research, v. 23, p. 501-514.

Bagnold, R. A., 1941, The physics of blown sand and desert dunes: London, Methuen & Co. Ltd, 265 p.

Blakey, R., 2007, http://jan.ucc.nau.edu/~rcb7/

Bridge, J. S., 2003, Rivers and floodplains; forms, processes, and sedimentary record: United Kingdom, Blackwell Publishing: Oxford, United Kingdom.

Bridge, J. S., and Tye, R. S., 2000, Interpreting the dimensions of ancient fluvial channel bars, channels, and channel belts from wireline-logs and cores, AAPG Bulletin: United States, American Association of Petroleum Geologists : Tulsa, OK, United States, p. 1205-1228.

Canter, L.O., Skinner, O., Sonnenfield, M., 2008, Facies and Mechanical Stratigraphy of the Middle Bakken, Mountrail County, North Dakota, AAPG Rocky Mountain Section 2008 Technical program: Denver, USA.

Cantrell, D. L., 2006, Cortical fabrics of Upper Jurassic ooids, Arab Formation, Saudi Arabia; implications for original carbonate mineralogy, Sedimentary Geology: Netherlands, Elsevier : Amsterdam, Netherlands, p. 157-170.

Cattaneo, A., and Steel, R. J., 2003, Transgressive deposits; a review of their variability, Earth-Science Reviews: Netherlands, Elsevier: Amsterdam, Netherlands, p. 187-228.

Davies, P. J., Bubela, B., and Ferguson, J., 1978, The formation of ooids, Sedimentology: International, Blackwell: Oxford-Boston, International, p. 703-729.

Davis, R. A., Jr., Cuffe, C. K., Kowalski, K. A., and Shock, E. J., 2003, Stratigraphic models for microtidal tidal deltas; examples from the Florida Gulf Coast, Marine Geology: Netherlands, Elsevier : Amsterdam, Netherlands, p. 49-60.

Dodd, J. R., Zuppann, C. W., Harris, C. D., Leonard, K. W., and Brown, T. W., 1993, Petrologic method for distinguishing eolian and marine grainstones, Ste. Genevieve Limestone (Mississippian) of Indiana, *in* Keith, B. D., and Zuppann, C. W., eds., AAPG Studies in Geology: United States, American Association of Petroleum Geologists : Tulsa, OK, United States, p. 49-59.

Donahue, J., 1969, Genesis of oolite and pisolite grains; an energy index, Journal of Sedimentary Petrology: United States, Society of Economic Paleontologists and Mineralogists : Tulsa, OK, United States, p. 1399-1411.

Dumonceaux, G. M., 1984, Stratigraphy and depositional environments of the Three Forks Formation (Upper Devonian), Williston Basin, North Dakota: University of North Dakota, 189 p.

Esteban, M., and Pray, L. C., 1983, Pisoids and pisolite facies (Permian), Guadalupe Mountains, New Mexico and West Texas: Federal Republic of Germany, Springer-Verlag : Berlin, Federal Republic of Germany, 503-537 p.

Evans, G., Murray, J. W., Biggs, H. E. J., Bate, R., and Bush, P. R., 1973, The Oceanography, Ecology, Sedimentology and Geomorphology of Parts of the Trucial Coast Barrier Island Complex, Persian Gulf: Federal Republic of Germany, Springer-Verlag, New York, 233-277 p.

Fabricius, F. H., 1977, Geological history of the eastern Mediterranean since late Miocene, Rapports et Proces Verbaux des Reunions - Commission Internationale pour l'Exploration Scientifique de la Mer Mediterranee: France, Commission Internationale pour l'Exploration Scientifique de la Mer Mediterranee : Paris, France, p. 109-110.

Fluegel, E., 2004, Microfacies of carbonate rocks; analysis, interpretation and application: Federal Republic of Germany, Springer: Berlin, Federal Republic of Germany, 976 p.

Frishman, S. A., and Behrens, E. W., 1969, Geochemistry of oolites, Baffin Bay, Texas, Abstracts with Programs - Geological Society of America: United States, Geological Society of America (GSA) : Boulder, CO, United States, p. 71-71.

Gerhard, L. C., Anderson, S. B., Carlson, C. G., and LeFever, J. A., 1982, Geological development, origin, and energy resources of the Williston Basin, North Dakota: AAPG Bulletin, v. 66, no. 8, p. 989-1020.

Glennie, K. W., 1970, Developments in SedimentologyDesert sedimentary environments, Developments in Sedimentology: Netherlands, Elsevier : Amsterdam-Oxford-New York, Netherlands.

Gripp, K., 1961, Ueber den Abtrag durch Rippelfelder, Neues Jahrbuch fuer Geologie und Palaeontologie. Monatshefte: Federal Republic of Germany, E. Schweizerbart'sche Verlagsbuchhandlung : Stuttgart, Federal Republic of Germany, p. 474-477.

Harms, J. C., 1969, Hydraulic significance of some sand ripples, Geological Society of America Bulletin: United States, Geological Society of America (GSA) : Boulder, CO, United States, p. 363-396.

Hunt, D., and Tucker, M. E., 1992, Stranded parasequences and the forced regressive wedge systems tract; deposition during base-level fall, Sedimentary Geology: Netherlands, Elsevier : Amsterdam, Netherlands, p. 1-9.

Hunter, R. E., 1977, Basic types of stratification in small eolian dunes, Sedimentology: International, Blackwell : Oxford-Boston, International, p. 361-387.

Kahle, C. F., 1974, Ooids from Great Salt Lake, Utah, as an analogue for the genesis and diagenesis of ooids in marine limestones, Journal of Sedimentary Petrology: United States, Society of Economic Paleontologists and Mineralogists : Tulsa, OK, United States, p. 30-39.

Kassler, P., 1973, The Structural and Geomorphic Evolution of the Persian Gulf: Federal Republic of Germany, Springer-Verlag, New York, 11-32 p.

Kendall, C. G. S. C., 2009, http://strata.geol.sc.edu/

-, 2008, First view of the cyanobacterial mats and strandline evaporite/carbonate deposits of Abu Dhabi; a personal retrospective, GeoArabia [Manama]: Bahrain, Gulf Petrolink in Bahrain: Manama, Bahrain, p. 156-157.

-, 1969a, Geomorphology of a recent shallow-water carbonate province; Khor Al Bazam, Trucial Coast, southwest Persian Gulf, *in* Skipwith, P. A. d. E., ed., Geological Society of America Bulletin: United States, Geological Society of America (GSA) : Boulder, CO, United States, p. 865-891.

-, 1969b, Holocene shallow-water carbonate and evaporite sediments of Khor al Bazam, Abu Dhabi, southwest Persian Gulf, *in* Skipwith, S. P. A. D. e., ed., American Association of Petroleum Geologists Bulletin: United States, American Association of Petroleum Geologists : Tulsa, OK, United States, p. 841-869.

Kent, D. M., and Christopher, J. E., 1994, Geological history of the Williston Basin and Sweetgrass Arch, *in* Mossop, G. D., and Shetson, I., eds., Geological atlas of the western Canada sedimentary basin: Calgary, AB, Canada, Canadian Society of Petroleum Geologists and Alberta Research Council.

Kukal, Z., and Saadallah, A., 1973, Aeolian Admixtures in the Sediments of the Northern Persian Gulf: Federal Republic of Germany, Springer-Verlag, New York, 115-121 p.

Leclair, S. F., and Bridge, J. S., 2001, Quantitative interpretation of sedimentary structures formed by river dunes, Journal of Sedimentary Research: United States, Society of Economic Paleontologists and Mineralogists: Tulsa, OK, United States, p. 713-716.

LeFever, J. A., 1991, History of Oil Production from the Bakken Formation, North Dakota, *in* Hansen, W. B., ed., 1991 Guidebook to Geology and Horizontal Drilling of the Bakken Formation: Billings, MT, Montana Geological Society, p. 3-17.

Loreau, J. P., and Purser, B. H., 1973, Distribution and Ultrastructure of Holocene Ooids in the Persian Gulf: Federal Republic of Germany, Springer-Verlag, New York, 279-328 p.

McKee, E. D., 1966, SedimentologyStructures of dunes at White Sands National Monument, New Mexico (and a comparison with structures of dunes from other selected areas), Sedimentology: International, Blackwell : Oxford-Boston, International.

McKee, E. D., Douglass, J. R., and Rittenhouse, S., 1971, Deformation of lee-side laminae in eolian dunes, Geological Society of America Bulletin: United States, Geological Society of America (GSA) : Boulder, CO, United States, p. 359-378.

McKee, E. D., and Tibbitts, J. G. C., 1964, Primary structures of a seif dune and associated deposits in Libya, Journal of Sedimentary Petrology: United States, Society of Economic Paleontologists and Mineralogists : Tulsa, OK, United States, p. 5-17.

McLaren, S. J., 2004, Late Quaternary vadose carbonate diagenesis in coastal and desert dune and beach sands; Is there a palaeoclimatic signal?, *in* Gardner, R., ed., Earth Surface Processes and Landforms: United Kingdom, Wiley & Sons : Chichester, United Kingdom, p. 1441-1458.

Otto, G. H., 1938, The sedimentation unit and its use in field sampling, Journal of Geology: United States, University of Chicago Press : Chicago, IL, United States, p. 569-582.

Pitman, J. K., Price, L. C., and LeFever, J. A., 2001, Diagenesis and fracture development in the Bakken Formation, Williston Basin: Implications for reservoir quality in the Middle Member: U.S. Geological Survey Professional Paper, no. 1613.

Plint, A. G., and Nummedal, D., 2000, The falling stage systems tract; recognition and importance in sequence stratigraphic analysis, Geological Society Special Publications: United Kingdom, Geological Society of London : London, United Kingdom, p. 1-17.

Pollastro, R. M., 2008, Fact Sheet - U. S. Geological SurveyAssessment of undiscovered oil resources in the Devonian-Mississippian Bakken Formation, Williston Basin Province, Montana and North Dakota, 2008, *in* Cook, T. A., Roberts, L. N. R., Schenk, C. J., Lewan, M. D., Anna, L. O., Gaswirth, S. B., Lillis, P. G., Klett, T. R., and Charpentier, R. R., eds., Fact Sheet - U. S. Geological Survey: United States, U. S. Geological Survey : Reston, VA, United States.

Posamentier, H. W., and Morris, W. R., 2000, Aspects of the stratal architecture of forced regressive deposits, Geological Society Special Publications: United Kingdom, Geological Society of London : London, United Kingdom, p. 19-46.

Purser, B. H., 1973, The Persian Gulf: New York - Heidelburg - Berlin, Springer-Verlag, p. 471.

Purser, B. H., and Loreau, J. P., 1973, Aragonitic, Supratidal Encrustations on the Trucial Coast, Persian Gulf: Federal Republic of Germany, Springer-Verlag, New York, 343-376 p.

Rampino, M. R., and Sanders, J. E., 1981, Evolution of the barrier islands of southern Long Island, New York, Sedimentology: International, Blackwell: Oxford-Boston, International, p. 37-47.

Reineck, H. E., and Singh, I. B., 1975, Depositional sedimentary environments, with reference to terrigenous clastics: United States, Springer-Verlag: New York, N. Y., United States.

Richter, D. K., 1983, Calcareous ooids; a synopsis: Federal Republic of Germany, Springer-Verlag : Berlin, Federal Republic of Germany, 71-99 p.

Sanders, J. E., and Kumar, N., 1975, Evidence of shoreface retreat and in-place 'drowning' during Holocene submergence of barriers, shelf off Fire Island, New York, Geological Society of America Bulletin: United States, Geological Society of America (GSA) : Boulder, CO, United States, p. 65-76.

Sedgwick, P. E., and Davis, R. A., Jr., 2003, Stratigraphy of washover deposits in Florida; implications for recognition in the stratigraphic record, Marine Geology: Netherlands, Elsevier : Amsterdam, Netherlands, p. 31-48.

Sharp, R. P., 1963, Wind ripples, Journal of Geology: United States, University of Chicago Press : Chicago, IL, United States, p. 617-636.

-, 1966, Kelso Dunes, Mojave Desert, California, Geological Society of America Bulletin: United States, Geological Society of America (GSA) : Boulder, CO, United States, p. 1045-1073.

Shinn, E. A., 1973, Carbonate Coastal Accretion in an Area of Longshore Transport, NE Qatar, Persian Gulf: Federal Republic of Germany, Springer-Verlag, New York, 179-191 p.

Simone, L., 1981, Ooids; a review, Earth-Science Reviews: Netherlands, Elsevier: Amsterdam, Netherlands, p. 319-355.

Simons, D. B., and Richardson, E. V., 1966, Resistance to flow in alluvial channels, U. S. Geological Survey Professional Paper: United States, U. S. Geological Survey : Reston, VA, United States, p. J1-j61.

Simons, D. B., Richardson, E. V., and Nordin, C. F., Jr., 1965, Sedimentary structures generated by flow in alluvial channels, Special Publication - Society of Economic Paleontologists and Mineralogists: United States, SEPM (Society for Sedimentary Geology) : Tulsa, OK, United States, p. 34-52.

Smith, M. G., and Bustin, R. M., 1996, Lithofacies and paleoenvironments of the Upper Devonian and Lower Mississippian Bakken Formation, Williston Basin: Bulletin of Canadian Petroleum Geology, v. 44, no. 3, p. 495-507.

Sperr, J. T., 1990, Exploration models for Bakken Shale reservoirs, Williston Basin, North Dakota, AAPG Bulletin: United States, American Association of Petroleum Geologists : Tulsa, OK, United States, p. 1345-1345.

Sumner, D. Y., and Grotzinger, J. P., 1993, Numerical modeling of ooid size and the problem of Neoproterozoic giant ooids, Journal of Sedimentary Petrology: United States, Society of Economic Paleontologists and Mineralogists : Tulsa, OK, United States, p. 974-982.

Wagner, C. W., and Van der Togt, C., 1973, Holocene sediment Types and Their Distribution in the Southern Persian Gulf: Federal Republic of Germany, Springer-Verlag, New York, 123-155 p.

Wanless, H. R., 1981, Fining-upwards sedimentary sequences generated in seagrass beds, Journal of Sedimentary Petrology: United States, Society of Economic Paleontologists and Mineralogists : Tulsa, OK, United States, p. 445-454.

Wanless, H. R., and Tedesco, L. P., 1993, Comparison of oolitic sand bodies generated by tidal vs. wind-wave agitation, AAPG Studies in Geology: United States, American Association of Petroleum Geologists : Tulsa, OK, United States, p. 199-225.

Warren, J. K., 2006, Evaporite; sediments, resources, and hydrocarbons: New York, NY, Springer Berlin Heidelberg, 1035 p.

Webster, R. W., 1982, Analysis of petroleum source rocks of the Bakken Formation (Devonian and Mississippian) in North Dakota: University of North Dakota, 150 p.

Wilkinson, B.H., 2004, Facies mosaics across the Persian Gulf and around Antigua; stochastic and deterministic products of shallow-water sediment accumulation, *in* Drummond, C.N., ed., Journal of Sedimentary Research, Volume 74: United States, Society of Economic Paleontologists and Mineralogists : Tulsa, OK, United States, p. 513-526.

Williams, P. F., and Rust, B. R., 1969, The sedimentology of a braided river, Journal of Sedimentary Petrology: United States, Society of Economic Paleontologists and Mineralogists : Tulsa, OK, United States, p. 649-679.

Wright, V. P., and Azeredo, A. C., 2006, How relevant is the role of macrophytic vegetation in controlling peritidal carbonate facies?; clues from the Upper Jurassic of Portugal, Sedimentary Geology: Netherlands, Elsevier : Amsterdam, Netherlands, p. 147-156.

CHAPTER 4. GEOMETRY AND RECOGNITION OF OOLITIC TIDAL CHANNELS IN ANCIENT RAMP SETTINGS: MODERN ANALOGS FROM THE PERSIAN GULF

Abstract

Oolitic tidal channels are one of the most poorly understood carbonate depositional environments. The few studies that have been conducted focus exclusively on their internal structure along attached shelves and isolated platforms, while oolitic tidal channels in ramp settings have been largely neglected. In order to better understand the shape and dimensions of tidal channels, this study presents the results of a survey of the proximal edge of a recent carbonate ramp in the Persian Gulf. Tidal channels documented in satellite imagery show a large variety of forms, orientations, and dimensions, and are aligned parallel, perpendicular or oblique to the shoreline. Planforms are remarkably similar to terrestrial fluvial systems, and transitions between meandering, braided, and anastomosing patterns occur. Oolitic channel widths vary by three orders of magnitude and range from 0.50 meters in Kuwait, to a maximum of 430 meters in Saudi Arabia. Channel lengths can be 25 km, whereas depths typically range between 1-5 meters. This study shows that tidal channels seem to be controlled by the same parameters that also apply to their fluvial counterparts, and can therefore be integrated into existing fluvial classification schemes. This facilitates predictions of tidal channel dimensions based upon models of fluvial systems. Channel forms are highly influenced by the composition of bank material they cut into: wide straight channels form where

banks consist of non-cohesive oolitic-skeletal sands, whereas those with prolific cyanobacterial growth are prone to sinuous channels. Tidal channel planform geometry, however, is not easily predicted from core data but can be observed in 3D seismic images instead. Spectral decomposition of seismic horizon slices and attribute maps based on seismic stratal slices are recommended.

4.0 Introduction

In recent years research on carbonate sand geometry has focused on wave- and tide-dominated sand accumulations in the Florida Shelf and the Bahamas (Wanless and Dravis, 2008; Harris and Ellis, 2008; Kaczmarek and Hasiuk, 2008; Rankey et al., 2008). Facies models developed for such high relief shelves and isolated platforms cannot be applied to ramps due to differences in relief and associated sedimentary processes (Purser, 1973). The limited knowledge about the dimensions and geometry of ooid accumulations in ramp settings have resulted in a series of problems for the oil and gas industry. Sheet-like carbonate sand accumulations, which occur in the Bahamas, dominate current sedimentology literature (Westphal et al., 2004; Davies, 2000; Chuber and Pusey, 1985; Ruppel, 1984). When such sheet-like models are used in the oil and gas industry to simulate oolitic reservoirs in ramp settings, and predict long-term field performance, the vast majority make erroneous predictions of changes in reservoir fluid volume and pressure. Ooid accumulations in ramp settings show a wide array of forms and dimensions, none of which can be characterized as a sheet in the sense of Friend (1979, 1983).

One of the least understood settings for ooid accumulations is tidal channels (cf. Jindrich, 1969). Modern oolitic tidal channel networks can be observed along coastlines of the Persian Gulf in the United Arab Emirates (UAE), Saudi Arabia, Qatar and Kuwait. The present study focuses on the morphology of three tidal channel networks in the UAE, Qatar, and Kuwait and the recognition of ancient oolitic tidal channels in ancient carbonate ramp successions. These networks were selected because: 1) their channels are conducive to the formation and accumulation of ooids (Taylor and Illing, 1969; Loreau and Purser, 1973; Al-Zamel et al., 2007), and because 2) their channel plan forms are affected by bank cohesion controlled by abundance of cyanobacterial mats. The purpose of this paper is to provide geometrical and dimensional data which can be used to better predict, interpret and understand ancient hydrocarbon-bearing tidal channel oolites.

4.1 Previous work

During the period 1961-1968 a consortium of 31 authors from the Imperial College of London, the Kiel University and the Shell Research Group carried out extensive research in the Persian Gulf to document geology, geomorphology and environmental factors that control carbonate precipitation in ramp settings. This research resulted in a monograph (Purser, 1973), which is the most comprehensive account of Persian Gulf geology. Sections of this monograph focus on recent carbonate facies (Wagner and Van Der Togt, 1973), recent depositional environments of Qatar (Shinn, 1973), and modern oolitic accumulations throughout the Persian Gulf (Loreau and Purser, 1973). Detailed bathymetry and lithofacies maps were created as part of this consortium and these were used to locate, identify and map the features described in the present study. Loreau and Purser (1973) defined and documented several oolitic accumulations such as tidal channels, coastal embayments, ebb deltas, beaches, and eolianites. These accumulations were sampled through dredging from boats and the diagnostic sedimentary features of these environments were recorded. Although the work done by Loreau and Purser (1973) is still the definitive publication on ooids from the Persian Gulf, they made very few inferences on the geometry and dimensions of ooid accumulations. Therefore, a detailed investigation of geometrical and dimensional properties of these sediment bodies was conducted by the author of this paper.

4.2 Methodology

Satellite images of the modern Persian Gulf were acquired from NASA Visible Earth, NASA World Wind and Google Earth. Google Earth 4.2 allows measurement of geomorphic features on the computer screen using a measuring tool. Software engineers at Google's New York City office were contacted to determine the accuracy of this measuring tool. Measurements using this tool are accurate to within one meter if the image is displayed in map view mode (Oral communication with Alexander Vogenthaler at Google New York). Accuracy is higher for features in areas with low topographic relief. Since all the coastal features measured were in areas with dips as low as one degree, the tool had high accuracy.

1700 km of the modern coastline along the Persian Gulf were surveyed for tidal channels between the Shat-Al-Arab Delta in Iraq and the town of Bukha in Oman (Fig.4.0). The selection criteria included 1) high resolution satellite coverage, 2) accessibility for fieldwork, and 3) pristine condition of coastline. The Shat-Al-Arab area lies at the border of Kuwait and Iraq and due to security concerns this delta was not visited. The town of Bukha lies close to the United Arab Emirates and Oman border; beyond this town the coastline is characterized by a narrow rocky

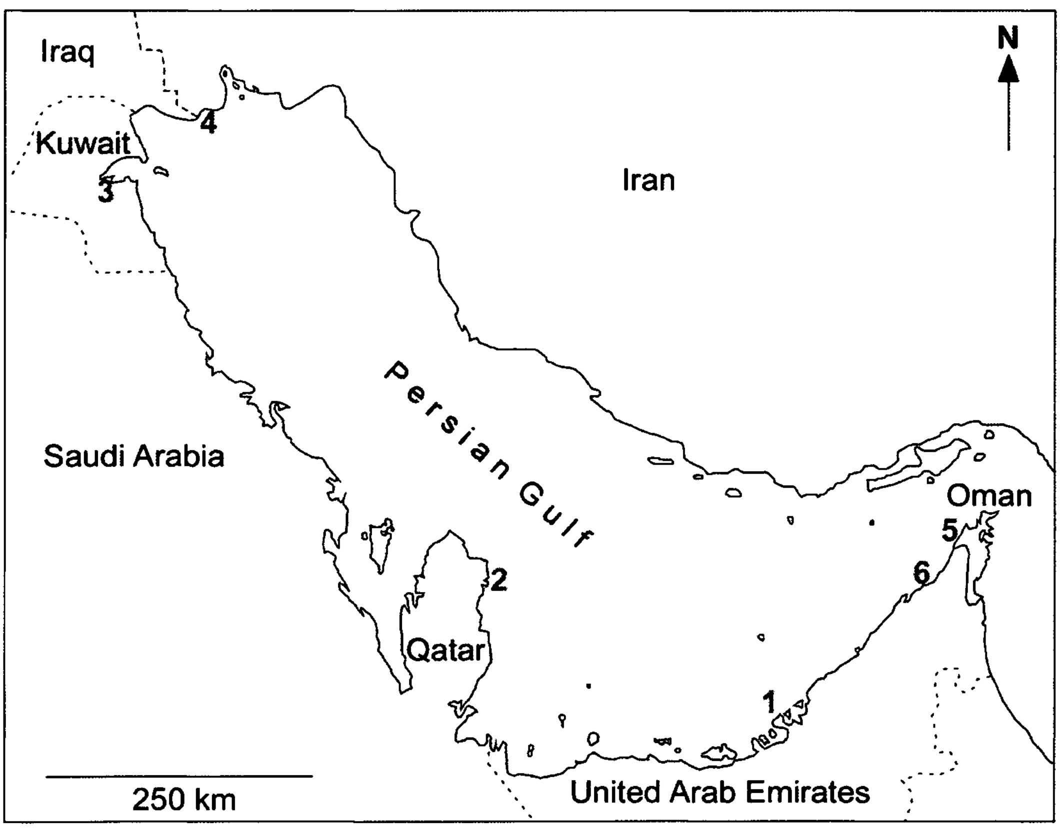

Figure 4.0. Map of Persian Gulf showing study area (shaded portion). 1) Abu Dhabi 2) Dakhira, Qatar 3) Kuwait Bay 4) Shat al-Arab Delta 5) Bukha 6) Ras-al-Khaimah. Fieldwork was conducted at coastlines along Abu Dhabi and Kuwait.

beach, which is not conducive to ooid formation.

The tidal channels mapped in this study were compared with lithofacies diagrams illustrated in Wagner and Van Der Togt (1973). Oolitic accumulations in tidal channels in the United Arab Emirates were sampled by Loreau and Purser (1973). Field locations for this study include the coastline in northern Kuwait Bay and along Abu Dhabi (Fig.4.0). During field work, shallow trenches were excavated to observe bedforms, and samples were collected to create petrographic slides. These slides were used to identify features diagnostic of ooids developed in tidal channels.

Fluvial morphometric parameters which were considered appropriate for analysis of tidal channels by Hofstede (2006) were used to characterize modern channel networks along the coastline of Abu Dhabi and Ras-al-Khaimah in the UAE (Fig.4.0), and the Dakhira area of Qatar (Fig.4.0). These included channel width, depth, w/d ratio, and sinuosity. Bathymetry data from Loreau and Purser (1973) were used to document depths, and satellite images from Google were used to measure widths along 104 data points in the tidal channel network along Abu Dhabi. Both channel networks in Qatar and Abu Dhabi were divided using the stream magnitude schemes of Shreve (1966, 1967). Sinuous channels in Qatar and Ras-al-Khaimah were classified using number, symmetry of bends and conformity of bends in the sense of Allen (1982). Channels in all locations were then surveyed for bar development to understand evolution of channel patterns, and these were compared with models based on field and lab observations by Bridge (1985, 1993).

4.3 Regional setting and study area

The Persian Gulf covers an area of approximately 2,380,000 square kilometers and is regarded as a model of an ideal carbonate ramp (Burchette and Wright, 1992). For a detailed treatment of environmental conditions that affect carbonate precipitation in the Persian Gulf, the reader is referred to Purser and Seibold (1973). Oolitic sands accumulate on the western margin of the Persian Gulf along the proximal edge of the ramp (Wilkinson, 2004). This section describes the geomorphic conditions at the inner ramp of the Persian Gulf where modern oolitic tidal channels were studied.

4.3.0 United Arab Emirates

Field and satellite image data from the United Arab Emirates were acquired from oolitic tidal channels along the Trucial Coast near the emirate of Abu Dhabi and near the Oman border from the emirate of Ras al-Khaimah (Fig.4.0). These channels vary in depth from 1-5 meters (Loreau and Purser, 1973). The geomorphology and recent sediments of the Trucial coast were first described in detail by Kendall (1969). Several 'T-shaped' barrier islands line the coast and are separated from a gently sloping beach by a large, shallow lagoon dominated by mangroves (Alsharhan and El-Sammak, 2004; Al-Habshi et al., 2007). Cyanobacterial mats flourish in the intertidal zone along the beach, and in local, topographically elevated areas within lagoons (Kendall, 1968). The sediments of the lagoon are primarily composed of poorly-consolidated, non-cohesive lime mud and minor (<9%) skeletal sand (Howari and El-Saiy, 2008). Tidal channel networks incise into these mud flats, grain-rich lagoonal sediments and underlying Pleistocene eolian sandstone (Kendall, 2008). Individual channels are distributed between barrier islands and form large flood tidal deltas along their seaward margins (Alsharhan and Kendall, 2003). Tidal range seaward and landward of the barrier islands is 2.5 meters and 1.0 meter, respectively (Evans et al., 1973). A gypsum-rich sabkha dominated by halophytes lies landward of the lagoon and tidal channel network (Boer and Gliddon, 1998; Evans et al., 1964).

The tidal channel observed at Ras-al-Khaimah incises into cyanobacterial mats and alluvium shed from the Oman Mountains. Unlike the coastline along Abu Dhabi, the beach at Ras-al-Khaimah is narrow and lacks an associated barrier island complex. Sediments along the coast are enriched in skeletal sands relative to mud-rich lagoonal facies (Alsharhan and El-Sammak, 2004).

4.3.1 Kuwait

Shallow (<0.50 meter) tidal channel networks were studied along the south-western margins of Kuwait Bay in the vicinity of Al-Jahra (Fig.4.0). Tidal range along this coastline is approximately 4 meters (Al-Zamel et al., 2007). Due to their small size, these channels cannot be resolved in current satellite imagery, therefore morphometric analyses were not conducted for these channels. Field photographs and oolitic sand samples were collected from this locality. The tidal channels along Kuwait Bay form on a mud-rich coastal plain dominated by algae, and incise into well-consolidated reefal limestone of Miocene age (Al-Zaidan et al., 2006, Al-Zamel et al., 2007). Tidal channels contain aragonitic ooid-rich sand that shows current ripples. During the time of observation this sand was coated with a fine calcareous organic-rich mud film that is 1-2 mm thick. Small (1-2 meters across) tidal pools developed in the intertidal zone contain green algae. The intertidal zone is characterized by intense bioturbation by grazing cerithid gastropods, and burrows of crabs which feed on the algae (Al-Zamel and Al-Sarawi, 1998; ElSayed and Albakri, 1994). Landwards of the intertidal zone is a broad, flat coastal sabkha, dominated by halophytes (Boulos and Aldosari, 1994; Saleh et al., 1999; Al-Hurban and Gharib, 2004). Wind-transported carbonate and quartz clasts are blown from carbonate bluffs further inland onto the supratidal sabkha and intertidal zone (Al-Hurban and Hersi, 2008). Kuwait Bay lies sea-ward of the intertidal zone and contains mainly medium to coarse grained ooid/quartz sands (Alghadban, 1990).

4.3.2 Qatar

Oolitic tidal channel networks studied are located in the Al-Dakhira National Reserve in northeastern Qatar. Satellite images show a dendritic tidal channel network amongst dark-grey patches of cyanobacterial mats (Figs. 4.9, 4.10). These channels are 1.0-1.5 meters deep (Shinn, 1973a). Tidal range along the coastline varies between 0.5-1.4 meters depending on local meteorological conditions (Taylor and Illing, 1969). Aragonite and high-magnesium calcite cements tend to precipitate in the intertidal zone, forming distinct horizons of surface and near-surface hardgrounds (Taylor and Illing, 1969). Tidal channels incise into cyanobacterial mats which encrust pelletal muds, silt, skeletal grains and calcareous hardgrounds (Shinn, 1973a). Mangroves form localized forests along certain sections of the coastline, whereas only isolated mangroves can be observed in the tidal channel network (Al-Khayat and Jones, 1999). Landwards of the intertidal zone is a coastal dolomitic and gypsiferous sabkha with isolated eolian sand ridges, and outcrops of Eocene dolomite (Shinn, 1973a; 1973b). Seaward, the intertidal zone grades into a shallow (2 meters) lagoon with highly bioturbated pelletal muds and minor amounts of skeletal sand (Shinn, 1973a).

4.4 Geometries of modern channel networks

The morphological diversity in modern channel networks investigated during this course of this study reveals a kaleidoscope of shapes and dimensions. If the traditional channel pattern classification schemes of Rust (1978), Miall (1977) and Schumm (1981) are applied to modern tidal channels in the Persian Gulf, meandering, braided, anastomosing, and straight channel forms can be documented. Bridge (2003) cautioned against classifying fluvial channels, into these forms, as their patterns can depend on flow stage and the scale of observation. In the case of tidal channels, which can be completely submerged during high tide and exposed during low tide, this warning is valid and important. Patterns of tidal channels change rapidly within relatively short distances, therefore classification terms such as 'braided' and 'meandering' are only used on a reach-scale.

4.4.0 *Tidal Channels of the United Arab Emirates*

Abu Dhabi

Several large straight channels run in a shore-perpendicular direction along the Abu Dhabi Coast (Fig. 4.1). Data were collected from one of these channel networks which drains an area of approximately 17 square kilometers during low tide. The network shows a dendritic pattern near the shoreline but has a single channel throughout the lagoon (Fig. 4.2). Depths of channels range from 1-5 meters, and width ranges between 1.2-438 meters with an average width of 30 meters. The relationship between W/D ratio and stream magnitude in the sense of Shreve (1966, 1967) is represented by Figure (4.5). Sinuosity is low and ranges between 1-1.2 and the average sinuosity is 1.03 (Fig. 4.3). The banks of these channels lack well-developed levees and are characterized by cohesionless oolitic-skeletal sand. Large alternate bars can be observed in satellite images and their orientation suggests a dominant flood tide Fig. (4.7). Figure (4.6) shows a disproportionately high number of magnitude 1 streams in the study area. This high number is explained by the occurrence of several small seepage streams that join large channels (Fig. 4.6). The sinuosity and bifurcation ratio of channels increase within short distances in a landward direction, as channels flow from an area of poorly cohesive oolitic-skeletal sand and into cohesive cyanobacterial mats (Fig. 4.8).

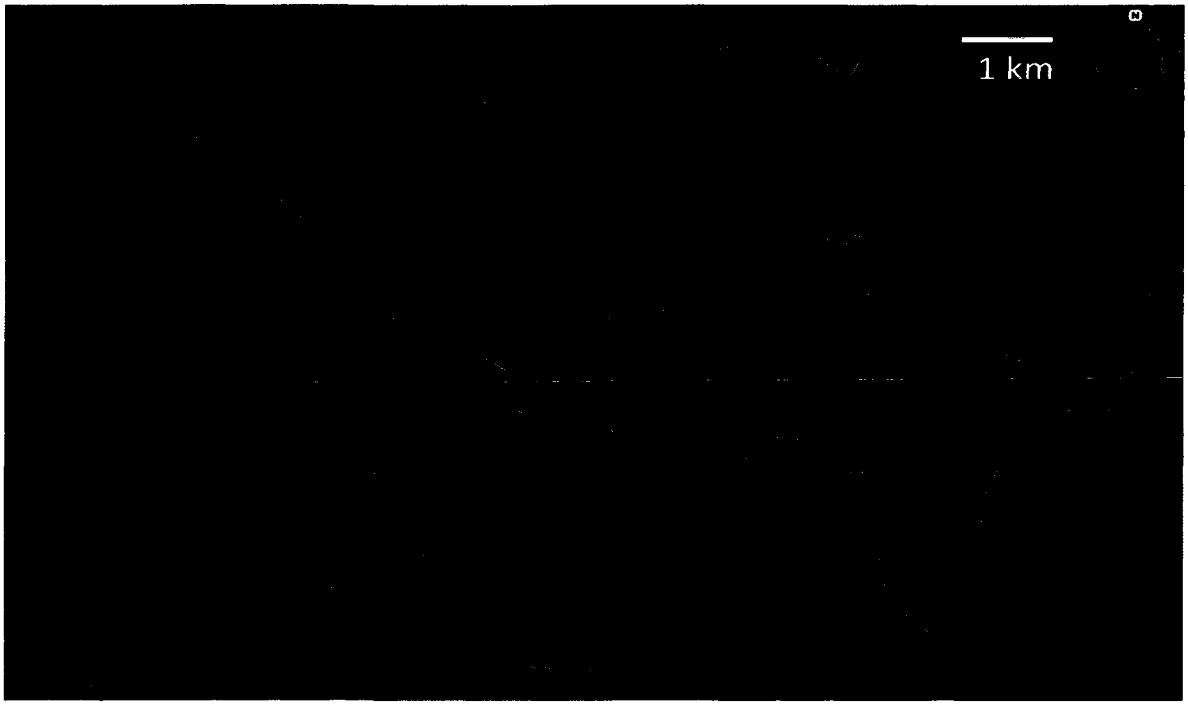

Figure 4.1. Study area along Sadiyat Island near Abu Dhabi. Rectangle shows area enlarged below

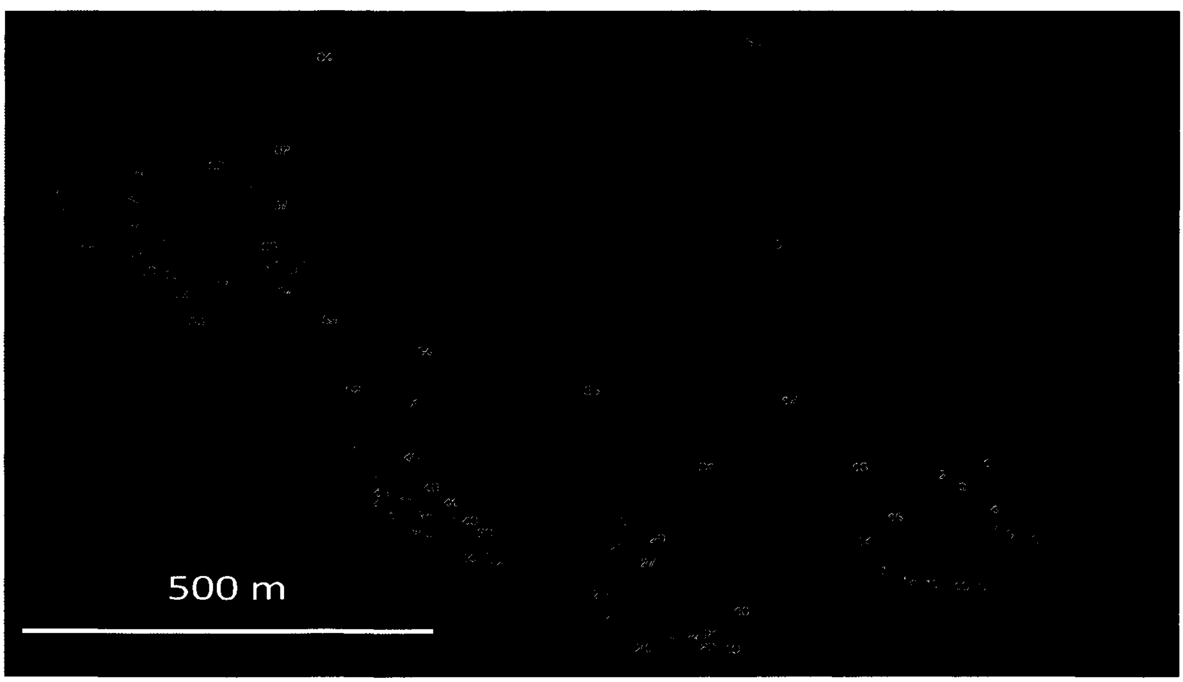

Figure 4.2. Detail of study area along Sadiyat Island in the UAE. Numbers note data points where channel width and depths were measured. Data is provided in Appendix B.

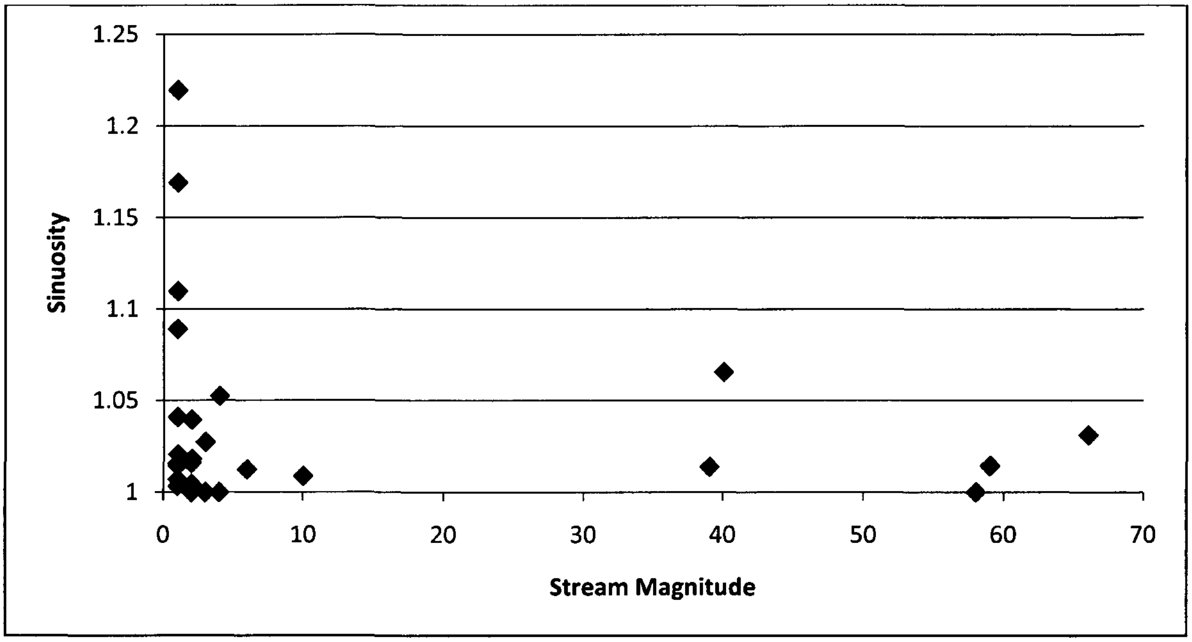

Figure 4.3. Sinuosity versus stream magnitude from tidal channels in Abu Dhabi. Note the higher sinuosity associated with magnitude 1 streams.

Ras-al-Khaimah

Unlike the shore-perpendicular channel network of Abu Dhabi, a single large isolated channel near the town of Al Rams in Ras-al-Khaimah runs parallel to the coastline. The morphometric parameters of the channel were measured along a reach between A and A' (Fig. 4.9). Three simple, regular, meander loops were observed; 2 are symmetric and 1 is asymmetric. Variations in channel width were recorded at 6 points (Fig. 4.9). The sinuosity of this channel reach is 1.63. The channel margins lie within the intertidal zone and form a boundary with supratidal eolian sediments. Cyanobacterial mats have colonized banks and point bars within the channel belt. Therefore, the banks of this channel are fairly cohesive. The meandering reach at Ras al-Khaimah can be classified as single phase, wider at bends, with no bars, following Brice (1974).

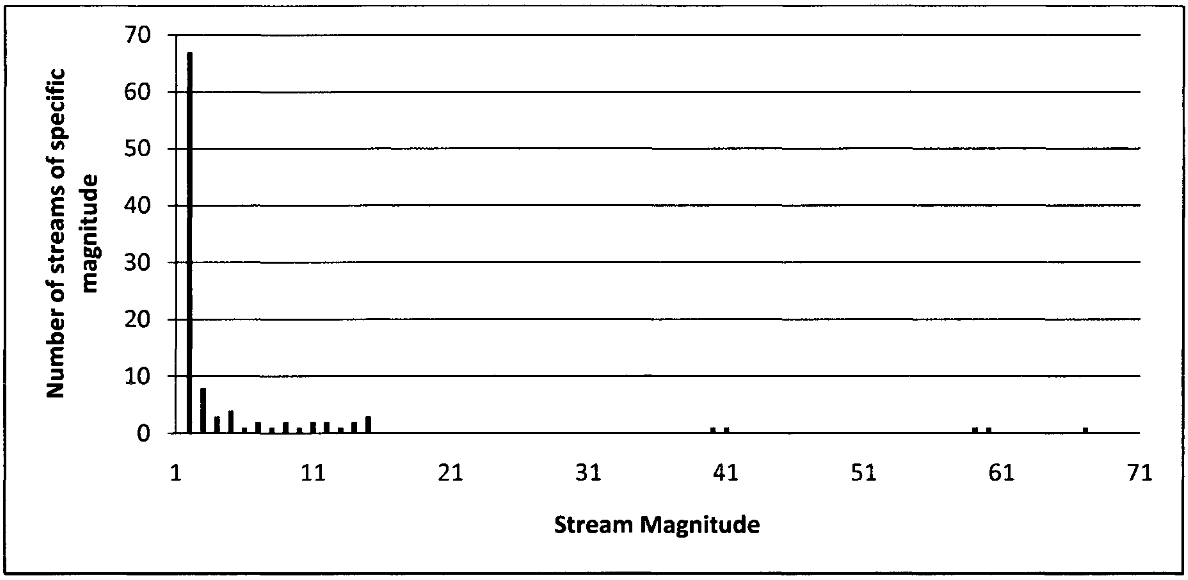

Figure 4.4. Histogram of stream magnitude from tidal channels in Abu Dhabi. There is an unusually high concentration of magnitude 1 streams in the network due to abundance of seepage streams.

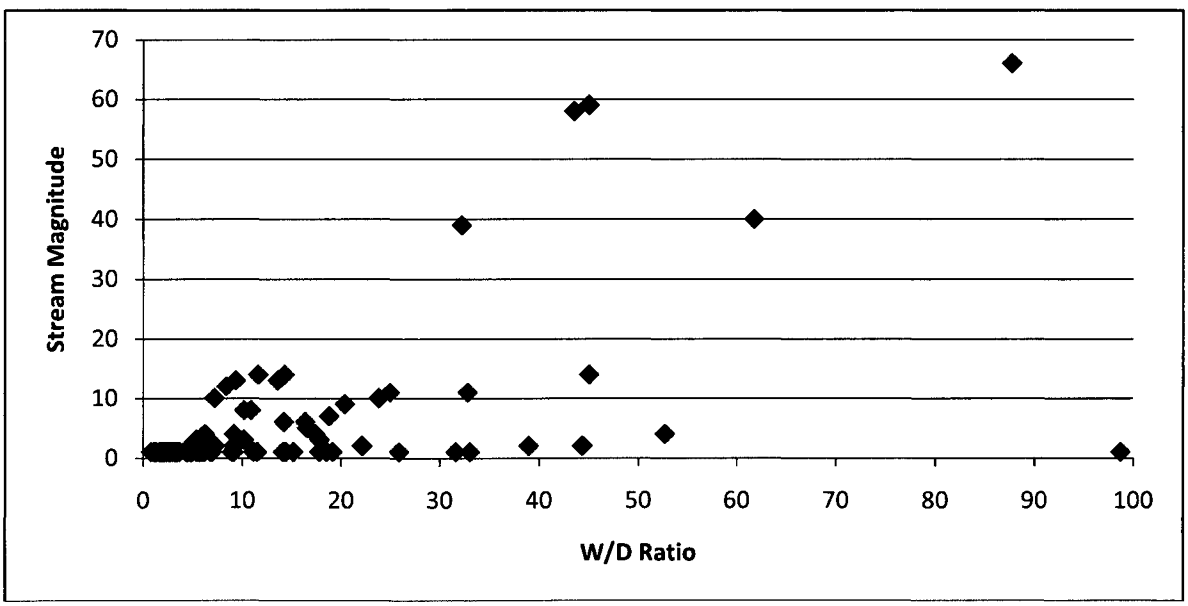

Figure 4.5. Plot of aspect ratio versus stream magnitude from tidal channel in Abu Dhabi. W/D ratio shows a gradual increase in streams of higher magnitude.

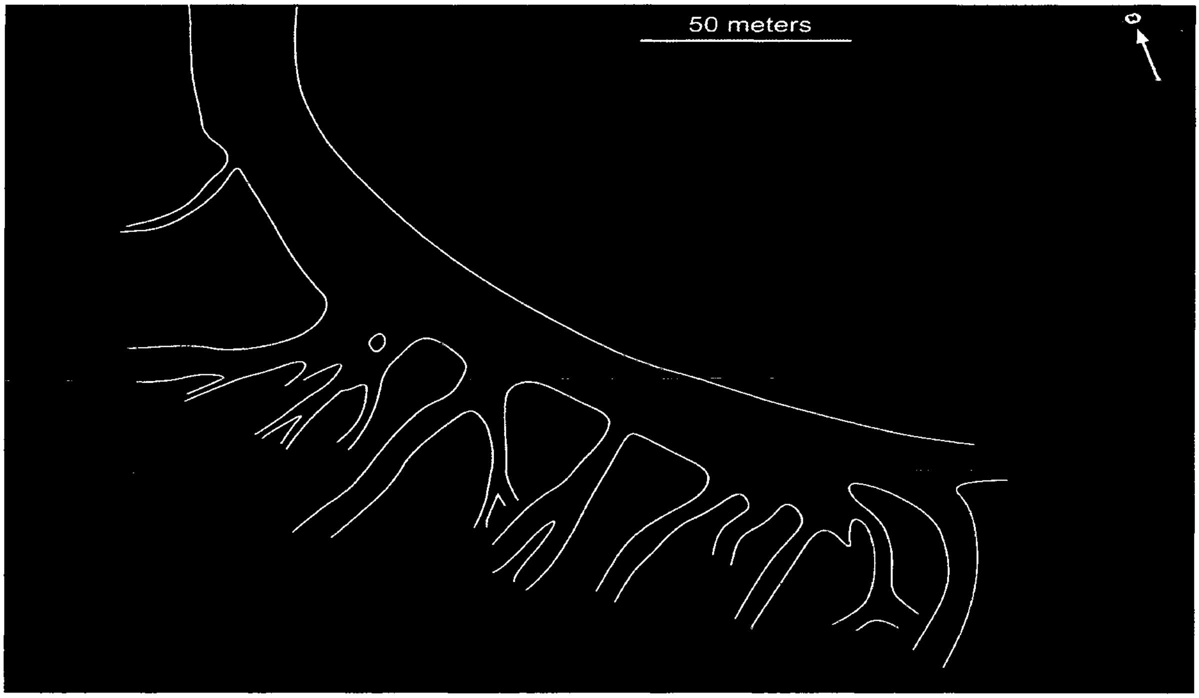

Figure 4.6. Seepage streams along a large tidal channel in Abu Dhabi, UAE.

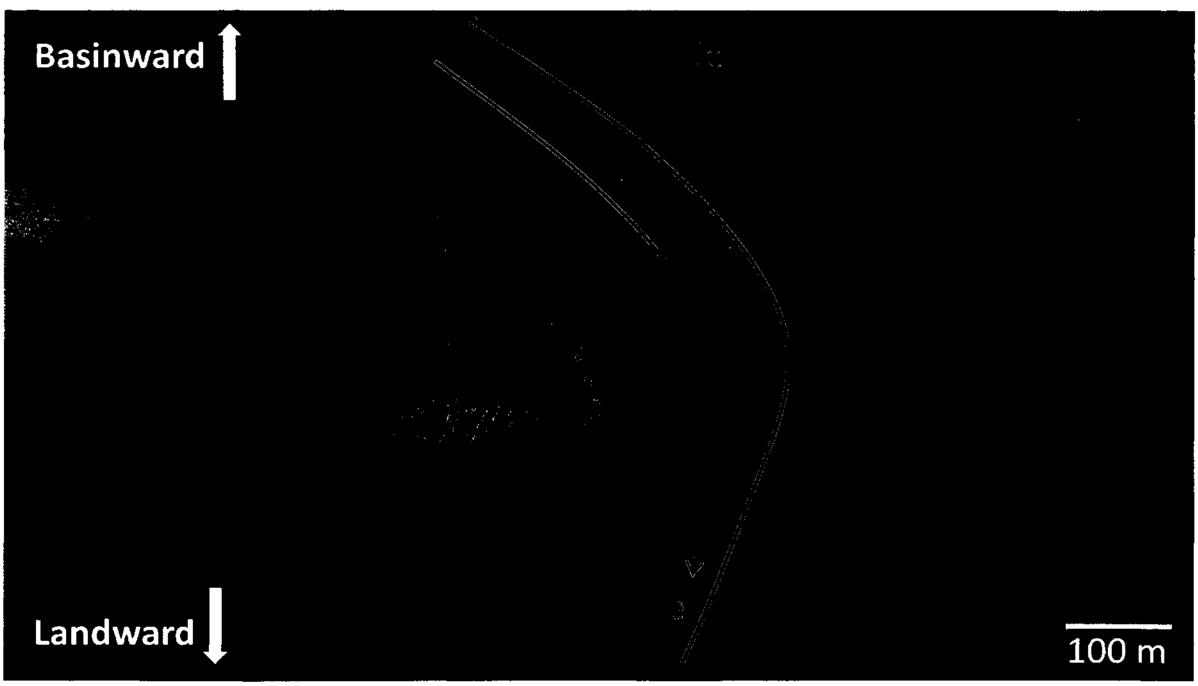

Figure 4.7. Unit bars showing dominant flood tide in a tidal channel in Abu Dhabi.

Figure 4.8. High sinuosity channels developed in a zone of prolific cyanobacterial mat growth, Abu Dhabi, UAE.

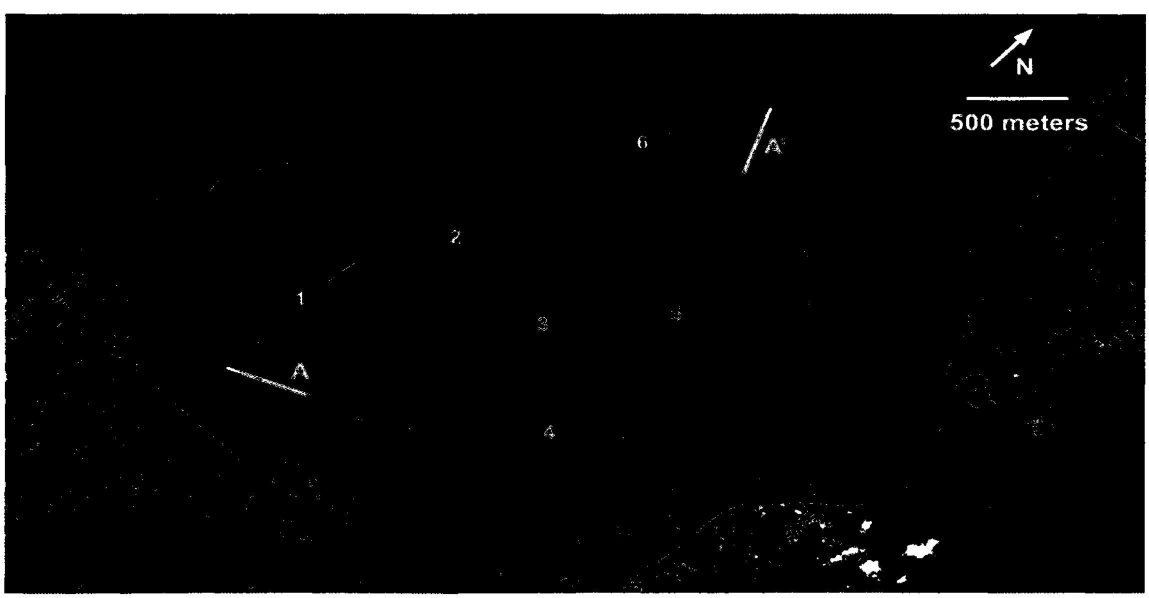

Figure 4.9. Meandering channel showing selected reach and data collection points (numbers in yellow), Ras al-Khaimah, United Arab Emirates.

4.4.1 Tidal Channels of Qatar

The tidal channels of Qatar in the study area form a dense dendritic network that drains into an isolated tidal lagoon. The channels have high sinuosity, irregular meanders and develop on a flat coastal plain with isolated mangroves. Channel banks and beds are cohesive as channels incise through cyanobacterial mats to well-cemented calcified hardgrounds (Taylor and Illing, 1969; Shinn, 1973a).

The depth of one these channels determined by Shinn (1973a) was approximately 1.5 meters. Sinuosity in the studied channels ranges between 1.35 and 1.97 with an average of 1.60 (Figs. 4.10, 4.11).The meandering patterns observed in the tidal channels of Qatar are best characterized as two phase, bimodal bankfull, irregular width, with no bars in the sense of Brice (1974). *4.4.2*

4.4.2 Petrography of oolitic channel sands

Samples of recent tidal channel sediment were collected from channels in Kuwait and Abu Dhabi. Samples in Abu Dhabi were collected from the banks of a tidal channel, whereas samples from Kuwait were collected from the channel bed and from the top of bars during low tide.Thin sections of these reveal subtle differences in coastal processes that dominate these localities.

Abu Dhabi

This microfacies is composed of approximately 60 percent ooids, 35 percent skeletal fragments, 4 percent intraclasts and less than 1 percent pellets (Fig. 4.12A).

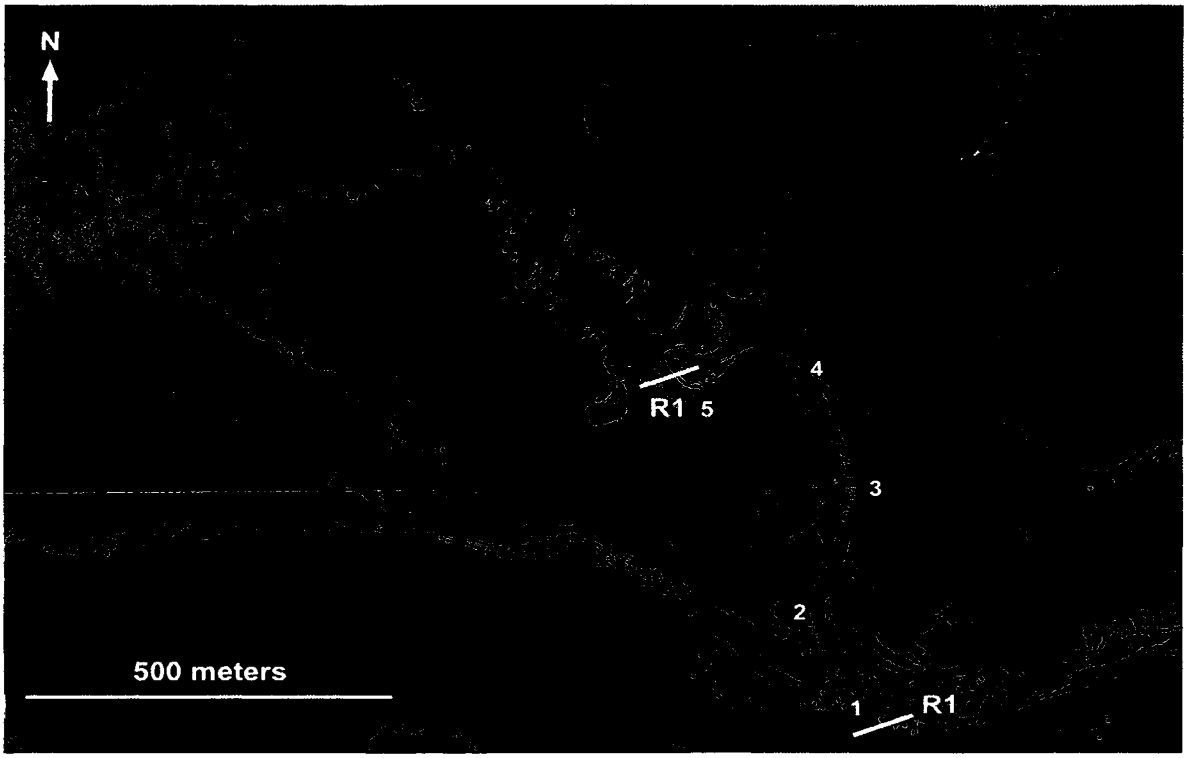

Figure 4.10. Selected reach (R1-R1) and data collection points along northeastern Qatar. Dark grey areas are cyanobacterial mats. Data taken at points (yellow) is listed in Appendix B. Area within red rectangle is enlarged in Fig. 4.10.

Ooids are tangential (concentric), circular, complete (unbroken), and show a large variation in sizes, symmetry and development (Fig. 4.12A). Although ooids with well developed cortices were documented, there is a large number of ooids that show only one superficial coating. Nuclei consist of quartz grains and skeletal fragments (Figs. 4.12B, 4.12D). No signs of boring or encrustation were observed in the ooids, and the outermost cortical lamellae show a smooth unbroken surface. Skeletal grains form the largest grains within the sample and contain fragments of pelecypods (70%), gastropods (20%), benthic foraminifera (7%), echinoderm plates (3%), and algae (<1%). Skeletal grains are medium-well

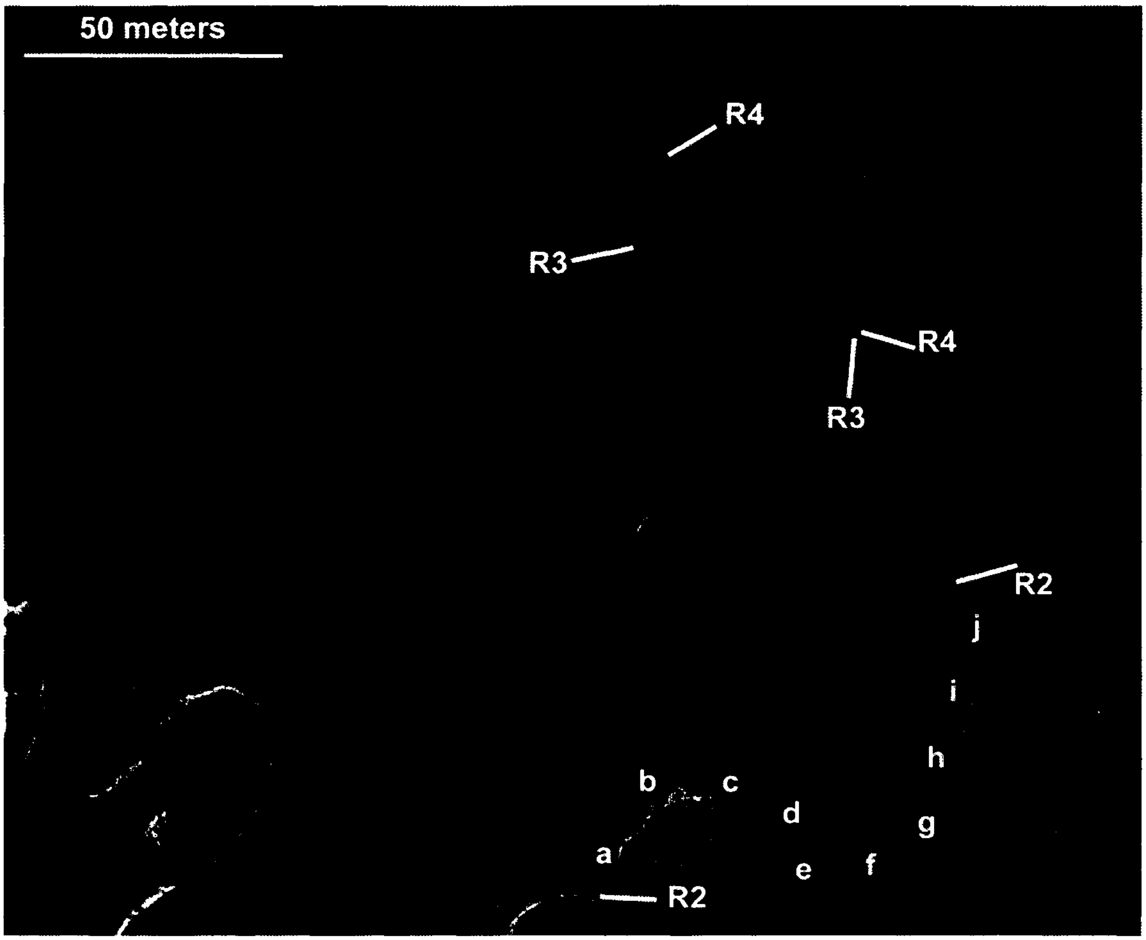

Figure 4.11. Selected reach and data collection points along northeastern Qatar. Isolated mangroves line some of the channels. Grey-green color is imparted by cyanobacterial mats. Data taken at points (yellow) is listed in Appendix B.

rounded, and show micritization. Peloidal wackestone intraclasts occur as large well rounded grains. Pellets are rare and show a distinct oval shape and early calcite cementation.

Kuwait

Ooids in this sample are highly micritic, which makes it difficult to determine their internal structure. However, a few ooids show well developed tangential cortices around nuclei of primarily large quartz grains and minor skeletal fragments (Fig. 4.12C). Approximately 85 percent of the sample consists of ooids, 10 percent of skeletal fragments, 4 percent of large uncoated grains and less than 1 percent of intraclasts. The ooids show a large grain size variation, tend to be asymmetric, and most have irregular shapes. The outermost cortical lamellae show abrasion in almost all the ooids but none are broken (Fig. 4.12C). No borings were observed in the ooids. Rare skeletal fragments include benthic foraminifera and gastropods. A small number of large quartz clasts in this sample remain uncoated, whereas most have at least one superficial micritic coating (Figs. 4.12D, 4.12E). Intraclasts are rare and include fragments of skeletal packstones.

Interpretation of petrography

These data, along with published descriptions in Loreau and Purser (1973) and Taylor and Illing (1969), can be used to deduce some general characteristics of oolitic tidal-channel fill in ramp settings. Sediments tend to be grain supported and the dominant grain type is ooids. The percentage of ooids ranges from 10-90% depending on what part of the channel is sampled. The abundance of ooids increases in a basinward direction, whereas the abundance of skeletal fragments increases in a landward direction (Loreau and Purser, 1973, Shinn, 1973a). Tidal channels along the coastline of Abu Dhabi terminate in large ebb deltas, but their sediments can be distinguished by the absence of boring. Boring by encrusting organisms leads to macroscale degradation of ooid grains and is proportional to bottom stability (Wanless and Tedesco, 1993). None of the ooids collected during the course of this study showed any evidence of boring. This may be due to higher energy levels within the channels that prevent encrustation on ooids. On the other hand, ooids from ebb deltas along the Abu Dhabi coastline show intense boring (Kendall, 2008). No broken ooids were observed in tidal channels, and most show a high level of symmetry. Symmetry of ooids is directly proportional to hydraulic turbulence; therefore, ooids in tidal channels generally tend to be symmetrical (Freeman, 1962). Some ooids collected from Kuwait Bay show slight asymmetry. This may be due to the topography of the tidal flats in the study area. Small ponds develop on the tidal flats and these can trap ooids. Ooids trapped in these ponds are removed from zones of turbulence and in a stable environment they tend to develop irregular coats. When channels migrate laterally, these ooids are re-introduced into tidal channels. All ooids in samples contain tangential coats which range from superficial to thick. Nuclei of ooids vary somewhat between Abu Dhabi and Kuwait. The high influx of eolian-transported sand along the *Shamal* wind-dominated coastline of Kuwait leads to an abundance of quartz nuclei in ooids. The restricted Kuwait Bay also tends to develop high salinities and this leads to an impoverished fauna (Al-Hurban and Ghraib, 2004; Al-Zamel and Al-Sarawi, 1998). The samples from Abu Dhabi were collected from the distal ends of tidal channels where lower salinities allow for large populations of mollusks. Therefore, the nuclei of ooids in Abu Dhabi tend to contain more skeletal fragments. Peloids, intraclasts, and botryoidal grains are uncommon in samples from both localities.

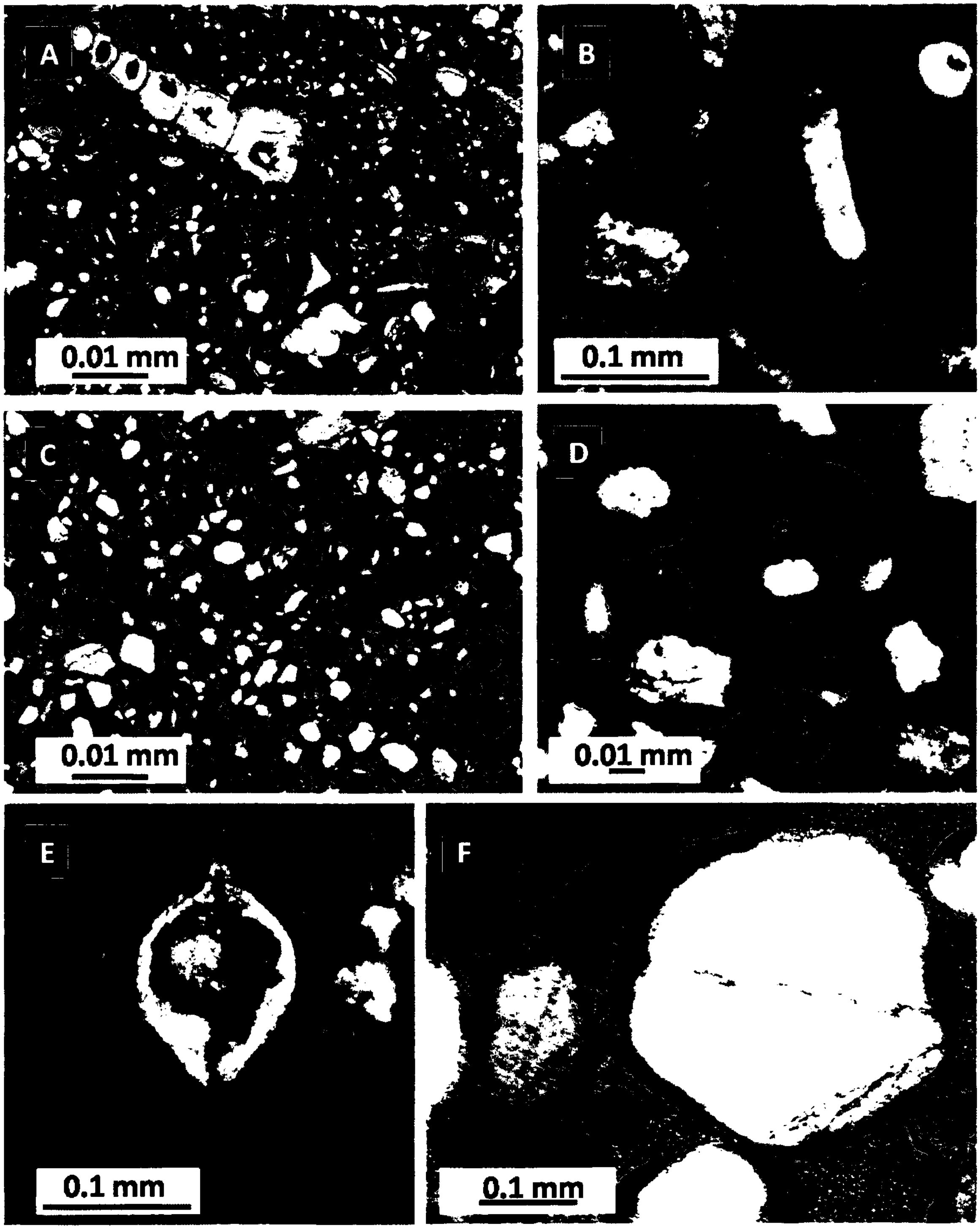

Figure 4.12. A) Grain assemblage of Abu Dhabi sample showing abundance of skeletal material B) Tangential coats on skeletal grain in Abu Dhabi C) Grain assemblage of Kuwait sample showing presence of several quartz grains D) Ostracod nucleus (Abu Dhabi) E) Superficial coatings on quartz grains (Kuwait) F) Magnified quartz grain showing micritic rim.

4.5 Guidelines for the recognition of ancient tidal channel oolites in ramp settings using sub-surface data

The assignment of a particular environment of deposition to ancient oolites in the sub-surface can be a daunting task. The guidelines proposed here are recommendations based upon current technologies and knowledge base on ooids from published studies. These guidelines are proposed for ramp settings only, therefore their application to attached shelves or isolated platforms is not recommended. This section is organized according to the most readily available and commonly used sub-surface datasets used in the oil and gas industry.

4.5.0 Three dimensional seismic imaging

Modern oolitic tidal channels form shallow, ribbon-like, low aspect ratio sediment bodies, which makes them difficult to detect in two-dimensional seismic lines. The main problem in stratigraphic plays is the detection of thin beds (Yilmaz, 1987). Three-dimensional seismic volumes allow the interpreter to view data in map view and greatly enhance the probability of detecting subtle seismic geomorphic features.

The full potential of three-dimensional seismic imaging for the description of ancient depositional systems has only recently been appreciated (Davies, 2004). This breakthrough technology has led to the formulation of seismic geomorphology, which Posamentier (2000) defined as the study of depositional systems using 3D-derived images. Posamentier (2004) presented several examples from marginal marine to deepwater settings where channel networks and associated geomorphic features were observed. Wood (2003; 2007) refined and applied these techniques to reflection seismic data from ancient fluvial systems using seismic slices.

Three 'slicing' methods are used to view seismic attributes such as amplitude or instantaneous phase. The first of these is the time slice, which is extracted from a seismic volume at a constant seismic two-way travel time (Zeng, 2006). Seismic time slices, however, do not depict actual paleotopography, and therefore have limited application in stratigraphic studies. The second method is the seismic horizon slice, which illustrates the seismic attribute along a seismic reflection. The seismic reflection may or may not coincide with a constant two-way seismic travel time, depending on whether dip is present. This method works well for sheet-like geometries but has limited applicability towards detecting ribbon-like sediment bodies such as tidal channels. Ethridge (2007) highlighted the use of the seismic stratal slices to image planform geometry of fluvial systems. In this technique, the interpreter divides variable-thickness vertical intervals between two laterally continuous reflections into uniformly spaced subintervals (Zeng, 2006). By doing so, the average value of the seismic attribute is displayed in map view, and is a close approximation of an instant in geological time. Application of this technique to Pliocene fluvial deposits in the Gulf of Mexico has allowed interpreters to view subtle changes in fluvial systems in high resolution (Zeng et al., 2001). Morphological parameters used to describe and classify fluvial systems can also be applied to tidal channels (Hofstede, 2006). Therefore, the construction of strata slices in three-dimensional seismic volumes should be useful in interpreting ancient oolitic tidal channels. Miall (2002, 2006) used seismic slices to identify tidal channels in Pleistocene strata of the Malay Basin.

Several seismic attributes have been used to image ancient fluvial successions, but the majority of these have been used to recognize sand packages in surrounding overbank fines (Davies, 2005). The acoustic impedance contrast between sandstone and mudstone produces sufficient reflections to allow observation of channel forms in seismic lines. Modern oolitic tidal channels, such as those formed along the coastline of Abu Dhabi, contain a fill of ooids and skeletal grains, and incise through unconsolidated materials that are variable locality to locality and include lime mudflats, skeletal sandflats, semi-consolidated cyanobacterial mats and consolidated Pleistocene ooid-rich eolianites (Loreau and Purser, 1973; Alsharhan and Kendall, 2003; Kendall, 2008). The Pleistocene eolianites contain primarily quartz grains, ooids and skeletal grains (Loreau and Purser, 1973; Alsharhan and Kendall, 2003; Kendall, 2008). The Pleistocene eolianites contain primarily quartz grains, ooids and skeletal grains (Kirkham and Evans, 2008). This would suggest that channel-fill and surrounding strata may have similar densities and similar seismic velocities in areas where channels incise through Pleistocene eolianites. In this particular case the boundary between channel fill and surrounding matrix would not generate an impedance contrast conducive for seismic observability. Unlike the channel networks of Abu Dhabi, the channels in the Dakhira area of Qatar incise through cyanobacterial mats to a well-cemented carbonate layer, and those at Kadmah Bay in Kuwait incise into a well-lithified reefal limestone (Shinn 1973a; Al-Zamel et al., 2007). A

P-wave velocity of approximately 4100 m/s is assumed for the oolitic-peloidal-skeletal packstone to grainstone channel-fill based on synthetic modeling of carbonates by Janson (2007). When the P-wave velocity of the channel-fill is compared with velocities of coral reef limestones (5618 m/s) and algal boundstones (6485 m/s), an impedance contrast strong enough to generate a reflection along channel boundaries is likely (Anselmetti et al., 1997; Wunderlich, 2008). Therefore, oolitic tidal channels that incise through lithologies significantly different in density will have a higher probability of being detected in seismic stratal slices.

A useful technique for detection of thin beds in three-dimensional seismic volumes is spectral decomposition (Laughlin et al., 2003). Because higher frequencies image thinner beds and lower frequencies image thicker beds, reflection amplitude maps inherently contain information on bed thickness. An amplitude extraction map based upon a strata slice can be used to decompose the seismic signal into its constituent frequencies (Hall and Trouillot, 2004). The interpreter can 'tune-in' to a particular frequency and since the strength of reflections bounding a bed are affected by bed thickness and frequency, can not only detect bed thickness variations but also accurately predict bed thickness (Partyka, 1999). Since high-frequency response of a reflector can be attenuated by the presence of fluids, spectral decomposition can also be used to detect hydrocarbons in a bed (Castagna, 2003). These attributes render spectral decomposition a powerful tool to better understand ancient tidal channels.

4.5.1 *Wireline logs*

Tidal channels incise into underlying materials (Kendall, 2009) and would therefore form sharp erosional contacts along their base. On well logs this would produce sharp, blocky contacts similar to those of fluvial channels, as noted by Miall (2004). Because of similar processes of channel macroform formation, tidal channels, like fluvial channels are expected to fine upwards. This characteristic is particularly useful if the lithology is known because most modern oolitic accumulations such as tidal deltas, tidal bars, and coastal embayments are inherently progradational and would produce coarsening upward successions in the log signature (Swenson et al., 2005). However, this characteristic alone does not suffice for an accurate interpretation of oolitic tidal channels, and should be used in conjunction with other data sets. Bridge and Tye (2000) created a detailed suite of hypothetical vertical profiles through different parts of a fluvial channel. The striking similarity between fluvial channel bedforms and those of oolitic tidal channels as demonstrated by Gonzalez and Eberli (1997), suggests that these profiles could be useful in interpretation of ancient tidal channels.

Xu (2007) presented a detailed study of siliciclastic tidal channels based on borehole image logs. In this study, he summarized some of the major diagnostic features of tidal channels as multiple cross sets bounded by low-angle bounding surfaces where each set shows a consistent foreset dip azimuth. Bases of channel fill elements are draped with thin mud (<10 cm) and mud intraclasts. Mud drapes, being less conductive, appear as dark bands, whereas coarse grained particles such as ooids will appear as light bands. Shell lags at the base of channels can also be detected on a cm-scale on borehole image logs (Ekstrom, 1987). Siliciclastic channel-fill can be distinguished from carbonate filled channels by using density and elemental analysis logs.

4.6 Discussion

Due to similarity in form and processes of channel macroform formation between tidal and fluvial channels, this study used the fluvial morphometric parameter approach proposed by Hofstede (2006). It is important to note, however, that this methodology is 180 degrees out of phase with the tidal channel descriptions made by Shinn (1983). According to Shinn (1983, page 193), 'tidal flats are analogous to river deltas turned wrong side out, that is, the sea, rather than the land, is the sediment source and channels with their distributaries branching in a landward direction provide the pathway for sediment delivery.' Following Hofstede (2006), this study considered the landward channels that join and form a large trunk as channel tributaries. This allowed the assignment of stream magnitude to tidal channel networks in UAE and Qatar in the sense of Shreve (1966, 1967). We argue that sediment is not sourced from the sea as suggested by Shinn (1983) and is rather formed within the tidal channels, as documented by Loreau and Purser (1973). Therefore, since the sea is not the sediment source, it cannot be regarded as a drainage basin, and the channels in a landward direction would act as tributaries that collect water from lagoons during receding tides and flush them into the open ocean. Channel-fills in the tidal networks in UAE, Qatar, and Kuwait contain a mixture of ooids which form and accumulate within the channels, wind blown quartz grains and skeletal fragments, e.g of gastropods and benthic foraminifera that inhabit these channels (Taylor and Illing 1969; Loreau and Purser 1973; Picha 1978; Al-Zamel et al., 2007). Even the nuclei of ooids contain either skeletal fragments of the aforementioned fauna or wind-transported quartz grains (Fig. 4.12D, 4.12E). Although all tidal networks documented by Loreau and Purser (1973) and this study contain similar grain types and sizes, the planform geometry of channels varies significantly. Therefore, like their fluvial counterparts, data from tidal channels support the argument that facies are seldom diagnostic of planform type (Brierly 1989; Brierly and Hickin 1991). Tidal channels in the Persian Gulf show a highly diverse assemblage of channel planforms, and no generalizations can be made regarding their geometries. Channel forms generated by tidal processes show remarkable similarities to terrestrial fluvial systems, and if the fluvial classification schemes of Miall (1977), Rust (1978) and Schumm (1981) are applied to tidal channels, then all four end-members are represented in the Persian Gulf (Fig. 13A). It should be noted that certain tidal channels along the margins of the Persian Gulf have been affected by anthropogenic changes. For example, the braided tidal channel illustrated in Figure (4.12B) shows a meandering planform for most of its reach (Fig. 4.8). The image in this study was taken adjacent to a dam in Ras al-Khaimah, UAE. Variations in discharge by the dam may have caused this particular section to develop a braided channel form.

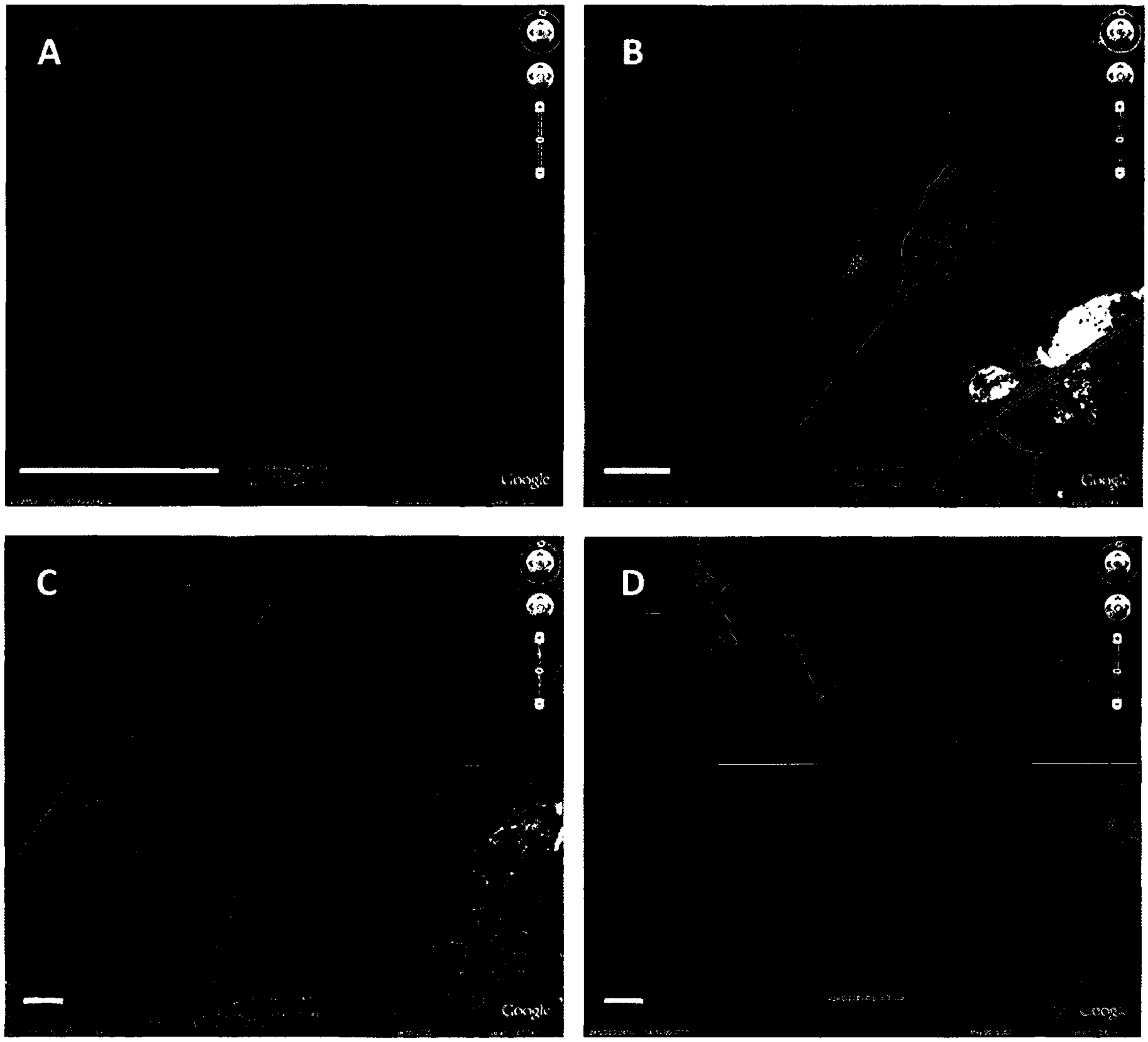

Figure 4.13. A) Anastomosing channels in Kuwait B) Braided channel in Ras al-Khaimah C) Meandering Channel in Ras al-Khaimah D) Straight channel in Abu Dhabi (Scale bar is 500 meters).

However, 22 km south of this braided reach is another braided tidal channel that shows no signs of human interference. Therefore it is likely that tidal channels can develop braiding through the process of convergence, which Ethridge (2007) define as the situation in which different controls can produce similar results.

Figure (4.12A) shows an anastomosing pattern in the tidal channels along Kadmah Bay in Kuwait. Landwards of these channels is a large sewer that discharges wastewater into Kuwait Bay. Due to the lack of aerial photographs prior to construction of the sewer it is difficult to determine whether the discharge from the sewer caused incision into the mud-rich tidal flats, or whether the sewage discharge was accommodated in older tidal channels. Currently these tidal channels form and accumulate ooids, and this correspondence of tidal channels with the sewage discharge may be an example of the process of reoccupation similar to fluvial systems (Aslan 1999; Morozova and Smith 2000; Makaske et al., 2002). This is the only location along the western margins of the Persian Gulf that showed a distinct anastomosing pattern; therefore it may well be a result of anthropogenic activity. Increased discharge from the sewer may have led to higher rates of channel aggradation and increased avulsion frequencies which may have led to channel anastomosis. Unlike the tidal channels of the UAE, the channels of Qatar have well-developed channel belts. To establish a relationship between channel width (C_w) and Channel belt width (CBW) measurements were taken at ten points along the reach R2 (Fig. 4.10). There seems to be very little correlation between channel width and channel belt width. At data-point 'a' the channel is 0.5 meters wide whereas the channel belt width is 7.04 meters. However, at point 'j' the channel width is 1.91 meters whereas the channel belt width is only 6.5 meters. Relationships between fluvial channels and associated channel belt widths were tested on one of these channels and the predicted results from the equations did not match the actual measurements from the satellite images, which show an average channel belt width of 11.5 meters (Table 4.0). This lack of relationship between channel width and channel belt width can be interpreted in three ways. First, it is possible that there is no strong relationship between the width of tidal channels and their associated belt widths. Second, the images used to acquire data may have been taken at a time of ebb tides where channels were in low-flow stage. This is most likely because high tide happens only once in 12 hours, and it would be a coincidence if the image was acquired during high tide. Third, this could be an underfit stream occupying a channel created during an older tidal regime.

Tidal channels documented in this study do not show a preferred orientation with respect to the coastline and can be shore-parallel, perpendicular or oblique. The only discernable trend in planform geometry of tidal networks documented in this study is the relationship between channel sinuosity (P) and occurrence of cyanobacterial mats. This phenomenon was noted when straight channels of a network in the UAE were compared with sinuous channels in Qatar. The mean sinuosity of the UAE channels which incise into unconsolidated oolitic-skeletal sands is 1.03, whereas channels in Qatar that have incised into cohesive cyanobacterial mats have an average sinuosity of 1.60. The filamentous texture of cyanobacteria coupled with the binding of sediment particles to their muscilagenous sheath may have resulted in greater cohesion along channel banks. Figure (4.13) shows a straight channel in the UAE developed in oolitic-skeletal material entering a zone colonized by cyanobacterial mats, and instantaneously shows an increase in sinuosity. Channels developed on these mats in Qatar tend to be much narrower (mean P= 3.34 meters) than those in UAE (mean P = 30.75). Sinuosity is inversely proportional to W/T, therefore channels in Qatar with cohesive banks tend to be narrow whereas those in Abu Dhabi tend to be wide (Schumm 1960a, 1968; Ferguson, 1973). Sinuosity can be affected by slope, water and sediment discharge, and bank cohesion (Schumm, 1960b, 1961). However, the channel networks in Abu Dhabi and Qatar develop on slopes of extremely low gradient (<0.01 degree) and host similarly sized sediment clasts. Therefore, the fundamental difference between these two locations is bank cohesion.

Equation	Reference	Results (W_{cb} in meters)
$W_{cb} = 17.6\ W$	Jefferson (1902)	21.8
$W_{cb} = 17.38W,\ 14W$	Inglis (1949)	21.55, 17.36
$W_{cb} = 3.4\ W^{1.1}$	Leopold and Wolman (1960)	4.30
$W_{cb} = 4.5\ W$	Zeller (1967)	5.58
$W_{cb} = 7.53\ W^{1.01}$	Lorenz et al (1985)	9.35
$W_{cb} = 4.3\ W^{1.12}$	Williams (1986)	5.6

Table 4.0. Calculation of Channel belt width using channel width of a tidal channel in Qatar.

A comparable situation was described comprehensively by Schumm (1963).He noted that streams which developed on the same valley slopes on the Great Plains of the U.S. tend to form very different plan form geometries. A detailed investigation based on several gauging stations along rivers with sinuosity ranging from 1.0-2.1 showed that the sinuosity was a function of several parameters. These controlling parameters included the percentage of clay-silt in the perimeter of the channel, a high percentage of clay-silt in the banks, and the proportions of sediment load. Modern channels which incise through fibrous peat in the Rhine-Meuse delta of the Netherlands also tend to show high sinuosity (Tornqvist, 1993). The sinuous tidal channels of Qatar incise into cyanobacterial mats and develop on both modern and ancient carbonate hardgrounds, and have very low gradient reaches (Taylor and Illing 1969; Shinn 1973a). Based on these criteria, they are classified as stable channels in the sense of Hooke (2007). Gibling (2006) proposed a comprehensive classification scheme for fluvial channels, and created a category of 'fixed river systems' for such stable channels. These are defined as bodies that show little evidence for lateral migration of channels and bars. A few of these may even contain tidal structures and marine fossils (Gibling, 2006 page 755). Although no depth data are available for the channels in Qatar, Gibling (2006) predicts such fixed channels to have W/T less than 15. Straight channels along the Abu Dhabi coastline lack cohesive margins, can be 24 km long, up to 400 meters wide and have W/T ratios that range from 1.1 – 98.6 with an average of 12.92. Satellite images of these channels show no signs of avulsion or lateral migration. Channel belts are absent, as they form in a shallow (<7 meters) lagoon. Therefore, they do not conform to any fluvial model proposed by Gibling (2006). The tidal channel measured in Ras al-Khaimah meanders for a length of 15 km, has a maximum channel width of 320 meters and forms a distinct channel belt 2 km in width. Figure (4.9) shows that cut-bank erosion on the seaward margin of these channels has extended the channel belt into an adjacent eolian dune field. Such channels would be best described as mobile channel belts of the meandering type according to the classification scheme of Gibling (2006). He documents a maximum thickness of 38 meters, channel belt widths less than 15 km and typically less than 3 km for mobile channel belts in terrestrial fluvial settings. However, without intensive coring of point bars associated with the Ras al-Khaimah channel, it is difficult to deduce whether the areas between meander loops which appear to be point bars indeed contain lateral accretion deposits, and if these deposits contain oolitic grainstones.

4.7 Conclusions

The diversity of patterns and variability in dimensions of oolitic tidal channels has received very little attention. This paper has sought to highlight the kaleidoscope of shapes and forms in modern tidal channels, and provided guidelines for the recognition of such channels in ancient carbonate ramps.

1. Tidal channel width ranges from 0.50 m in Kuwait to 430 meters along the Saudi coast. The maximum recorded length of channels is along the Trucial Coast, which can run up to 25 km from the coastline to terminal ebb deltas. Based on the fluvial classification of Gibling (2006), some tidal channels can be classified as fixed 'river' systems, which are documented to contain sand bodies that are thin (3-15 m), less than 150 meter wide, with W/T commonly less than 15 in the terrestrial realm. Tidal channels along northeastern Qatar exemplify this type in a tidal setting. Mobile channel belts of the meandering type can have

deposits up to 38 meters thick, channel belts less than 15 km wide and are represented by large shore-parallel channels along the coastline of Ras al-Khaimah in the UAE. Straight channels of Abu Dhabi do not fit well into the Gibling (2006) classification scheme and have aspect ratios that range from 1.1 – 98.6 with an average of 12.92, widths up to 400 meters, and depths of 5 meters.

2. Planform geometry of tidal channels can be described as meandering, braided, anastomosing and straight. Channels documented in this study are oriented perpendicular, parallel or oblique to the shoreline.

3. Ancient tidal channels can be best observed in seismic strata slices in the sense of Zeng (2006). Miall (2002, 2006) successfully observed tidal channels in Pleistocene strata of the Malay basin using seismic slices. Spectral decomposition has been a highly successful tool in the detection of fluvial channels and is expected to perform just as well for tidal channels.

4. Bimodal cross sets, sharp flat bases, fining upwards motifs, and densities of 2.71-2.89 g/cm^3, are useful but not diagnostic criteria that can be used to identify oolitic tidal channels in the ancient record. Readers are referred to Xu (2007) for a detailed treatment of clastic tidal channel diagnosis using borehole image logs.

5. Channel fills can be characterized as poorly sorted, grain-supported assemblages of ooids and skeletal grains of variable size. Ooids tend to be tangential, range from well developed to superficial, may show abrasion in the outermost lamella, have nuclei of skeletal and quartz grains, show symmetry, lack of borings, and are complete (unbroken).

6. Modern channels show an increase in sinuosity in zones with abundant cyanobacterial growth and straight channels in areas of unconsolidated bank materials. In the ancient record, channels incised in algal boundstones should be expected to have higher sinuosities than those developed into grainstones.

4.8 Acknowledgements

Many individuals provided ideas that led to this project. These ideas were conceived from thoughtful discussions with the Saudi-PNZ Group at Chevron, and the Middle Eastern Team at ExxonMobil. Petro Papazis introduced me to reservoir simulation and the importance of geological data inserted into these models. Anthony Sandomierski encouraged A.J. to focus on carbonate ramp settings and the utility of ooids in diagnostic ancient environments. Fieldwork in Kuwait would not have been possible without the help of Wahab Sadeqi. Richard Marston provided valuable insights into controlling parameters of fluvial channel patterns. Dennis Harry was kind enough to review the section on geophysical methods that can be used to recognize ancient tidal channels. We also wish to thank Frank Ethridge, Ellen Wohl and John Ridley for reviewing and improving an earlier version of this manuscript.

4.9 References

Al Habshi, A., Youssef, T., Aizpuru, M., and Blasco, F., 2007, New mangrove ecosystem data along the UAE coast using remote sensing, p. 309-319.

Al-Hurban, A., and Gharib, I., 2004, Geomorphological and sedimentological characteristics of coastal and inland sabkhas, Southern Kuwait: Journal of Arid Environments, v. 58, p. 59-85.

Al-Hurban, A.E., and Hersi, A.A., 2008, Sedimentomorphic mapping of Jal Az-Zor escarpment, northern Kuwait, using GIS methods: Kuwait Journal of Science & Engineering, v. 35, p. 93-126.

Al-Khayat, J.A., and Jones, D.A., 1999, A comparison of the macrofauna of natural and replanted mangroves in Qatar, Academic Press Ltd, p. 55-63.

Al-Zaidan, A.S.Y., Kennedy, H., Jones, D.A., and Al-Mohanna, S.Y., 2006, Role of microbial mats in Sulaibikhat Bay (Kuwait) mudflat food webs: evidence from delta C-13 analysis: Marine Ecology-Progress Series, v. 308, p. 27-36.

Al-Zamel, A., and Al-Sarawi, M., 1998, Late quaternary Sabkha sedimentation along Kadhmah Bay Coast, Kuwait, Arabian Gulf: Arab Gulf Journal of Scientific Research, v. 16, p. 471-495.

Al-Zamel, A., Al-Sarawi, M., and Khader, S., 2007, Coastal geomorphology, hydrodynamics, and biolithofacies in the intertidal and subtidal areas of Umm Al-Namil Island, Kuwait Bay, Kuwait: Journal of Coastal Research, v. 23, p. 501-+.

Alghadban, A. N., 1990, Holocene sediments in a shallow bay, southern coast of Kuwait, Arabian Gulf: Marine Geology, v. 92, p. 237-254.

Allen, J. R. L., 1982, Sedimentary Structures: Their Character and Physical Basis, Volume 1. Developments in Sedimentology 30. Elselvier Science Publishers, Amsterdam.

Alsharhan, A.S., and El-Sammak, A.A., 2004, Grain-size analysis and characterization of sedimentary environments of the United Arab Emirates coastal area: Journal of Coastal Research, v. 20, p. 464-477.

Alsharhan, A. S., and C. G. S. Kendall, 2003, Holocene coastal carbonates and evaporites of the southern Arabian Gulf and their ancient analogues: Earth-Science Reviews, v. 61, p. 191-243.

Anselmetti, F.S., von Salis, G.A., Cunningham, K.J., and Eberli, G.P., 1997, Acoustic properties of Neogene carbonates and siliciclastics from the subsurface of the Florida Keys: implications for seismic reflectivity: Marine Geology, v. 144, p. 9-31.

Aslan, A., 1999, Contrasting styles of Holocene avulsion, Texas Gulf Coastal Plain, USA, *in* Blum, M.D., ed., Special Publication of the International

Association of Sedimentologists, Volume 28: International, Blackwell : Oxford, International, p. 195-209.

Boer, B., and Gliddon, D., 1998, Mapping of coastal ecosystems and halophytes (case study of Abu Dhabi, United Arab Emirates): Marine and Freshwater Research, v. 49, p. 297-301.

Boulos, L., and M. Aldosari, 1994, Checklist of the flora of Kuwait: Journal of the University of Kuwait-Science, v. 21, p. 203-217.

Brice, J. C., 1974, Evolution of meander loops: Geological Society of America Bulletin, v. 85, p. 581-586.

Bridge, J. S., 1985, Paleochannel patterns inferred from alluvial deposits - A critical-evaluation: Journal of Sedimentary Petrology, v. 55, p. 579-589.

Bridge, J. S., 1993a, Description and interpretation of fluvial deposits - A critical perspective: Sedimentology, v. 40, p. 801-810.

Bridge, J. S., 1995, Description and interpretation of fluvial deposits - A critical perspective - Reply: Sedimentology, v. 42, p. 384-389.

Bridge, J. S., 2003, Rivers and floodplains; forms, processes, and sedimentary record: United Kingdom, Blackwell Publishing: Oxford, United

Bridge, J. S., and R. S. Tye, 2001, Interpreting the dimensions of ancient fluvial channel bars, channels, and channel belts from wireline logs and cores (vol 84, pg 1205, 2000): Aapg Bulletin, v. 85, p. 365-365.

Brierley, G. J., 1989, River planform facies models - The sedimentology of braided, wandering and meandering reaches of the Squamish River, British-Columbia: Sedimentary Geology, v. 61, p. 17-35.

Brierley, G. J., and E. J. Hickin, 1991, Channel planform as a non-controlling factor in Fluvial Sedimentology - The case of the Squamish River floodplain, British-Columbia: Sedimentary Geology, v. 75, p. 67-83.

Burchette, T. P., and V. P. Wright, 1992, Carbonate ramp depositional systems: Sedimentary Geology, v. 79, p. 3-57.

Castagna, J. P., 2003, Identifying stratigraphy and fluids using spectral decomposition; the current state of the art, Bulletin of the Houston Geological Society, United States, Houston Geological Society : Houston, TX, United States, p. 19-19.

Chuber, S., and W. C. Pusey, 1985, Productive Permian carbonate cycles, San Andres Formation, Reeves Field, West Texas Casebooks in earth science: United States, Springer-Verlag : New York, NY, United States, 289-307 p.

Davies, R., 2000, Reservoir geology of the Middle Minagish Member (Minagish Oolite), Umm Gudair Field, Kuwait, *in* C. Hollis, C. Bishop, R. Gaur, and A. A. Haider, eds., Special Publication - Society for Sedimentary Geology, United States, Society for Sedimentary Geology (SEPM) : Tulsa, OK, United States, p. 273-286.

__, 2004, 3D seismic technology; are we realising its full potential?, *in* S. A. Stewart, J. A. Cartwright, M. Lappin, R. Johnston, S. I. Fraser, and A. R. Brown, eds., Memoirs of the Geological Society of London, United Kingdom, Geological Society of London : London, United Kingdom, p. 1-9.

—, 2005, Geologic processes in sedimentary basins inferred from three-dimensional seismic imaging, *in* Posamentier, H.W., ed., GSA Today, Volume 15: United States, Geological Society of America (GSA) : Boulder, CO, United States, p. 4-9.

Ekstrom, M. P., 1987, Formation imaging with microelectrical scanning arrays, *in* C. A. Dahan, M. Y. Chen, P. M. Lloyd, and D. J. Rossi, eds., Log Analyst, United States, Society of Professional Well Log Analysts : Houston, TX, United States, p. 294-306.

Elsayed, M. I., and D. Albakri, 1994, Geomorphology and sedimentary biosedimentary structures of the intertidal environment along the coast of Kuwait, North-Western Arabian Gulf: Geologische Rundschau, v. 83, p. 448-463.

Ethridge, F.G., 2007, Fluvial seismic geomorphology; a view from the surface, *in* Schumm, S.A., ed., Geological Society Special Publications, Volume 277: United Kingdom, Geological Society of London : London, United Kingdom, p. 205-222.

Evans, G., 1995, The Arabian Gulf; a modern carbonate-evaporite factory, a review, Cuadernos de Geologia Iberica = Journal of Iberian Geology, Spain, Consejo Superior de Investigaciones Cientificas, Universidad de Madrid : Madrid, Spain, p. 61-96.

Evans, G., J. W. Murray, H. E. J. Biggs, R. Bate, and P. R. Bush, 1973, The Oceanography, Ecology, Sedimentology and Geomorphology of Parts of the Trucial Coast Barrier Island Complex, Persian Gulf: Federal Republic of Germany, Springer-Verlag, New York, 233-277 p.

Evans, G., P. Skipwith, and C. G. S. Kendall, 1964, Origin of coastal flats sabkha of Trucial coast Persian Gulf: Nature, v. 202, p. 759-&.

Ferguson, R. I., 1973, Sinuosity of Supraglacial Streams, Geological Society of America Bulletin, United States, Geological Society of America (GSA) : Boulder, CO, United States, p. 251-255.

Freeman, T., 1962, Quiet water oolites from Laguna Madre, Texas, Journal of Sedimentary Petrology, United States, Society of Economic Paleontologists and Mineralogists : Tulsa, OK, United States, p. 475-483.

Friend, P. F., 1979, Vertical and lateral building of river sandstone bodies, Ebro Basin, Spain, *in* M. J. Slater, and R. C. Williams, eds., Journal of the Geological Society of London, United Kingdom, Geological Society of London : London, United Kingdom, p. 39-46.

__, 1983, Towards the field classification of alluvial architecture or sequence, Special Publication of the International Association of Sedimentologists, International, Blackwell: Oxford, International, p. 345-354.

Hall, M., and E. Trouillot., 2004, Predicting stratigraphy with spectral decomposition, 2004 CSEG National Convention Abstracts Volume, Calgary, Canada.

Hunter, R. E., 1977, Basic types of stratification in small eolian dunes, Sedimentology, International, Blackwell : Oxford-Boston, International, p. 361-387.

Gibling, M. R., 2006, Width and thickness of fluvial channel bodies and valley fills in the geological record: A literature compilation and classification: Journal of Sedimentary Research, v. 76, p. 731-770.

Gonzalez, R., and G. P. Eberli, 1997, Sediment transport and bedforms in a carbonate tidal inlet; Lee Stocking Island, Exumas, Bahamas: Sedimentology, v. 44, p. 1015-1030.

Harris, P.M., and J. Ellis, 2008, Satellite imagery and visualization of the Caicos Platform, *in* W. A. Morgan and P. M. Harris, eds., Developing Models and Analogs for Isolated Carbonate Platforms – Holocene and Pleistocene Carbonates of Caicos Platform, British West Indies, SEPM Core Workshop, United States, Society of Economic Paleontologists and Mineralogists, United States, p. 29-46.

Hofstede, J. L. A., 2006, Application of fluvial morphometric parameters and relations to Wadden Sea tidal drainage basins: Zeitschrift Fur Geomorphologie, v. 50, p. 193-207.

Howari, F. M., and A. K. El-Saiy, 2008, Characterization of recent sediments between Abu Dhabi and Dubai coasts, United Arab Emirates, with multiple analytical techniques: Journal of Coastal Research, v. 24, p. 74-82.

Hooke, J. M., 2007b, Complexity, self-organisation and variation in behaviour in meandering rivers, Geomorphology, Netherlands, Elsevier : Amsterdam, Netherlands, p. 236-258.

Hunter, R.E., 1977, Basic types of stratification in small eolian dunes, Sedimentology, Volume 24: International, Blackwell : Oxford-Boston, International, p. 361-387.

Inglis, C.C., 1949, The behaviour and control of rivers and canals (with the aid of models), Central Waterpower, Irrigation and Navigation Research Station Research Publication, v.13, part 1, Poona, India.

Janson, X., 2007, Three-dimensional geological and synthetic seismic model of Early Permian redeposited basinal carbonate deposits, Victorio Canyon, West Texas, *in* Kerans, C., Bellian, J.A., and Fitchen, W., eds., AAPG Bulletin, Volume 91: United States, American Association of Petroleum Geologists : Tulsa, OK, United States, p. 1405-1436.

Jefferson, M. S. W., 1902, National GeographicLimiting width of meander belts, National Geographic, United States, National Geographic Society : Washington, DC, United States.

Jindrich.V, 1969, Recent carbonate sedimentation by tidal channels in lower Florida Leys: Journal of Sedimentary Petrology, v. 39, p. 531-&.

Kaczmarek, S. E., and F. J. Hasiuk., 2008, Mapping surficial sediment distributions on Caicos Platform: A quantitative approach integrating statistical analysis of Landsat spectral data and field observations, *in* W. A. Morgan and P. M. Harris, eds., Developing Models and Analogs for Isolated Carbonate Platforms – Holocene and Pleistocene Carbonates of Caicos Platform, British West Indies, SEPM Core Workshop, United States, Society of Economic Paleontologists and Mineralogists, United States, p. 57-74.

Kendall, C. G. S. C., 1968, Recent algal mats of a Persian Gulf lagoon, *in* P. A. d'E. Skipwith B, ed., Journal of Sedimentary Petrology, United States, Society of Economic Paleontologists and Mineralogists : Tulsa, OK, United States, p. 1040-1058.

__, 1969, Geomorphology of a recent shallow-water carbonate province; Khor Al Bazam, Trucial Coast, southwest Persian Gulf, *in* P. A. d. E. Skipwith, ed., Geological Society of America Bulletin, United States, Geological Society of America (GSA) : Boulder, CO, United States, p. 865-891.

__, 2008, First view of the cyanobacterial mats and strandline evaporite/carbonate deposits of Abu Dhabi; a personal retrospective, GeoArabia [Manama], Bahrain, Gulf Petrolink in Bahrain : Manama, Bahrain, p. 156-157.

Kirkham, A., and G. Evans, 2008, Giant burrows in the Quaternary Limestones of Futaysi Island and Al Dabb'iya, Abu Dhabi Emirate, p. 324-331

Laughlin, K., Garossino, P., and G. Partyka, 2003, Spectral Decomposition for Seismic Stratigraphic Patterns, AAPG Search and Discovery Article#40096 (2003).

Leopold, L. B., 1960, River meanders, *in* M. G. Wolman, ed., Geological Society of America Bulletin, United States, Geological Society of America (GSA) : Boulder, CO, United States, p. 769-793.

Loreau, J. P., and Purser, B.H., 1973, Distribution and ultrastructure of Holocene ooids in the Persian Gulf, *in* B. H. Purser, ed., The Persian Gulf; Holocene Carbonate Sedimentation and Diagenesis in a Shallow Epicontinental Sea, Federal Republic of Germany, Springer-Verlag, New York, p. 471.

Lorenz, J. C., 1985, Determination of widths of meander-belt sandstone reservoirs from vertical downhole data, Mesaverde Group, Piceance Creek basin, Colorado, *in* D. M. Heinze, J. A. Clark, and C. A. Searls, eds., AAPG Bulletin, United States, American Association of Petroleum Geologists : Tulsa, OK, United States, p. 710-721.

Makaske, B., D. G. Smith, and H. J. A. Berendsen, 2002, Avulsions, channel evolution and floodplain sedimentation rates of the anastomosing upper Columbia River, British Columbia, Canada: Sedimentology, v. 49, p. 1049-1071.

Miall, A. D., 1977a, A review of the braided-river depositional environment, Earth-Science Reviews, Netherlands, Elsevier : Amsterdam, Netherlands, p. 1-62.

__, 2002, Architecture and sequence stratigraphy of Pleistocene fluvial systems in the Malay Basin, based on seismic time-slice analysis: AAPG Bulletin, v. 86, p. 1201-1216.

__, 2006, Reconstructing the architecture and sequence stratigraphy of the preserved fluvial record as a tool for reservoir development: A reality check: Aapg Bulletin, v. 90, p. 989-1002.

Morozova, G. S., and N. D. Smith, 2000, Holocene avulsion styles and sedimentation patterns of the Saskatchewan River, Cumberland Marshes, Canada: Sedimentary Geology, v. 130, p. 81-105.

Partyka, G., 1999, Interpretational applications of spectral decomposition in reservoir characterization, *in* J. Gridley, and J. Lopez, eds., Leading Edge [Tulsa, OK], United States, Society of Exploration Geophysicists : Tulsa, OK, United States, p. 353.

Picha, F., 1978, Depositional and diagenetic history of Pleistocene and Holocene oolitic sediments and sabkhas in Kuwait, Persian Gulf, Sedimentology, International, Blackwell: Oxford-Boston, International, p. 427-448.

Purser, B. H., 1973, The Persian Gulf; Holocene Carbonate Sedimentation and Diagenesis in a Shallow Epicontinental Sea, Federal Republic of Germany, Springer-Verlag, New York, p. 1-471.

Posamentier, H. W., 2000, Seismic stratigraphy into the next millennium; a focus on 3D seismic data, Annual Meeting Expanded Abstracts - American Association of Petroleum Geologists, United States, American Association of Petroleum Geologists and Society of Economic Paleontologists and Mineralogists (AAPG) : Tulsa, OK, United States, p. 118-118.

__, 2004, Seismic geomorphology; imaging elements of depositional systems from shelf to deep basin using 3D seismic data; implications for exploration and development, Memoirs of the Geological Society of London, United Kingdom, Geological Society of London : London, United Kingdom, p. 11-24.

Purser, B. H., and E. Seibold, 1973, The Principal Environmental Factors Influencing Holocene Sedimentation and Diagenesis in the Persian Gulf: Federal Republic of Germany, Springer-Verlag, New York, 1-9 p.

Rankey, E. C., B. Riegl, and K. Steffen, 2006, Form, function and feedbacks in a tidally dominated ooid shoal, Bahamas: Sedimentology, v. 53, p. 1191-1210.

Ruppel, S. C., 1984, The Chappel Formation (Mississippian) of the eastern Palo Duro Basin; development of a carbonate shoal, SEPM Core Workshop, United States, Society of Economic Paleontologists and Mineralogists, United States, p. 58-93.

Rust, B. R., 1978, A classification of alluvial channel systems, Memoir - Canadian Society of Petroleum Geologists, Canada, Canadian Society of Petroleum Geologists : Calgary, AB, Canada, p. 187-198.

Saleh, A., F. Al-Ruwaih, A. Al-Reda, and A. Gunatilaka, 1999, A reconnaissance study of a elastic coastal sabkha in Northern Kuwait, Arabian Gulf: Journal of Arid Environments, v. 43, p. 1-19.

Schumm, S. A., 1960a, The effect of sediment type on the shape and stratification of some modern fluvial deposits, American Journal of Science, United States, Kline Geology Laboratory, Yale University: New Haven, CT, United States, p. 177-184.

__, 1960b, The shape of alluvial stream channels in relation to sediment type, Journal of Geophysical Research, United States, American Geophysical Union: Washington, DC, United States, p. 1638-1638.

__, 1961, The effect of sediment type on the shape and stratification of some modern fluvial deposits; a reply, American Journal of Science, United States, Kline Geology Laboratory, Yale University : New Haven, CT, United States, p. 234-239.

__, 1963b, Sinuosity of alluvial rivers on the Great Plains, Geological Society of America Bulletin, United States, Geological Society of America (GSA) : Boulder, CO, United States, p. 1089-1099.

__, 1968, Speculations concerning paleohydrologic controls of terrestrial sedimentation, Geological Society of America Bulletin, United States, Geological Society of America (GSA) : Boulder, CO, United States, p. 1573-1588.

__, 1981, Evolution and response of the fluvial system, sedimentologic implications, Special Publication - Society of Economic Paleontologists and Mineralogists, United States, SEPM (Society for Sedimentary Geology) : Tulsa, OK, United States, p. 19-29.

Shinn, E. A., 1973a, Carbonate Coastal Accretion in an Area of Longshore Transport, NE Qatar, Persian Gulf: Federal Republic of Germany, Springer-Verlag, New York, 179-191 p.

__, 1973b, Recent Intertidal and Nearshore Carbonate Sedimentation around Rock Highs, E Qatar, Persian Gulf: Federal Republic of Germany, Springer-Verlag, New York, 193-198 p.

__, 1973c, Sedimentary Accretion along the Leeward, SE Coast of Qatar Peninsula, Persian Gulf: Federal Republic of Germany, Springer-Verlag, New York, 199-209 p.

__, 1983, Tidal flat environment, AAPG Memoir, United States, American Association of Petroleum Geologists: Tulsa, OK, United States, p. 171-210.

Shreve, R. L., 1966, Statistical law of stream numbers, Journal of Geology, United States, University of Chicago Press : Chicago, IL, United States, p. 17-37.

__, 1967, Infinite topologically random channel networks, Journal of Geology, United States, University of Chicago Press : Chicago, IL, United States, p. 178-186.

Swenson, J. B., C. Paola, L. Pratson, V. R. Voller, and A. B. Murray, 2005, Fluvial and marine controls on combined subaerial and subaqueous delta progradation: Morphodynamic modeling of compound-clinoform development: Journal of Geophysical Research-Earth Surface, v. 110, p. 1-16.

Taylor, J. C. M., and Illing, L.V., 1969, Holocene intertidal calcium carbonate cementation, Qatar, Persian Gulf, Sedimentology, International, Blackwell: Oxford-Boston, International, p. 69-107.

Tornqvist, T. E., 1993, Holocene alternation of meandering and anastomosing fluvial systems in the Rhine-Meuse Delta (central Netherlands) controlled by sea-level rise and subsoil erodibility, Journal of Sedimentary Petrology, United States, Society of Economic Paleontologists and Mineralogists : Tulsa, OK, United States, p. 683-693.

Wagner, C. W., and C. Van der Togt, 1973, Holocene sediment Types and Their Distribution in the Southern Persian Gulf: Federal Republic of Germany, Springer-Verlag, New York, 123-155 p.

Wanless, H. R., 1993, Comparison of oolitic sand bodies generated by tidal vs. wind-wave agitation, *in* L. P. Tedesco, ed., AAPG Studies in Geology, United States, American Association of Petroleum Geologists : Tulsa, OK, United States, p. 199-225.

Wanless, H.R., and J. J. Dravis., 2008, Role of storms and prevailing energy in defining sediment body geometry, composition, and texture on Caicos Platform, *in* W. A. Morgan and P. M. Harris, eds., Developing Models and Analogs for Isolated Carbonate Platforms – Holocene and Pleistocene Carbonates of Caicos Platform, British West Indies, SEPM Core Workshop, United States, Society of Economic Paleontologists and Mineralogists, United States, p. 13-20.

Westphal, H., G. P. Eberli, L. B. Smith, G. M. Grammer, and J. Kislak, 2004, Reservoir characterization of the Mississippian Madison Formation, Wind River Basin, Wyoming: Aapg Bulletin, v. 88, p. 405-432.

Williams, G. P., 1986, River meanders and channel size, Journal of Hydrology, Netherlands, Elsevier : Amsterdam, Netherlands, p. 147-164.

Wilkinson, B. H., 2004, Facies mosaics across the Persian Gulf and around Antigua; stochastic and deterministic products of shallow-water sediment accumulation, *in* C. N. Drummond, ed., Journal of Sedimentary Research, United States, Society of Economic Paleontologists and Mineralogists : Tulsa, OK, United States, p. 513-526.

Wood, L. J., 2003, Applying sequence stratigraphy and seismic stratal slice technology in the Gulf of Mexico, *in* T. Hentz, H. Zeng, M. DeAngelo, and S.

Dutton, eds., GasTips, United States, Hart Publications for Gas Research Institute : Potomac, MD, United States, p. 10-21.

__, 2007, Quantitative seismic geomorphology of Pliocene and Miocene fluvial systems in the northern Gulf of Mexico, U.S.A, Journal of Sedimentary Research, United States, Society for Sedimentary Geology : Tulsa, OK, United States, p. 713-730.

Wunderlich, A., 2008, Seismic Model of a Mixed Siliciclastic-Carbonate Ramp to Basin Transition: Southwest Paradox basin, Colorado and Utah, USA, Unpublished Diploma Thesis, Technische Universitaet, Freiberg, Germany, p. 103.

Xu, C., 2007, Interpreting shoreline sands using borehole images; a case study of the Cretaceous Ferron Sandstone Member in Utah, AAPG Bulletin, United States, American Association of Petroleum Geologists : Tulsa, OK, United States, p. 1319-1338.

Yilmaz, O., 1987, Seismic data processing Investigations in geophysics: United States, Soc. Explor. Geophys. : Tulsa, OK, United States.

Zeller, J., 1967, Meandering channels in Switzerland, Publication - Association Internationale d'Hydrologie Scientifique = Publication - International Association of Scientific Hydrology, International, International Association of Scientific Hydrology, International, p. 174-186.

Zeng, H., 2001, From seismic stratigraphy to seismic sedimentology; a sensible transition, Bulletin - Corpus Christi Geological Society, United States, Corpus Christi Geological Society : Corpus Christi, TX, United States, p. 9-16.

__, 2006, Seismic imaging? Try stratal slicing, AAPG Explorer, United States, American Association of Petroleum Geologists : Tulsa, OK, United States, p. 28-28.

CHAPTER 5. GEOPOLITICAL EFFECTS ON HYDROCARBON PRODUCTION FROM MIDDLE EASTERN OIL AND GAS FIELDS: A CASE STUDY FROM IRAQ

Abstract

Exploration and production companies often face challenges when attempting to strike a balance between appeasing authorities and exploiting hydrocarbons while maintaining sustainable development. Ethnically diverse Iraq contains proven petroleum reserves of 115 billion barrels. To allow access to this oil, the U.S. government drafted the Iraqi Oil and Gas Law. This law, which is unpopular with 70 percent of Iraqis, has not been implemented due to opposition from Kurds and Shi'a, the two groups that control all of Iraq's major oil fields. Kurds oppose the law because it provides the state government in Baghdad control over oil that can be potentially used to fund an independent Kurdish state. Shi'a oppose the law because of the nature of the contracts it proposes. The law promotes Production Sharing Agreements (PSAs), which are long-term (>50 years) contracts that allow foreign companies to own the state's oil without paying royalty. Foreign investors prefer such longterm contracts because it takes a decade to understand the production behavior of an oil field. Because of this dead-lock between foreign investors and the two ethnic groups, Iraq is currently the 11th largest producer; despite having the 2nd largest reserves in the world.

Policy recommendations in this study include amendments regarding oil fields in Kurdish territory and healthy alternatives to PSAs that would ensure the flow of

oil from Iraq while maintaining sustainable development. These include exclusion of oil fields in the Kurdish territory, which constitute only 3 percent of Iraq's oil reserves, from article 5a of the Iraqi Oil and Gas Law. This study recommends the use of contracts, such as Technical Service Agreements, that satisfy both the foreign oil companies and the Iraqi populace.

5.0 Introduction

Once hydrocarbons have been discovered, their exploitation is governed by economics of development and production. Infrastructure needs to be created that allows efficient transportation of oil and gas from the sub-surface to consumers. This process can be complicated if the political situation around oil and gas fields is not conducive to production. Such is the case in countries where either the government (Venezuela, Bolivia) or locals (Nigeria) oppose foreign intervention in oil production. Most Middle Eastern oil and gas fields are located in politically volatile zones. Whether these are in countries with economic sanctions (Iran), authoritarian monarchies (Saudi Arabia, Kuwait, UAE, Qatar, Bahrain, Oman), or in areas of sectarian crisis (Iraq), the geopolitical scene determines how hydrocarbons are produced. Using Iraq as a case study, this paper investigates the problems associated with maintaining sustainability during the exploitation of oil and gas from conflict zones. Local dissent against large corporations in such countries is often linked to corruption within the government. Funds generated by the government from oil royalties are not used to improve the quality of life for the general populace. Therefore, this study also recommends policies that will allow efficient development of oil and gas fields while ensuring sustainability for locals.

At 115 billion barrels of oil, Iraqi oil reserves are the third largest in the world (Energy Information Administration, 2007). Analysts show that this number may increase to 214 billion barrels once unexplored fields are added (Blanche, 2007a). Despite the richness of hydrocarbons, Iraq has the lowest reserve-to-production ratio of all major oil-producing countries (Sever, 2008). The reasons for this are political instability and the lack of infrastructure. Large Western oil companies such as ExxonMobil will not enter Iraq unless personnel on the ground feel safe (Ian Russell, personal communication, 2007). The security situation in Iraq has deteriorated as Iraq has replaced Afghanistan as a hot bed of Global Jihadism (Hegghammer, 2006). Corporations will not invest in Iraq unless a law safeguards their investments. According to James Paul, executive director of Global Policy Forum in New York, "the Exxons of the world know it is better to wait until legality is established in Iraq." To grant foreign companies access to Iraqi Oil, the Bush Administration introduced a draft of the Iraq Oil and Gas Law to the Iraqi parliament on February 27, 2007. Noori al-Maliki's government approved the law but could not implement it after opposition from Shi'a and Kurd representatives in parliament (Blanche 2007a). The law is still pending approval, and recently countries such as China have decided to take the risk and sign contracts with the Iraqi government even though the law has not been implemented. Western oil companies, such as ExxonMobil and ConocoPhillips, collaborate with the Northern Oil Company of Iraq on small-scale projects, but full-scale exploitation of Iraq's hydrocarbon reserves will not proceed until the Oil Law is approved.

5.1 Background

To fully appreciate the complexity surrounding sectarianism in Iraq and why it affects oil production, it is imperative to understand Iraq's post-colonial history. Iraq, like most countries in the Middle East, is an artifact of European style-nation state building. Prior to European occupation, the Ottoman Empire controlled Iraq in three parts, the northern Kurdish province of Mosul, the central province of Baghdad and the southern province of Basra. These divisions were based on the distribution of ethnic groups (Cleveland, 2004). In 1920 the British created the Mandate of Iraq and drew boundaries that would encompass northern and southern oil fields. In 1918 Sir Maurice Hankey, Britain's first Secretary of World War I wrote:

> Oil in the next war will occupy the place of coal in the present war, or at least a parallel place to coal. The only big potential supply that we can get under British control is the Persian (now Iran) and Mesopotamian (now Iraq) supply...Control over these oil supplies becomes a first class British war aim (Yergin, 1991).

Shortly after, the British appointed a Syrian, King Faisal, to govern Iraq. King Faisal signed a concession contract with the Iraq Petroleum Company, a consortium of British, French and American Oil Companies. The terms of the contract would last for 75 years (Muttitt, 2005).

Today, the some of the most prolific Iraqi Oil fields are in northern Iraq (Fig. 5.0), which is still dominated by the Kurds who seek independence and refuse to fly the Iraqi flag since US occupation in 2003. The largest oil fields (Fig. 5.0) are in the southwest in Shi'a controlled territory. Central Iraq has a large Sunni population but no major oil fields. Although the majority of Iraqis are Shi'a, ever since the British appointed Amir Faisal as King of Iraq in 1921, the political leaders have been Sunni. This has led to hostility between Shi'a and Sunni over decades, especially during the oppressive regime of Saddam Hussein, when Shi'a were persecuted. Since the removal of Saddam Hussein each of the three main groups, the Shi'a, Sunni and Kurd strive to control Iraq's oil wealth.

5.2 Opposition to the Oil Law

According to a recent survey, 70 percent of Iraqis oppose the Oil Law (Sever, 2008). However, the reasons for opposition vary from one group to another.

The greatest opposition comes from Kurds who control northern Iraq in the form of a semi-autonomous government (Kurdish Regional Government). Northern Iraq contains the famous Kirkuk and Tikrit oil fields. Currently, one third of all the oil produced in Iraq comes from Kurdish territory (Blanche 2007a). To the dismay of the central government in Baghdad, the Kurdish Regional Government (KRG) started providing leases to foreign oil companies in the beginning of 2004, before the Oil and Gas Law became public. Since then, they

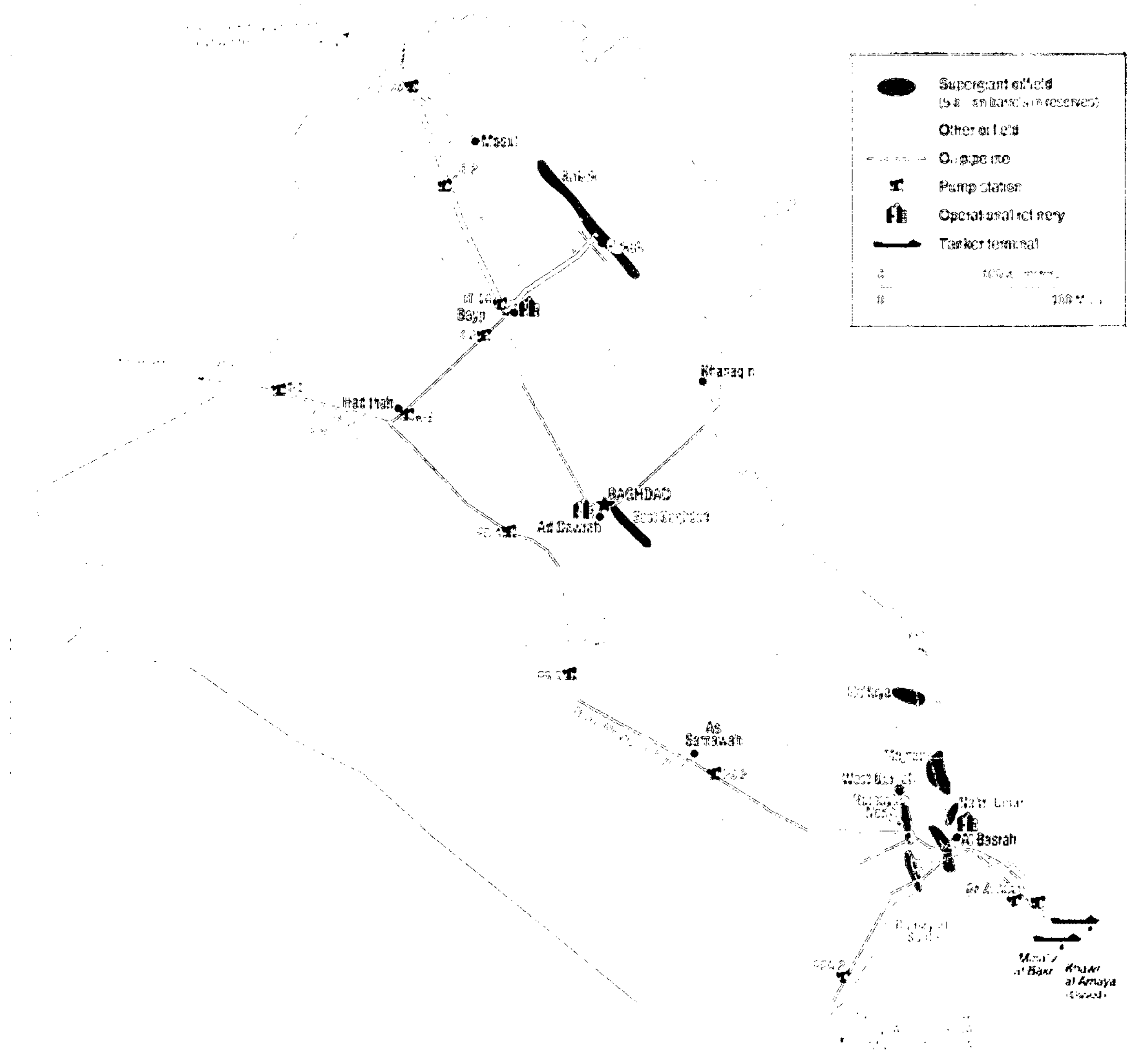

Figure 5.0. Location of Iraqi Oil and Gas Fields. Notice the presence of supergiant oil fields in the Kurdish and Shi'a dominated areas and their absence from Sunni dominated north-central Iraq. (image reproduced from University of Texas Middle East Center Webpage)

have been collaborating with Hunt Oil, Addax Oil and Gas, Heritage Oil Corporation, OMV and Perenco.

The majority of these companies (with the exception of Hunt) are European and Canadian mid-sized, independent operators who work on a very low profit margin and are willing to risk their reputation. They are opportunists who would rather increase the capital of their firm when the price of oil is high than wait for the state government in Baghdad to open public bidding for oil leases. The Kurdish Regional Government welcomes their business as it provides them not only with funding that can be used to gain independence but legitimacy as a form of government. To prevent the secession of Kurdistan from the rest of Iraq, the Oil Law explicitly states that the Iraqi Oil and Gas Council will make decisions on all dealings with international oil firms.

The Council of Representatives shall approve all international petroleum treaties related to Petroleum Operations that Iraq signs with other countries.

(Article 5a)

This law applies to Petroleum operations <u>in all the territory of the Republic of Iraq</u>, including the soil and subsoil on land, as well as inland waters and territorial waters.

(Article 1a)

The Kurds dislike the fact that decisions regarding oil in their territory are made by a Shi'a dominated government in Baghdad. Kurds have long sought autonomy and see oil as a source of funding that could potentially fund their independence struggle and boost economy once autonomy is achieved (Blanche, 2007b). The Kurds feel strongly about the status of Kirkuk and other large oil and gas fields within their territory. According to Massoud Barzani, the president of the Kurdish Regional Government, "There are five or six issues on which I will not compromise: Identity, borders, peshmergas, budget, the oil law and Kirkuk" (Blanche, 2007b).

The second group that opposes the Oil Law is the Shi'a. Dissent is expressed in the form of attacks on well sites, pipelines and refineries. Between April 2003 and May 2007, there were 400 attacks on Iraq's oil infrastructure (EIA, 2007). This affects the price of oil to consumers in the United States is because traders will add $4 to $8 to the price of a barrel of oil as "risk premium[2]" (Banerjee, 2004). It affects Iraq in the sense that, in 2005, Iraq had to spend $4 billion to $5 billion to import fuel (Glanz and Worth, 2006). The attacks of June 2004 on a major pipeline cost the country up to $1 billion in revenue (Wong and Glanz, 2004). Although most of these attacks are blamed on "insurgents," one group that is responsible for such activities is the Mahdi Army led by Moqtada al-Sadr. In July 2005, followers of al-Sadr joined the opposition on the draft oil law. According to Sheikh Salah al-Obiedi, a Sadr office spokesman, "we reject this unclear law that contains a number of points which prevent us from accepting it...this law has no grounding in Iraqi reality" (AFX News Limited, 2007). According to Nassar al-Rubaie, the spokesperson for al-Sadr's parliamentary bloc, "The most serious problem with the law is the production sharing agreements, which we categorically reject. Such agreements, which provide for foreign oil companies to share investments and profits with the state, would undermine Iraq's sovereignty in the short run and will strip it of its sovereignty in the long run."

---

[2] Risk premium is the difference in price between the expected value of a commodity and the actual value. It is added by traders to compensate for uncertainty associated with shipping and handling in a supply chain.

The concept of Production Sharing Agreements (PSAs) was started by Indonesia in the 1960s. PSAs are a political tool and, although the state controls oil, they are long-term (25-40 years) agreements that are not subject to change. Companies invest in infrastructure and when wells come online, the initial oil is termed 'cost oil.' This oil is tax-free and the companies do not pay royalties to the state. In theory, cost oil is used to cover the company's costs of setting up infrastructure. After this cost is recovered, further production is termed 'profit oil' and that is shared with the state itself. Profit oil may or may not be subject to taxes and royalty.

5.3 Policy recommendations

5.3.0 Amendments regarding oil fields in northern Iraq (Kurdish Territory).

The KRG signed their first contract with a Norweign oil company called DNO in 2004 (Muttitt, 2005). Since then they have signed contracts with Canadian, American, Turkish and Austrian oil companies (Oppel, 2007; Wong and Stolberg, 2007). These companies have been highly successful, and although most have PSAs with the KRG, they have added revenue to the KRG and indirectly funded the Kurdish independence movement. Although these companies are black-listed by Baghdad, that label does little to deter their daily operations in the most politically stable part of Iraq.

The state government in Baghdad seeks to control oil and gas fields located in Kurdish territory. A referendum for Kurdish autonomy which was to be held in 2007 has been delayed indefinitely (Farrell, 2007). Tensions around towns such as Kirkuk, where Saddam Hussein used ethnic cleansing to eradicate native Kurds and settle Shi'a in an effort to control oil and gas fields, are increasing as displaced Kurds return home (Farrell, 2007). Currently, Kurdish oil fields are the only facilities where foreign oil workers feel safe, and this sense of security encourages further investment by foreign companies. Implementation of the Iraqi oil law without amendments to exclude oil and gas fields from central government control could have dire consequences. The implementation will result in sectarian clashes between Kurds and Shi'a populations in volatile areas such as Kirkuk. Lack of security would send panic-stricken foreign oil workers home, and would harm the local economy.

Based on historic and current views held by the Kurds, and for the sake of security around northern oil and gas fields, this study recommends amending the law such that Kurdish territories are not included. Although currently one third of oil is produced in Kurdish territory, reserves in Kurdistan make up only 3 percent of Iraq's proven reserves (Al-Mehdieh, 2006). Although a more permanent solution would be to hold a referendum in Kirkuk and grant them autonomy, the issue of Kurdish independence is beyond the scope of this paper.

5.3.1 The nature of contracts

Production Sharing Agreements are mainly designed for countries where oil fields are small, often offshore, production costs are high, and exploration prospects are uncertain. They seem to work well in countries like Nigeria, Angola, Guinea, Brazil, or Indonesia where drilling is done in deepwater[3] (Anderson et al., 2000; Bruhn, 1998; Bruso et al., 2004; Chapin et al., 2002; Guritno et al., 2003) and the average well costs over $100 million. None of these conditions apply to Iraq, where fields are in the giant, super-giant and elephant categories, all are located onshore, production costs are low (~$10-20 million per well) and reservoirs are the most prolific hydrocarbon producers in the world. The reason that oil companies still prefer PSAs is their duration. It takes a minimum of 10 years of production history for geoscientists and engineers to develop a good understanding of how oil fields function[4]. The lengthy duration of a PSA allows this understanding to develop and keeps the operator of the field motivated to enhance recovery. Short-term contracts do not allow for such a knowledge base to develop and, since there is no long-term commitment, operators lack the motivation to continue applying techniques that would increase the longevity of the field.

Healthy alternatives to PSAs are Risk Service Contracts, Buyback Contracts, Development and Production Contracts, and Technical Service Contracts.

Risk Service Contracts are a model adopted by Algeria and Kuwait. In this model, a foreign company invests capital, and when the well comes online it reimburses its costs from oil sales and a fixed fee per barrel of oil produced. In

---

[3] Deepwater refers to wells drilled offshore in water depths that exceed 500 meters (1650 feet).

[4] 'Understanding of how oil fields function' here refers to the sub-surface changes in pressure, volume, and temperature in the reservoir. Data acquired over the years are used in history matching, reserve estimation, and updating simulation models.

this way the company determines profitability by increasing or decreasing production. The major risk with such service contracts is that if the company drills a dry well or the venture fails, then drilling costs cannot be recovered. Therefore, these are done in areas where risk of drilling dry holes is negligible. For a place like Iraq, where reservoirs are incredibly rich in hydrocarbons, these contracts would work very well.

Buyback Contracts were introduced by Iran in the 1990s. They differ from Risk Service Contracts in their shorter duration (5-7 years). Because of their exceedingly short duration they are not recommended for Iraq.

Development and Production Contracts were used by Iraq prior to the U.S. invasion. They allow a company to invest and investments can either be recovered through cash or oil. However, after a fixed period of 12 years the oilfield is turned over to the national oil company. The foreign company can continue getting oil at the market price or at a discounted rate if it chooses to sign a Technical Service Agreement with the national oil company.

A Technical Service Agreement (TSA) is when a company is hired to carry out certain services under contract for a limited amount of time in exchange for a fee (Muttitt, 2005). This is the most common type of contract that oil companies make with oil-rich states along the Persian Gulf. On September 5th 2008, China signed a 3 billion dollar TSA with Baghdad for the duration of 22 years. This was the largest oil deal Iraq has signed with a foreign country since 2003 (Goode and Mohammed, 2008). China will provide technical advisors, oil workers, and equipment and will help set-up infrastructure to develop the Adhab Field. This deal was initially signed with the Saddam Hussein regime back in 1997, and the original version was a PSA. However, the Chinese have shown a good grasp of Iraqi politics through the revision of the original contract into a TSA. Asim Jihad, a spokesperson for the Iraqi Oil Ministry, attributes this deal to China's "wide experience in this field."

Any one of these contract types would benefit Iraq by allowing it to control decisions regarding its oil, generating revenue, and using the technical expertise that foreign companies possess. For multinational companies it allows them to full access to Iraqi hydrocarbons with very little risk of failure. The terms of all these contracts are significantly shorter than PSAs, which allows both parties flexibility.

5.4 Conclusion

To appease the various rival factions in Iraq, it is important to establish a legal framework that is acceptable to the Iraqi people and oil companies. Policy recommendations in this paper are a small step towards enhanced recovery of hydrocarbons from Iraq while establishing a system that is fair to the Iraqi people. Other issues that have not been discussed in this paper are smuggling of crude oil to Syria and Jordan, and the role of American troops and foreign insurgents in Iraq. However, once foreign companies actively invest in Iraq and the general population of Iraq witness changes in security and infrastructure funded by oil revenues, the country will head towards greater stability. Insurgency thrives on chaos, and a stable Iraq will not be as attractive as a battleground.

5.5 Acknowledgements

I wish to thank Ian Russell at the Middle Eastern Business Unit at ExxonMobil and the Iraq Team at ConocoPhillips for taking the time and helping me understand the complexities surrounding oil recovery from Iraq.

5.6 References

AFX News Limited., 2007, Followers of al-Sadr join opposition on draft Iraq oil law. Forbes, July 5th.

Al-Mahdieh., 2006, Geographical distribution of Iraqi Oil Fields and its relation with the new constitution. Report by the Revenue Watch Institute.

Anderson, J.E., J. Cartwright, S.J. Drysdall, and N. Vivian., 2000, Controls on turbidite sand deposition during gravity-driven extension of a passive margin: Examples from Miocene sediments in Block 4, Angola. Marine and Petroleum Geology, v.17, p. 1165-1203.

Banerjee, N. 2004, Attacks Drive Price of Oil to $40 a Barrel. The New York Times, May 12.

Blanche, E. 2007, Dividing Iraq? *The Middle East.* Issue 383, p. 6-10.

Blanche, E. 2007, The battle for Iraqi Oil. *The Middle East*, Issue 381, p. 6-10.

Bruhn, C.H.L., 1998, Deep-water reservoirs from the eastern Brazilian rift and passive margin basin: AAPG International conference and exhibition, Rio de Janeiro, AAPG Short course notes no. 6.

Bruso, J.M.Jr, S. L. Getz, and R. W. Wallace., 2004, Geology will support further discoveries in the Gulf of Guniea's golden rectangle. Oil and Gas Journal, February 16th, p. 30-38.

Chapin, M., P. Swinburn, R. van der Weiden, D. Skaloud, S. Adesanya, D. Stevens, C. Varley, J. Wilkie, E. Brentjens, and M. Blaauw., 2002, Integrated seismic and subsurface characterization of Bonga Field, offshore Nigeria. The Leading Edge, v. 19, p. 1125-1131.

Cleveland, W.L. 2004, A history of the modern Middle East. Westview Press, Boulder.

Energy Information Administration, 2007, www.eia.gov

Farrell, S. 2007, As Iraqis Vie for Kirkuk's Oil, Kurds are pawns. New York Times, December 9th.

Glanz, J., R.F. Worth. 2006, Attacks on Iraq Oil Industry Aid vast Smuggling Scheme. The New York Times, June 4th.

Goode, E., Mohammed, R. 2008, Iraq signs oil deal with China worth up to $3 billion. *New York Times*, August 29th.

Guritno, E., L. Salvadori., M. Syaiful, I. Buson, A. Mortimer, F.B. Hakim., J. Dunham, J. Decker., and S. Algar., 2003, Deep-water Kutei Basin: A new petroleum province. Proceedings of the Indonesian Petroleum Association, 29th Annual Convention, October 22.

Hegghammer, T. 2006, Global Jihadism After the Iraq War. *Middle East Journal.* Volume 60.

Kramer, A.E. 2007, Iraq, With U.S. Support, Voids a Russian Oil Contract. *New York Times*, November 4th.

Muttitt, G. 2005, Crude Designs: The rip-off of Iraq's oil wealth. Platform publishing, p. 1-47.

Oppel, R.A. 2007, Kurds reach new oil deals, straining ties with Baghdad. New York Times, October 4th.

Sever, M., 2008, Oil and Politics in Iraq. *Geotimes*, Volume 53, p. 24-25.

Wong, E., and J. Glanz., 2004, The reach of war: The insurgency; 2 pipeline blasts halt oil exports at top Iraq port. The New York Times, June 16th.

Wong, E., S.G. Stolberg., 2007, Iraqi Blocs Opposed to Draft Oil Bill. New York Times, May 3rd.

Yergin, D. 1991. The Prize, Simon and Schuster, London, p. 188.

APPENDIX A: NON-PROPRIETARY CORE DESCRIPTIONS OF THE DEVONIAN-MISSISSIPPIAN BAKKEN FORMATION

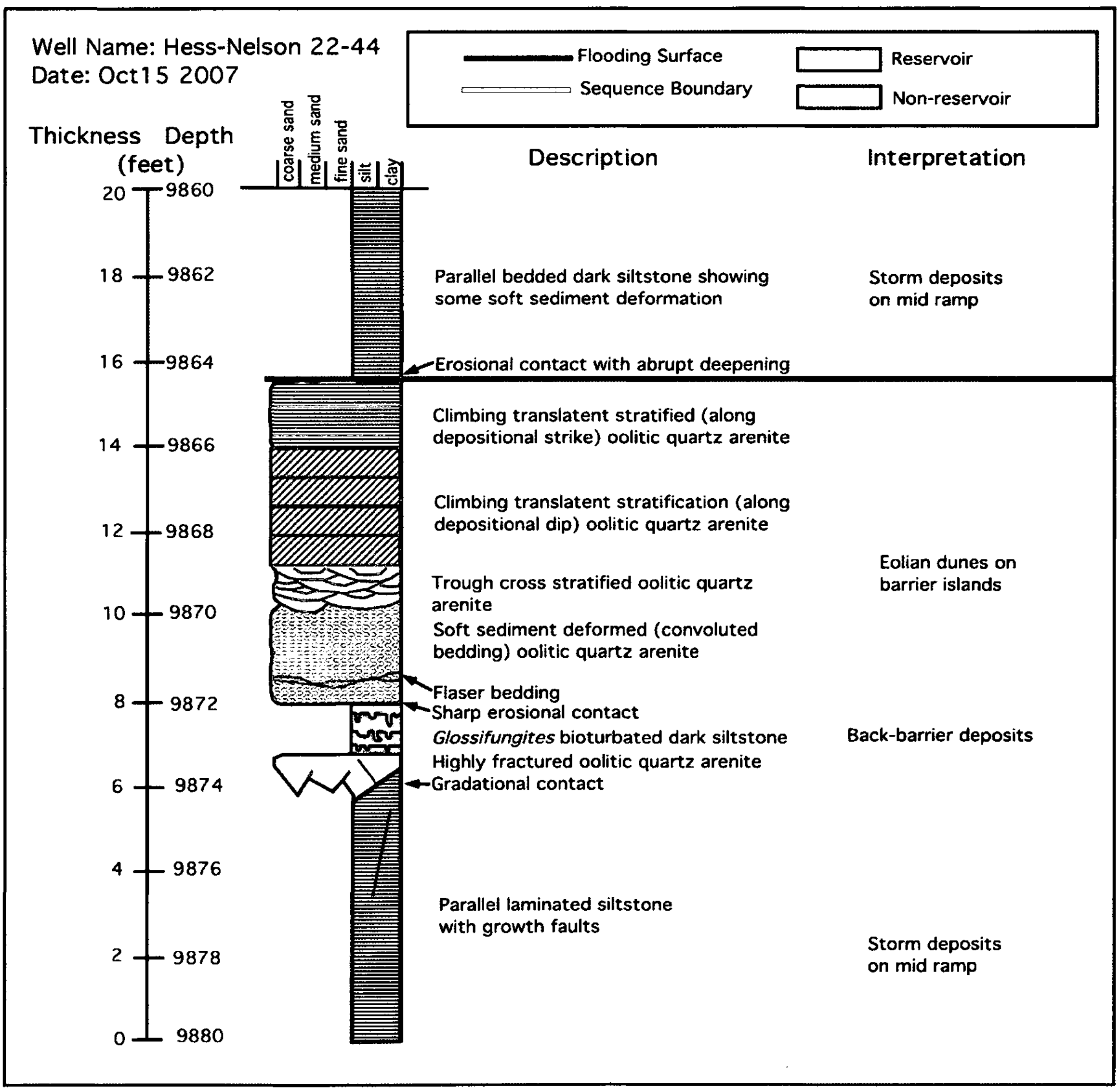

Well Name: Hess-Nelson 22-44
Date: Oct15 2007
Flooding Surface
Sequence Boundary
Reservoir
Non-reservoir
Thickness Depth
(feet)
coarse sand
medium sand
fine sand
silt
clay
Description
Interpretation
20 9860
18 9862
16 9864
14 9866
12 9868
10 9870
8 9872
6 9874
4 9876
2 9878
0 9880
Parallel bedded dark siltstone showing some soft sediment deformation
Storm deposits on mid ramp
Erosional contact with abrupt deepening
Climbing translatent stratified (along depositional strike) oolitic quartz arenite
Climbing translatent stratification (along depositional dip) oolitic quartz arenite
Eolian dunes on barrier islands
Trough cross stratified oolitic quartz arenite
Soft sediment deformed (convoluted bedding) oolitic quartz arenite
Flaser bedding
Sharp erosional contact
Glossifungites bioturbated dark siltstone
Back-barrier deposits
Highly fractured oolitic quartz arenite
Gradational contact
Parallel laminated siltstone with growth faults
Storm deposits on mid ramp

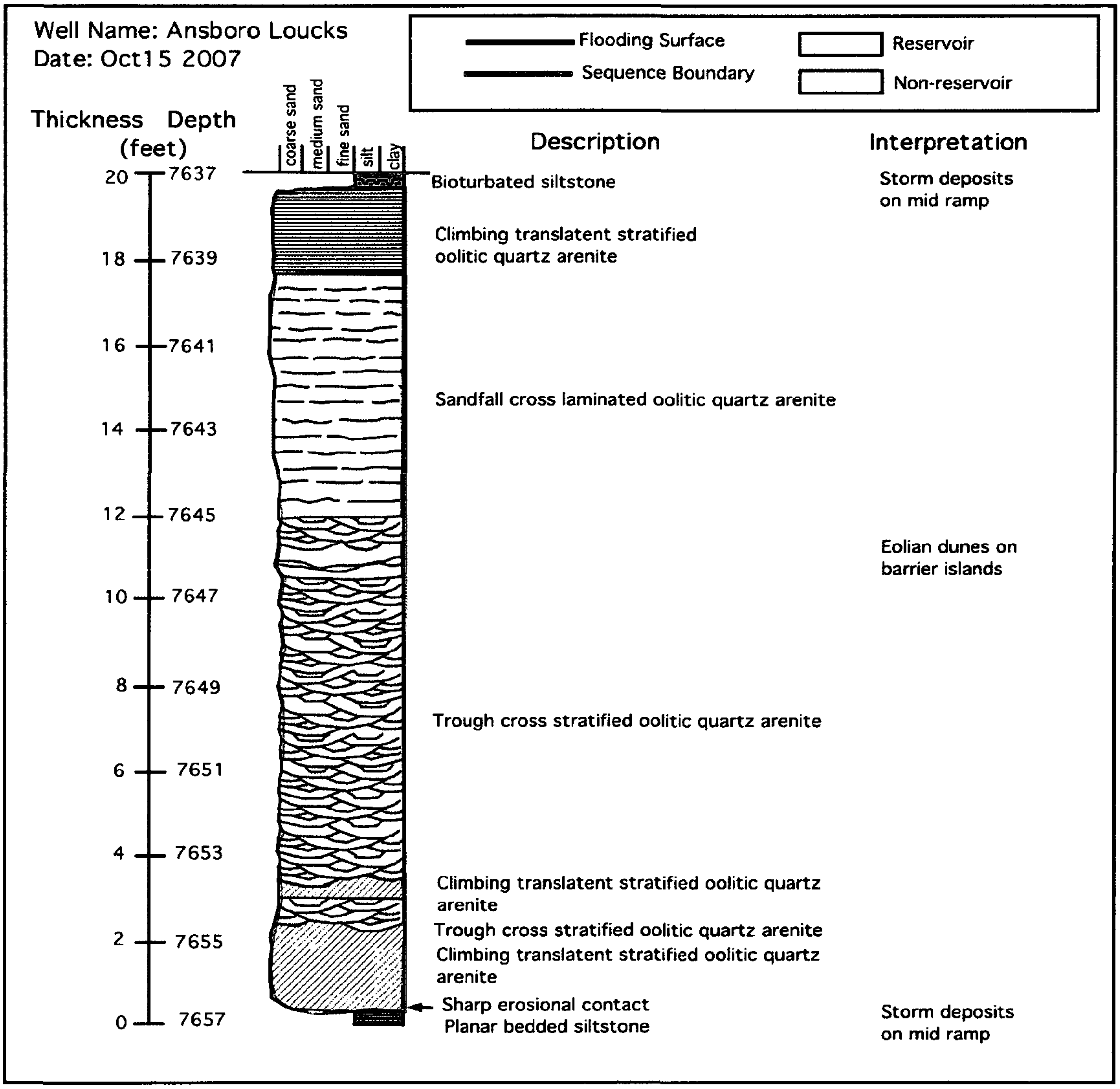
Well Name: Ansboro Loucks
Date: Oct15 2007
Flooding Surface
Sequence Boundary
Reservoir
Non-reservoir
Thickness (feet)
Depth
coarse sand
medium sand
fine sand
silt
clay
Description
Interpretation
20 7637
18 7639
16 7641
14 7643
12 7645
10 7647
8 7649
6 7651
4 7653
2 7655
0 7657
Bioturbated siltstone
Storm deposits on mid ramp
Climbing translatent stratified oolitic quartz arenite
Sandfall cross laminated oolitic quartz arenite
Eolian dunes on barrier islands
Trough cross stratified oolitic quartz arenite
Climbing translatent stratified oolitic quartz arenite
Trough cross stratified oolitic quartz arenite
Climbing translatent stratified oolitic quartz arenite
Sharp erosional contact
Planar bedded siltstone
Storm deposits on mid ramp

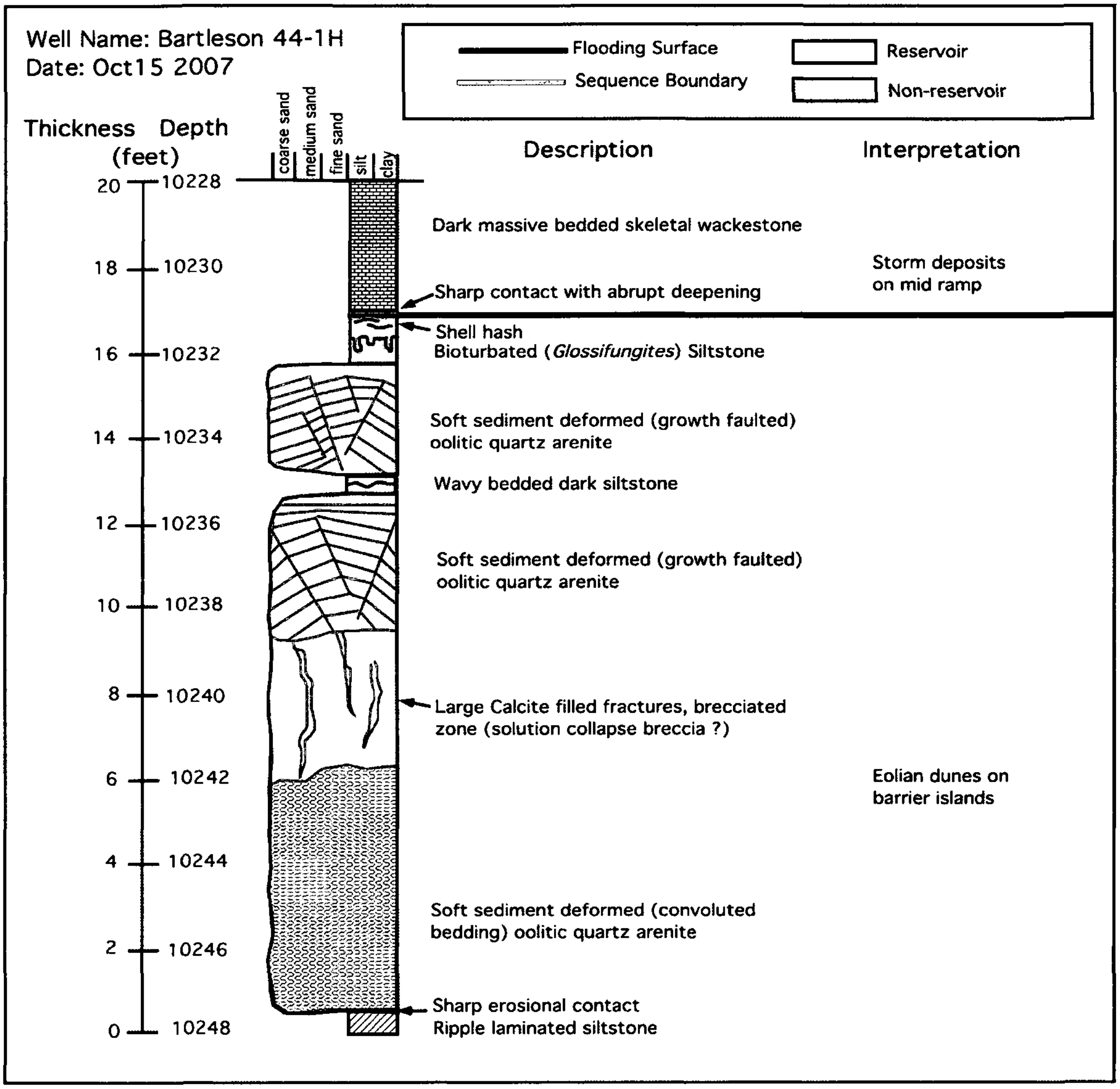
Well Name: Bartleson 44-1H
Date: Oct15 2007
Flooding Surface
Sequence Boundary
Reservoir
Non-reservoir
Thickness
Depth
(feet)
coarse sand
medium sand
fine sand
silt
clay
Description
Interpretation
20
10228
18
10230
16
10232
14
10234
12
10236
10
10238
8
10240
6
10242
4
10244
2
10246
0
10248
Dark massive bedded skeletal wackestone
Storm deposits on mid ramp
Sharp contact with abrupt deepening
Shell hash
Bioturbated (*Glossifungites*) Siltstone
Soft sediment deformed (growth faulted) oolitic quartz arenite
Wavy bedded dark siltstone
Soft sediment deformed (growth faulted) oolitic quartz arenite
Large Calcite filled fractures, brecciated zone (solution collapse breccia ?)
Eolian dunes on barrier islands
Soft sediment deformed (convoluted bedding) oolitic quartz arenite
Sharp erosional contact
Ripple laminated siltstone

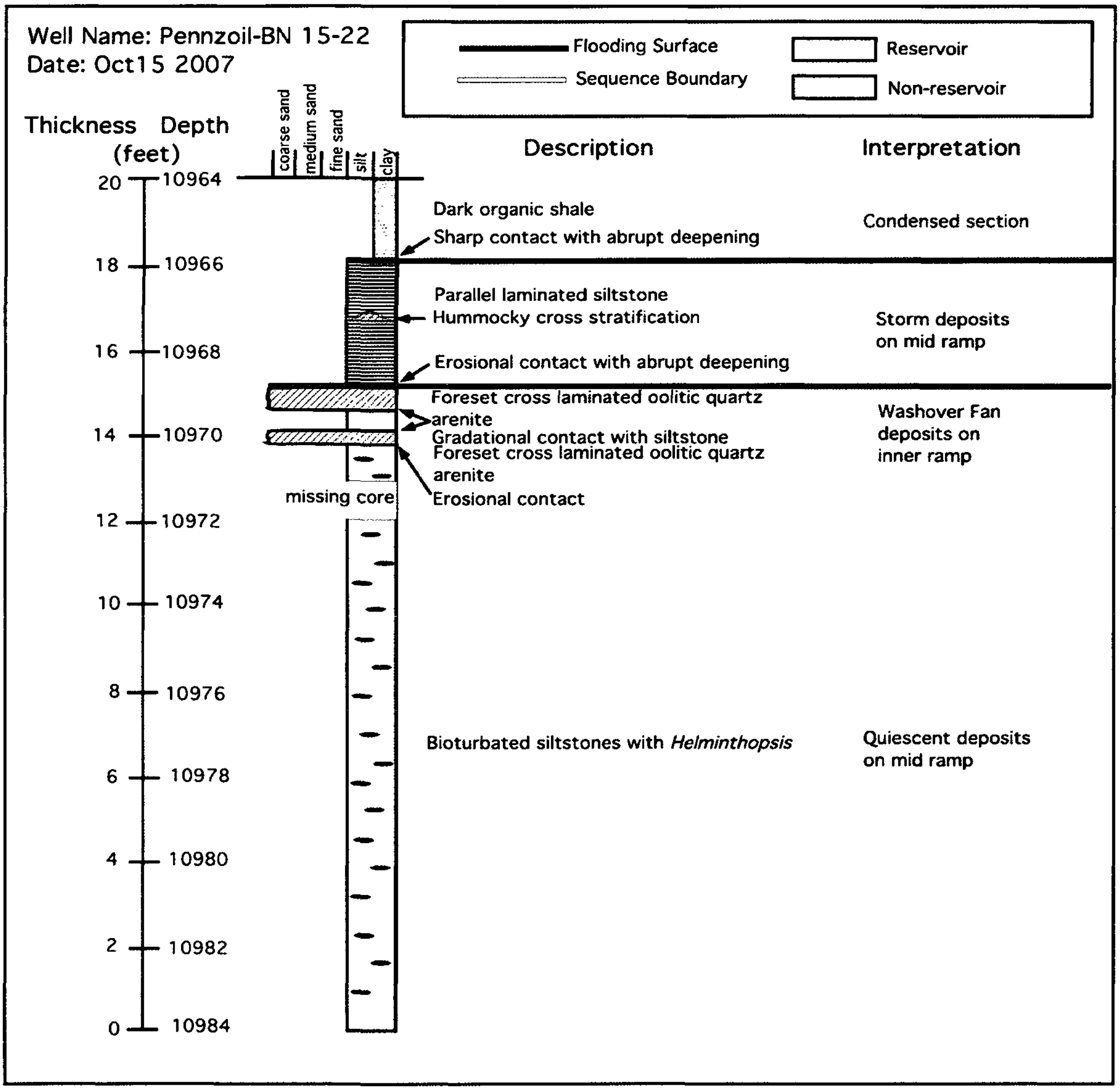
Well Name: Pennzoil-BN 15-22
Date: Oct15 2007
Flooding Surface
Sequence Boundary
Reservoir
Non-reservoir
Thickness Depth (feet)
coarse sand
medium sand
fine sand
silt
clay
Description
Interpretation
20 10964
18 10966
16 10968
14 10970
12 10972
10 10974
8 10976
6 10978
4 10980
2 10982
0 10984
Dark organic shale
Sharp contact with abrupt deepening
Condensed section
Parallel laminated siltstone
Hummocky cross stratification
Erosional contact with abrupt deepening
Storm deposits on mid ramp
Foreset cross laminated oolitic quartz arenite
Gradational contact with siltstone
Foreset cross laminated oolitic quartz arenite
Erosional contact
missing core
Washover Fan deposits on inner ramp
Bioturbated siltstones with *Helminthopsis*
Quiescent deposits on mid ramp

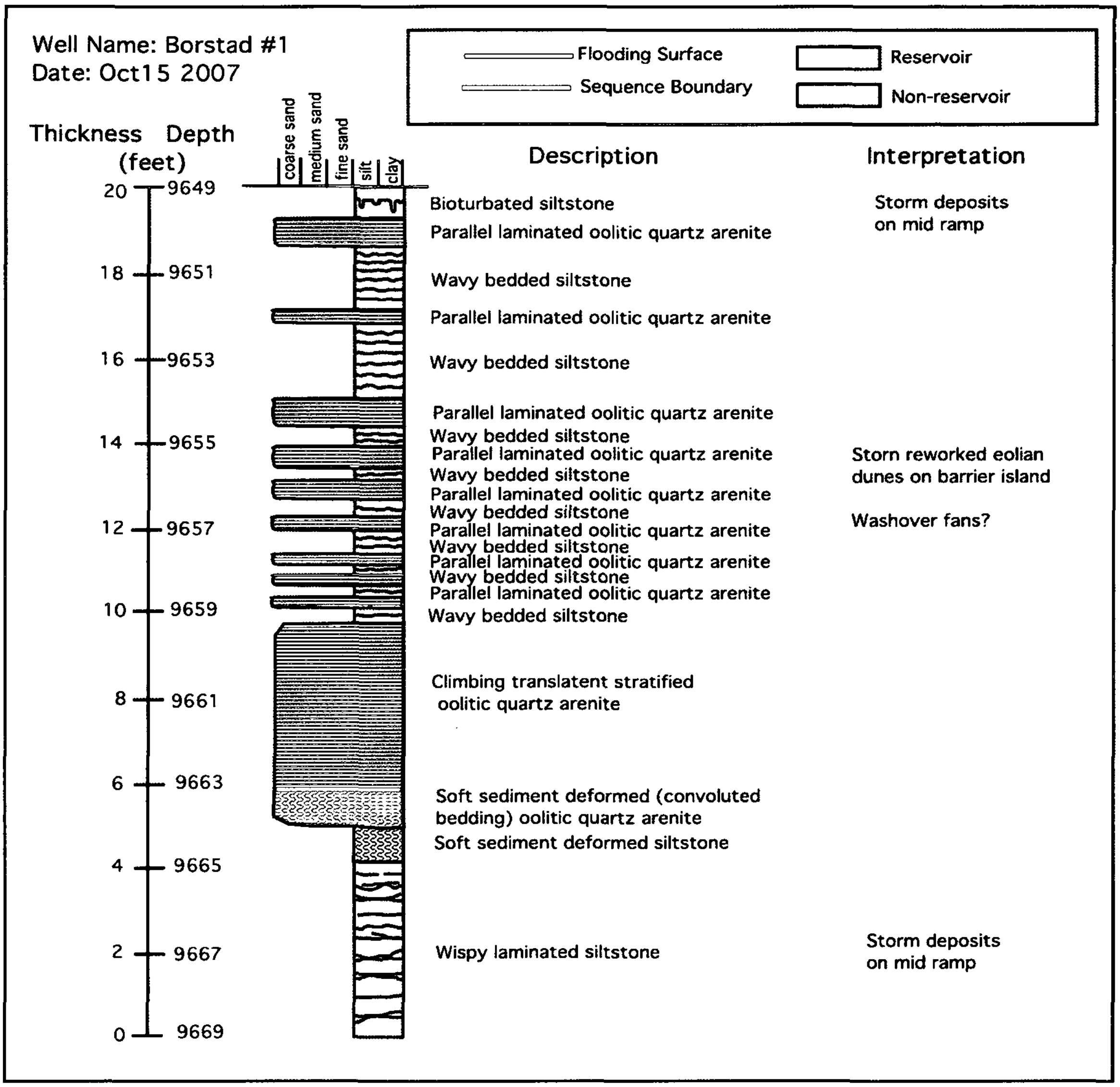
Well Name: Borstad #1
Date: Oct15 2007
Flooding Surface
Sequence Boundary
Reservoir
Non-reservoir
Thickness (feet)
Depth
coarse sand
medium sand
fine sand
silt
clay
Description
Interpretation
20
9649
18
9651
16
9653
14
9655
12
9657
10
9659
8
9661
6
9663
4
9665
2
9667
0
9669
Bioturbated siltstone
Parallel laminated oolitic quartz arenite
Wavy bedded siltstone
Parallel laminated oolitic quartz arenite
Wavy bedded siltstone
Parallel laminated oolitic quartz arenite
Wavy bedded siltstone
Parallel laminated oolitic quartz arenite
Wavy bedded siltstone
Parallel laminated oolitic quartz arenite
Wavy bedded siltstone
Parallel laminated oolitic quartz arenite
Wavy bedded siltstone
Parallel laminated oolitic quartz arenite
Wavy bedded siltstone
Parallel laminated oolitic quartz arenite
Wavy bedded siltstone
Climbing translatent stratified oolitic quartz arenite
Soft sediment deformed (convoluted bedding) oolitic quartz arenite
Soft sediment deformed siltstone
Wispy laminated siltstone
Storm deposits on mid ramp
Storn reworked eolian dunes on barrier island
Washover fans?
Storm deposits on mid ramp

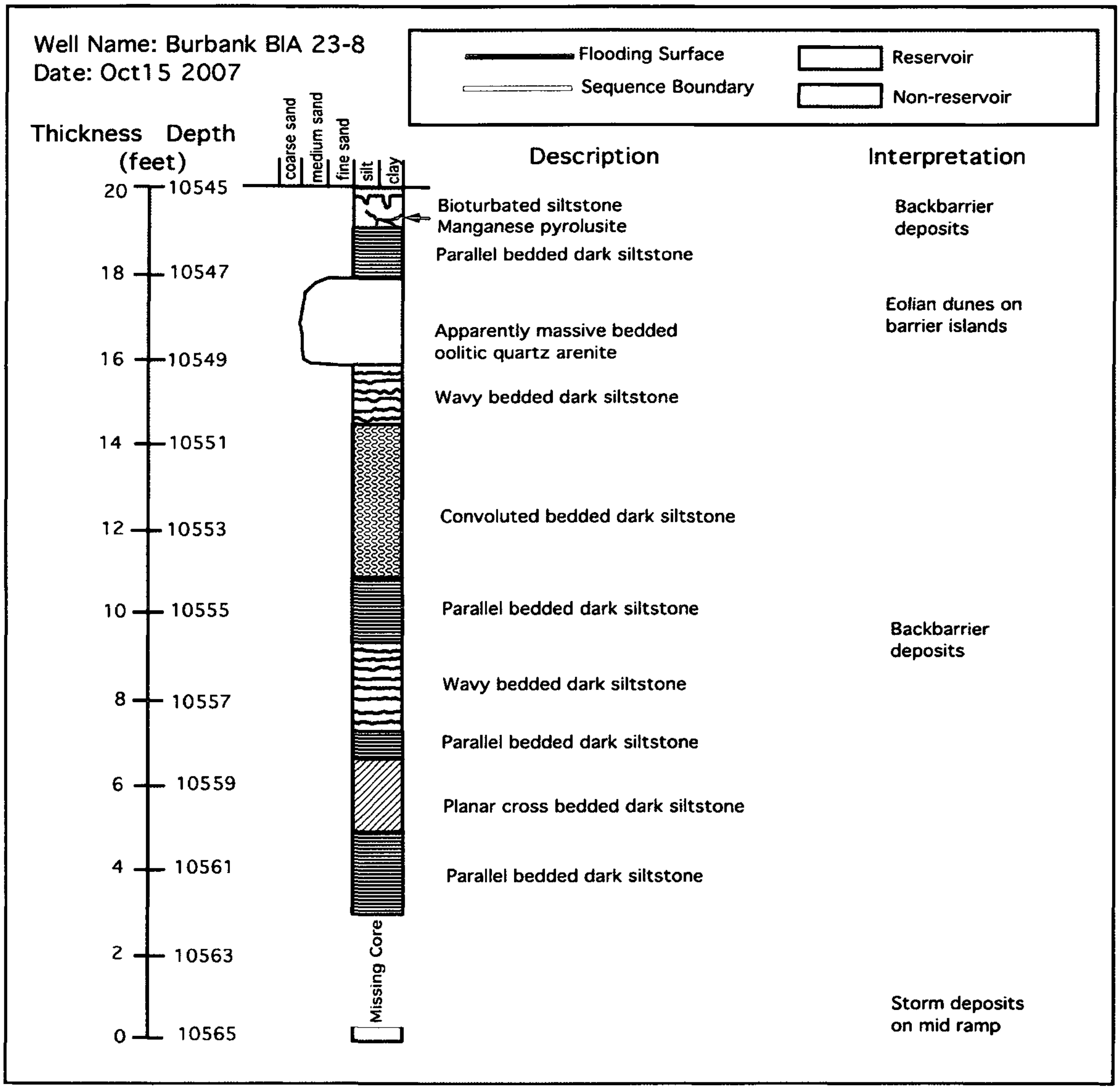

Well Name: Burbank BIA 23-8
Date: Oct15 2007
Flooding Surface
Sequence Boundary
Reservoir
Non-reservoir
Thickness
Depth
(feet)
coarse sand
medium sand
fine sand
silt
clay
Description
Interpretation
20 10545
18 10547
16 10549
14 10551
12 10553
10 10555
8 10557
6 10559
4 10561
2 10563
0 10565
Bioturbated siltstone
Manganese pyrolusite
Parallel bedded dark siltstone
Apparently massive bedded oolitic quartz arenite
Wavy bedded dark siltstone
Convoluted bedded dark siltstone
Parallel bedded dark siltstone
Wavy bedded dark siltstone
Parallel bedded dark siltstone
Planar cross bedded dark siltstone
Parallel bedded dark siltstone
Missing Core
Backbarrier deposits
Eolian dunes on barrier islands
Backbarrier deposits
Storm deposits on mid ramp

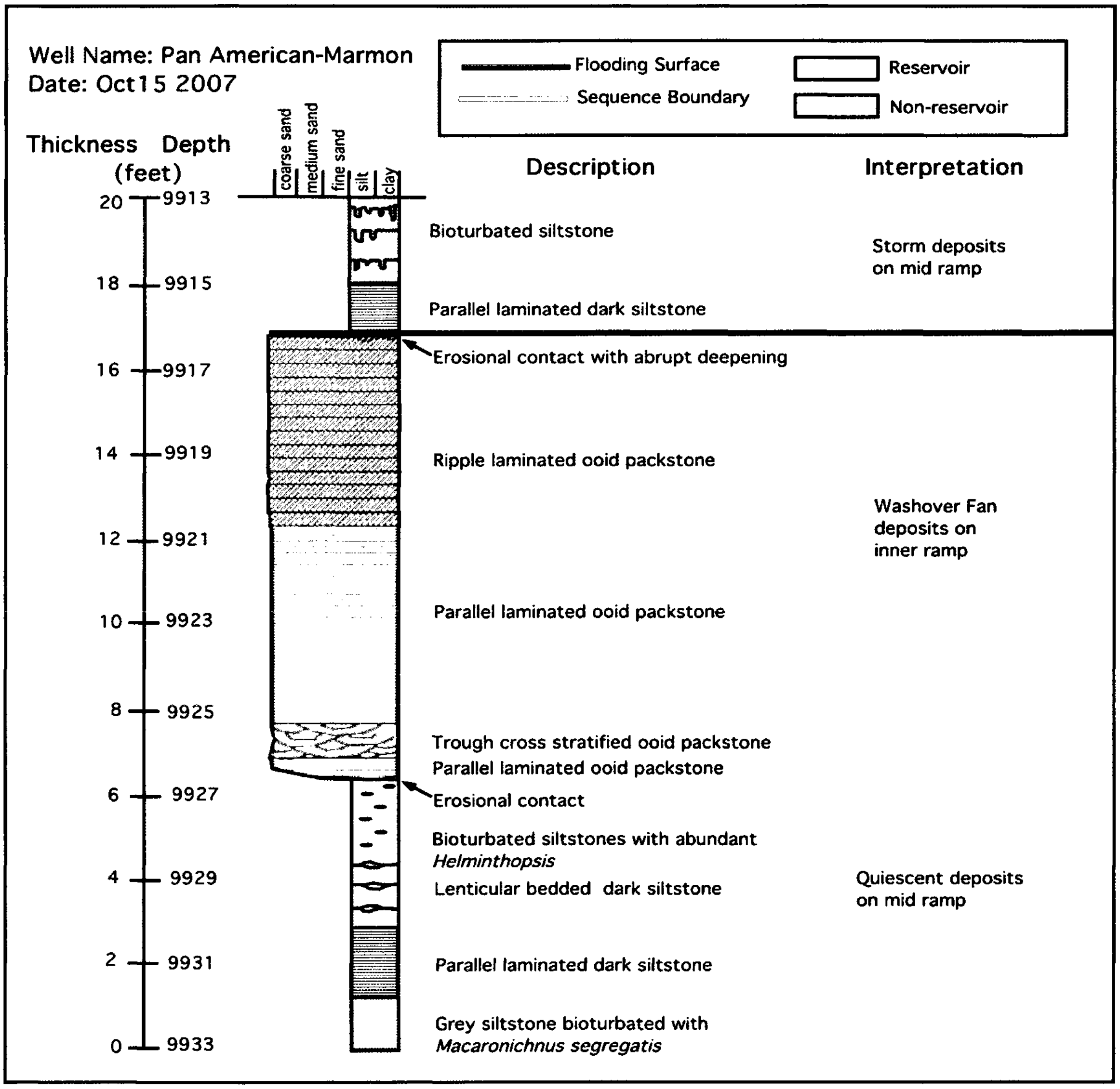
Well Name: Pan American-Marmon
Date: Oct15 2007
Flooding Surface
Sequence Boundary
Reservoir
Non-reservoir
Thickness Depth
(feet)
coarse sand
medium sand
fine sand
silt
clay
Description
Interpretation
20 9913
18 9915
16 9917
14 9919
12 9921
10 9923
8 9925
6 9927
4 9929
2 9931
0 9933
Bioturbated siltstone
Storm deposits on mid ramp
Parallel laminated dark siltstone
Erosional contact with abrupt deepening
Ripple laminated ooid packstone
Washover Fan deposits on inner ramp
Parallel laminated ooid packstone
Trough cross stratified ooid packstone
Parallel laminated ooid packstone
Erosional contact
Bioturbated siltstones with abundant *Helminthopsis*
Lenticular bedded dark siltstone
Quiescent deposits on mid ramp
Parallel laminated dark siltstone
Grey siltstone bioturbated with *Macaronichnus segregatis*

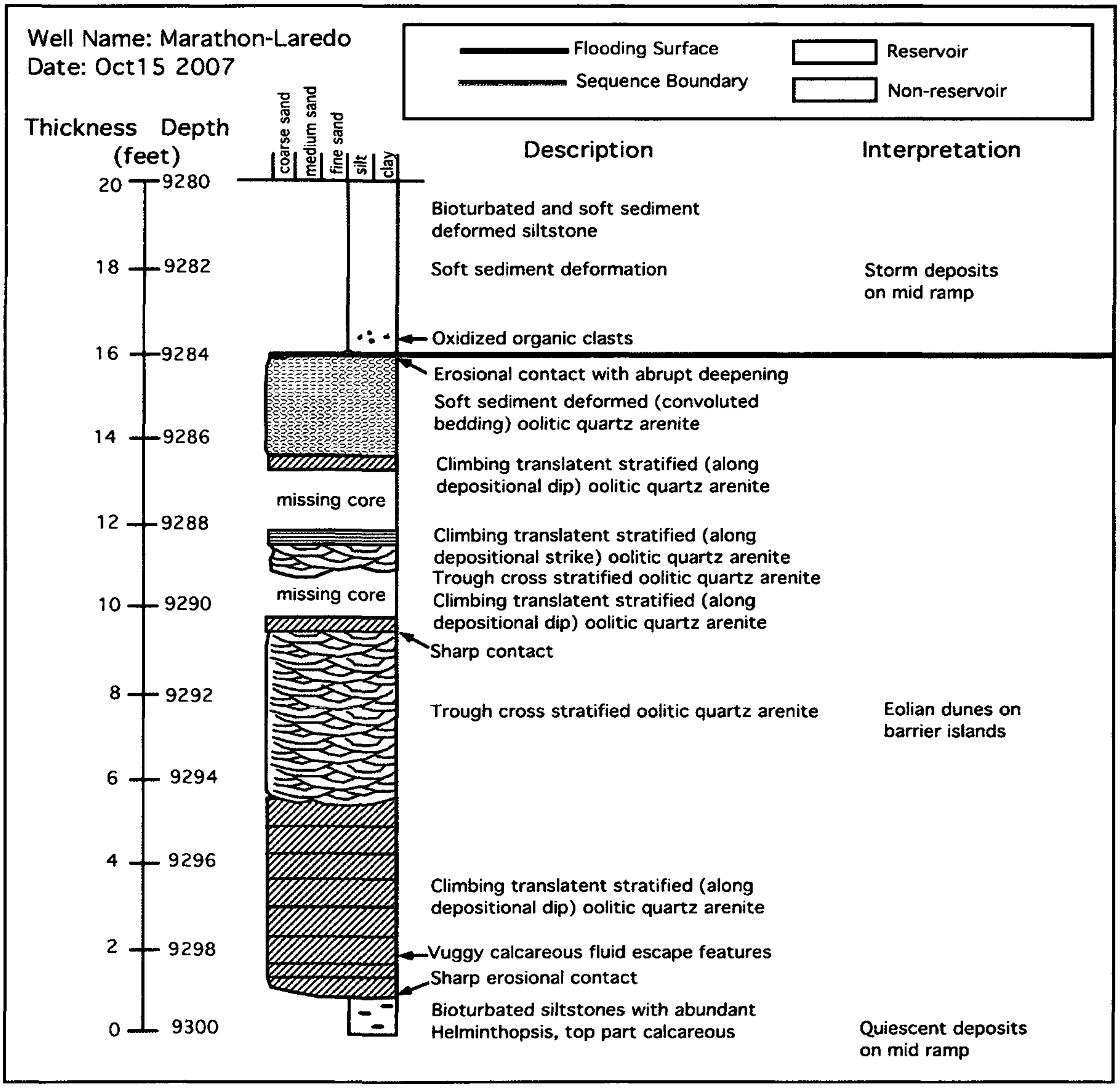
Well Name: Marathon-Laredo
Date: Oct15 2007
Flooding Surface
Sequence Boundary
Reservoir
Non-reservoir
Thickness
Depth
(feet)
coarse sand
medium sand
fine sand
silt
clay
Description
Interpretation
20 9280
18 9282
16 9284
14 9286
12 9288
10 9290
8 9292
6 9294
4 9296
2 9298
0 9300
Bioturbated and soft sediment deformed siltstone
Soft sediment deformation
Storm deposits on mid ramp
Oxidized organic clasts
Erosional contact with abrupt deepening
Soft sediment deformed (convoluted bedding) oolitic quartz arenite
Climbing translatent stratified (along depositional dip) oolitic quartz arenite
missing core
Climbing translatent stratified (along depositional strike) oolitic quartz arenite
Trough cross stratified oolitic quartz arenite
missing core
Climbing translatent stratified (along depositional dip) oolitic quartz arenite
Sharp contact
Trough cross stratified oolitic quartz arenite
Eolian dunes on barrier islands
Climbing translatent stratified (along depositional dip) oolitic quartz arenite
Vuggy calcareous fluid escape features
Sharp erosional contact
Bioturbated siltstones with abundant Helminthopsis, top part calcareous
Quiescent deposits on mid ramp

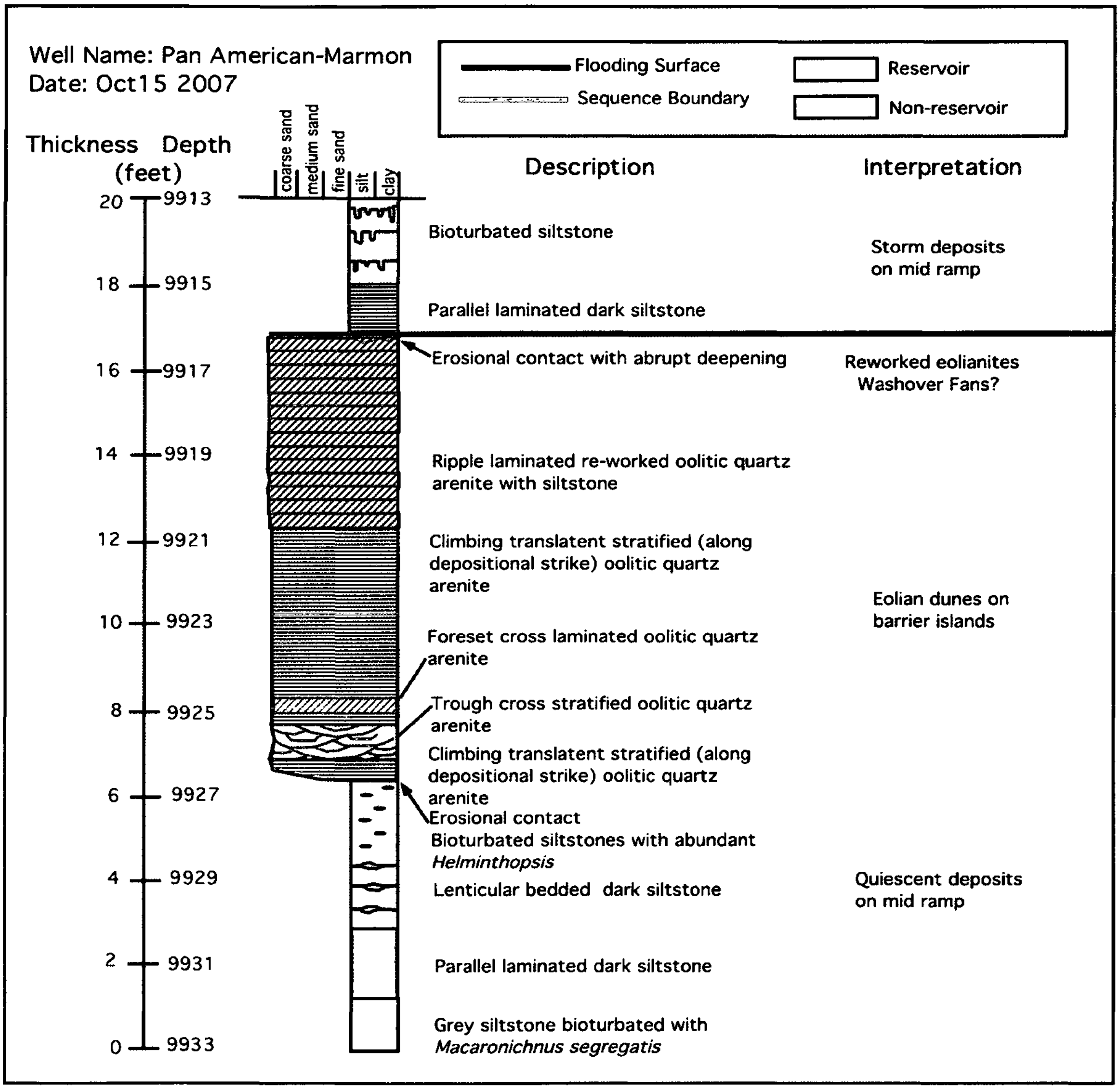
Well Name: Pan American-Marmon
Date: Oct15 2007
Flooding Surface
Sequence Boundary
Reservoir
Non-reservoir
Thickness (feet)
Depth
coarse sand
medium sand
fine sand
silt
clay
Description
Interpretation
20 9913
18 9915
16 9917
14 9919
12 9921
10 9923
8 9925
6 9927
4 9929
2 9931
0 9933
Bioturbated siltstone
Parallel laminated dark siltstone
Storm deposits on mid ramp
Erosional contact with abrupt deepening
Reworked eolianites Washover Fans?
Ripple laminated re-worked oolitic quartz arenite with siltstone
Climbing translatent stratified (along depositional strike) oolitic quartz arenite
Foreset cross laminated oolitic quartz arenite
Eolian dunes on barrier islands
Trough cross stratified oolitic quartz arenite
Climbing translatent stratified (along depositional strike) oolitic quartz arenite
Erosional contact
Bioturbated siltstones with abundant *Helminthopsis*
Lenticular bedded dark siltstone
Quiescent deposits on mid ramp
Parallel laminated dark siltstone
Grey siltstone bioturbated with *Macaronichnus segregatis*

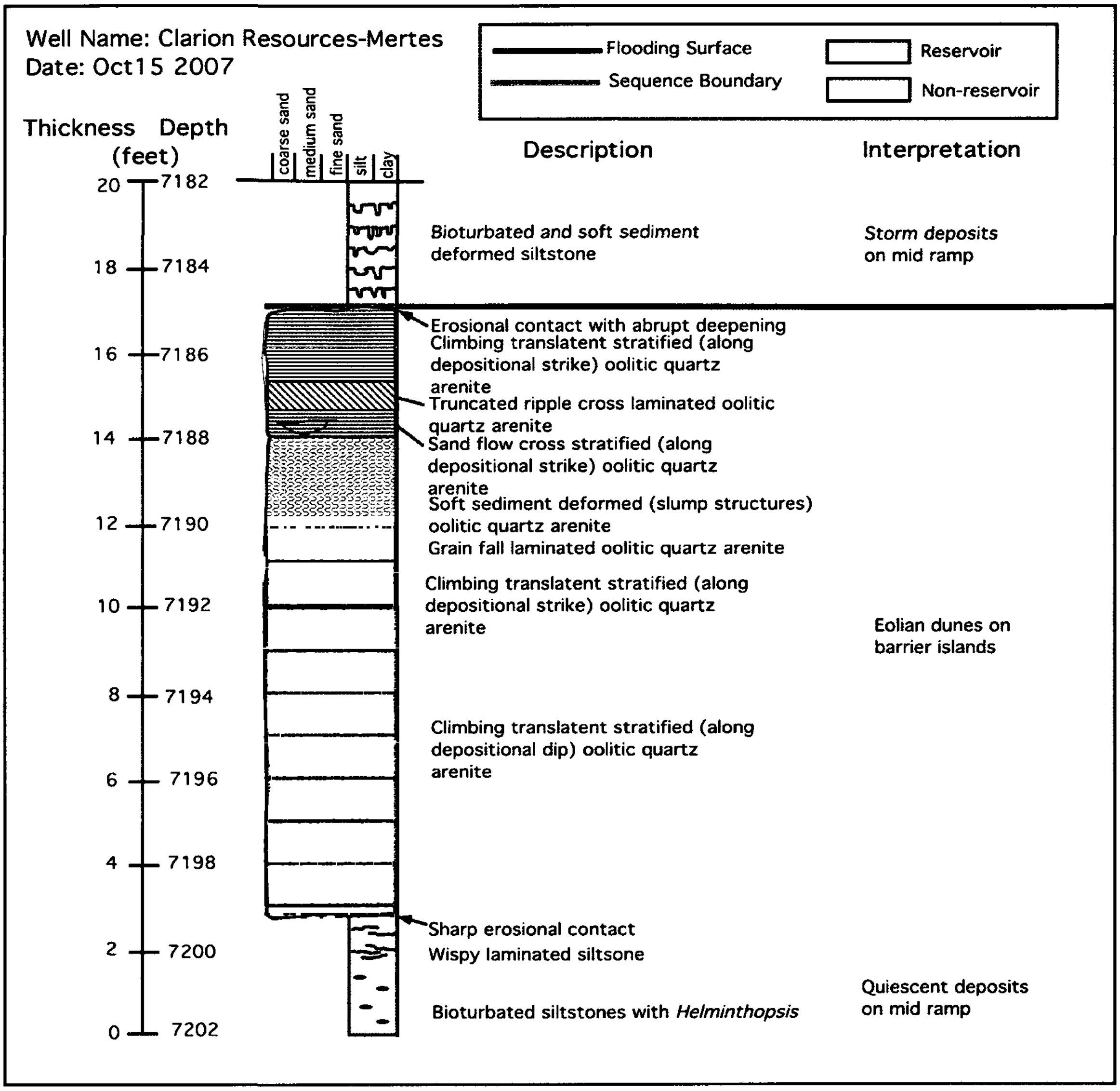

Well Name: Clarion Resources-Mertes
Date: Oct15 2007
Flooding Surface
Sequence Boundary
Reservoir
Non-reservoir
Thickness
Depth
(feet)
coarse sand
medium sand
fine sand
silt
clay
Description
Interpretation
20 7182
18 7184
16 7186
14 7188
12 7190
10 7192
8 7194
6 7196
4 7198
2 7200
0 7202
Bioturbated and soft sediment deformed siltstone
Storm deposits on mid ramp
Erosional contact with abrupt deepening
Climbing translatent stratified (along depositional strike) oolitic quartz arenite
Truncated ripple cross laminated oolitic quartz arenite
Sand flow cross stratified (along depositional strike) oolitic quartz arenite
Soft sediment deformed (slump structures) oolitic quartz arenite
Grain fall laminated oolitic quartz arenite
Climbing translatent stratified (along depositional strike) oolitic quartz arenite
Eolian dunes on barrier islands
Climbing translatent stratified (along depositional dip) oolitic quartz arenite
Sharp erosional contact
Wispy laminated siltsone
Bioturbated siltstones with Helminthopsis
Quiescent deposits on mid ramp

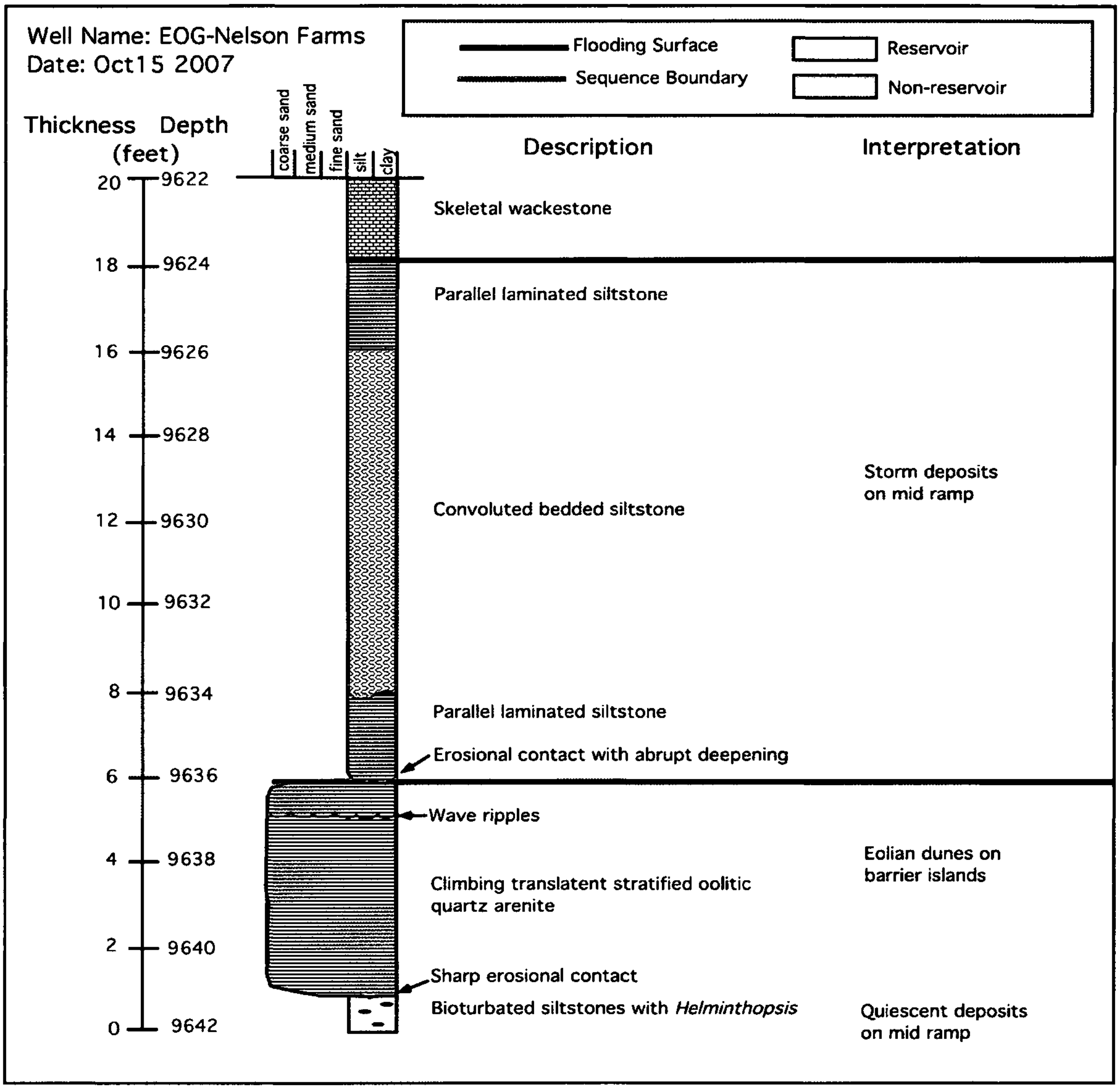

Well Name: EOG-Nelson Farms
Date: Oct15 2007
Flooding Surface
Sequence Boundary
Reservoir
Non-reservoir
Thickness
Depth
(feet)
coarse sand
medium sand
fine sand
silt
clay
Description
Interpretation
20
9622
18
9624
16
9626
14
9628
12
9630
10
9632
8
9634
6
9636
4
9638
2
9640
0
9642
Skeletal wackestone
Parallel laminated siltstone
Convoluted bedded siltstone
Storm deposits on mid ramp
Parallel laminated siltstone
Erosional contact with abrupt deepening
Wave ripples
Climbing translatent stratified oolitic quartz arenite
Eolian dunes on barrier islands
Sharp erosional contact
Bioturbated siltstones with *Helminthopsis*
Quiescent deposits on mid ramp

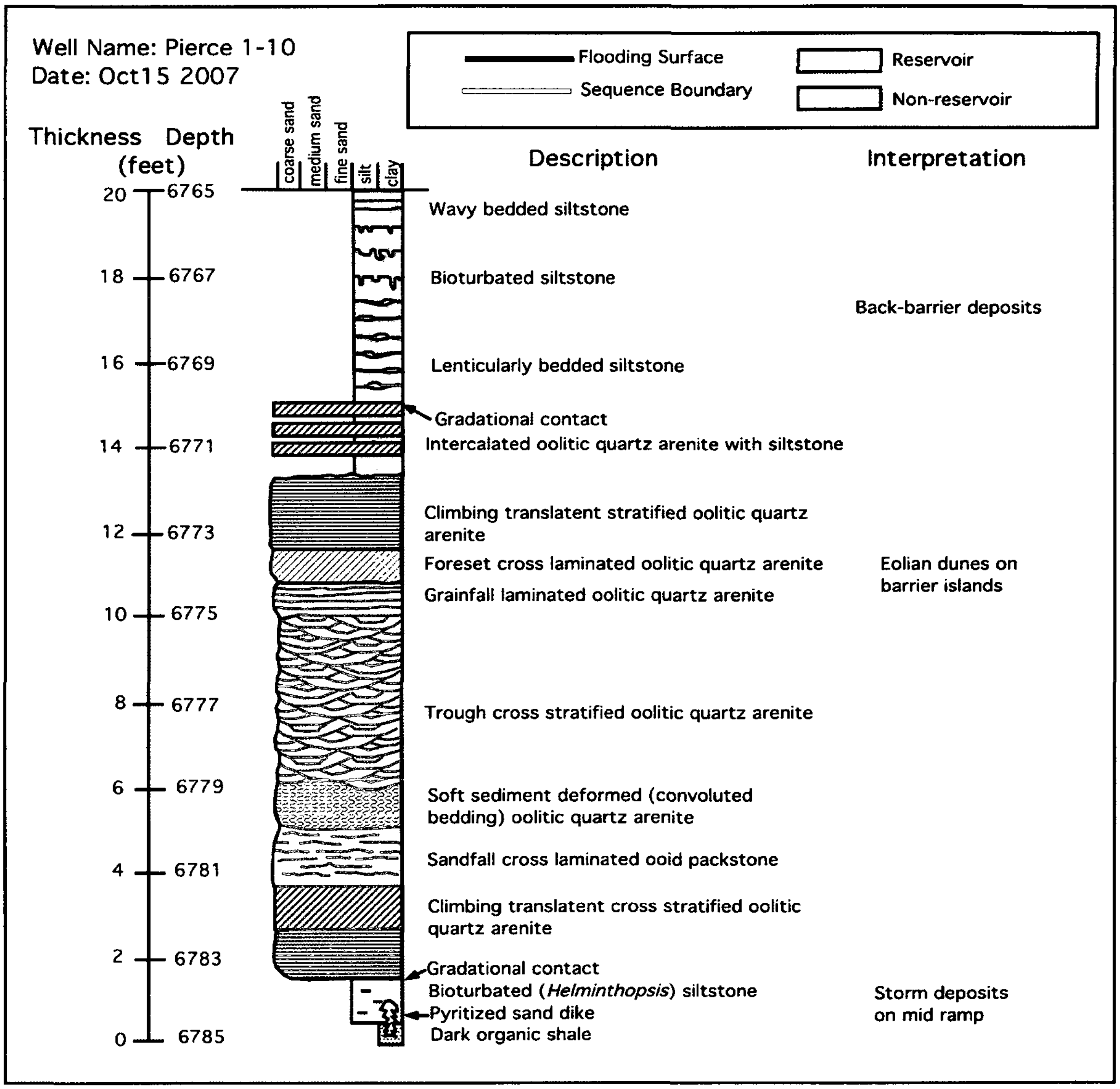
Well Name: Pierce 1-10
Date: Oct15 2007
Flooding Surface
Sequence Boundary
Reservoir
Non-reservoir
Thickness
Depth (feet)
coarse sand
medium sand
fine sand
silt
clay
Description
Interpretation
20
18
16
14
12
10
8
6
4
2
0
6765
6767
6769
6771
6773
6775
6777
6779
6781
6783
6785
Wavy bedded siltstone
Bioturbated siltstone
Back-barrier deposits
Lenticularly bedded siltstone
Gradational contact
Intercalated oolitic quartz arenite with siltstone
Climbing translatent stratified oolitic quartz arenite
Foreset cross laminated oolitic quartz arenite
Eolian dunes on barrier islands
Grainfall laminated oolitic quartz arenite
Trough cross stratified oolitic quartz arenite
Soft sediment deformed (convoluted bedding) oolitic quartz arenite
Sandfall cross laminated ooid packstone
Climbing translatent cross stratified oolitic quartz arenite
Gradational contact
Bioturbated (Helminthopsis) siltstone
Storm deposits on mid ramp
Pyritized sand dike
Dark organic shale

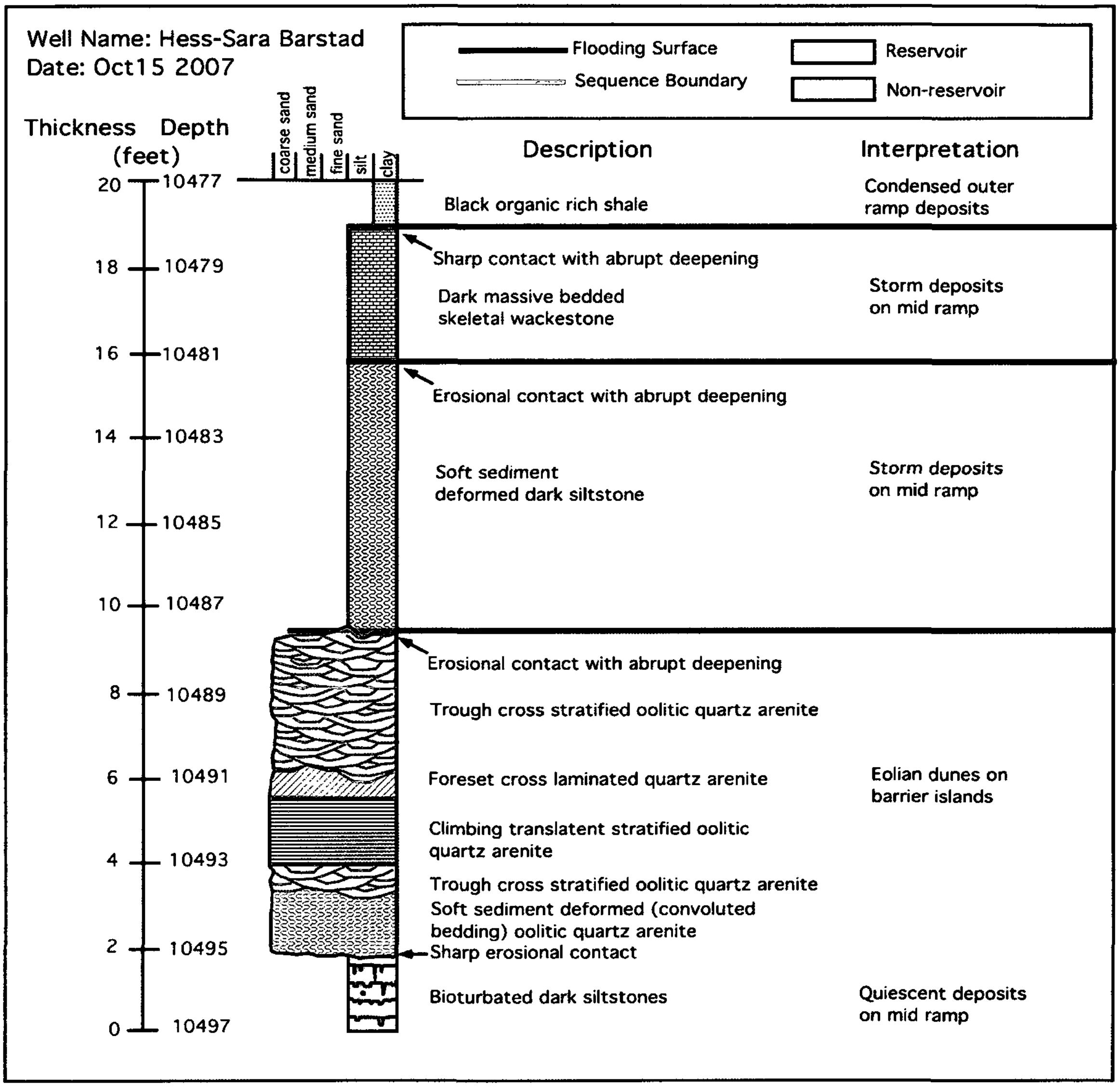

Well Name: Hess-Sara Barstad
Date: Oct15 2007
Flooding Surface
Sequence Boundary
Reservoir
Non-reservoir
Thickness Depth (feet)
coarse sand
medium sand
fine sand
silt
clay
Description
Interpretation
20 10477
18 10479
16 10481
14 10483
12 10485
10 10487
8 10489
6 10491
4 10493
2 10495
0 10497
Black organic rich shale
Condensed outer ramp deposits
Sharp contact with abrupt deepening
Dark massive bedded skeletal wackestone
Storm deposits on mid ramp
Erosional contact with abrupt deepening
Soft sediment deformed dark siltstone
Storm deposits on mid ramp
Erosional contact with abrupt deepening
Trough cross stratified oolitic quartz arenite
Foreset cross laminated quartz arenite
Eolian dunes on barrier islands
Climbing translatent stratified oolitic quartz arenite
Trough cross stratified oolitic quartz arenite
Soft sediment deformed (convoluted bedding) oolitic quartz arenite
Sharp erosional contact
Bioturbated dark siltstones
Quiescent deposits on mid ramp

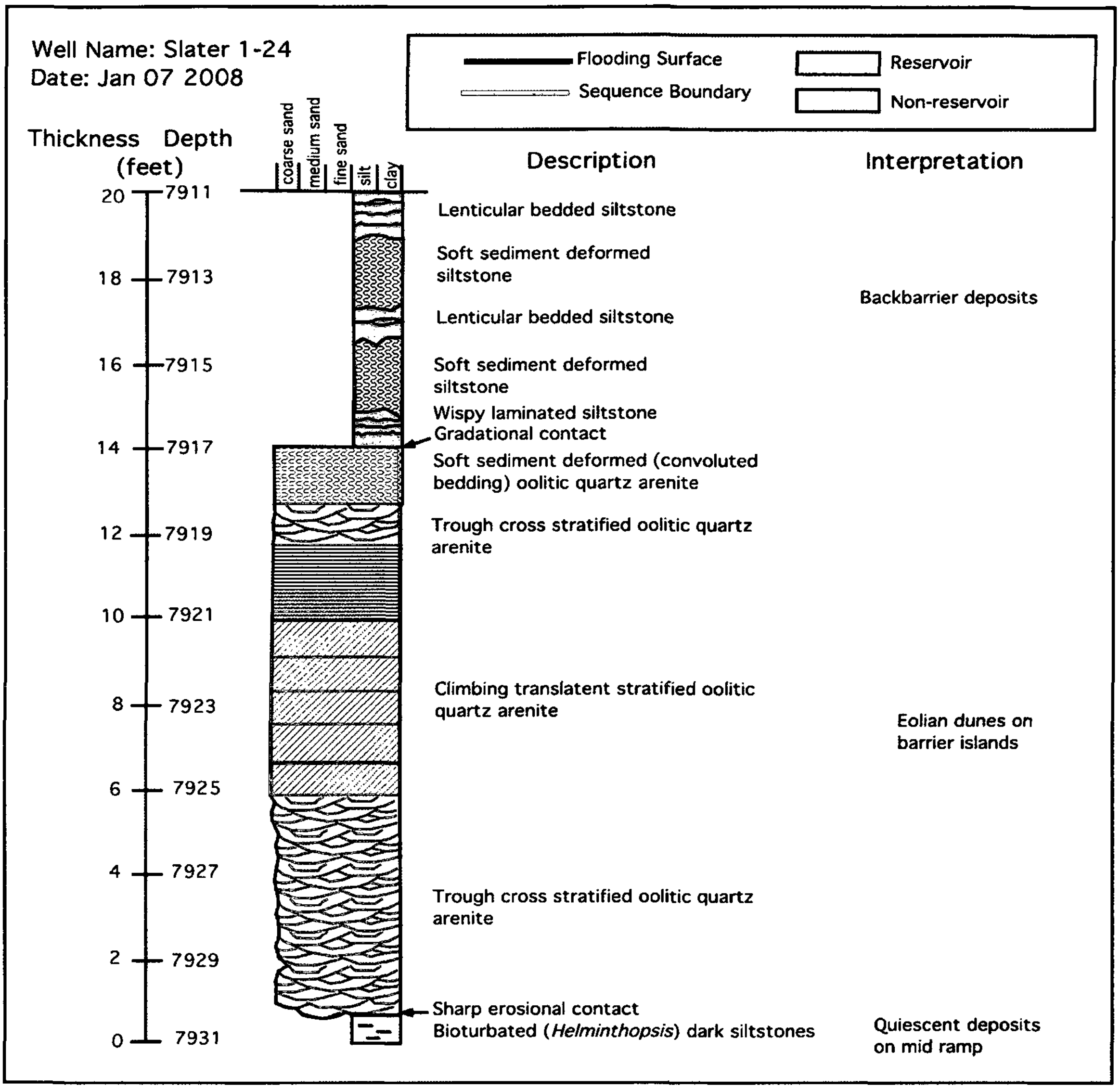
Well Name: Slater 1-24
Date: Jan 07 2008
Flooding Surface
Sequence Boundary
Reservoir
Non-reservoir
Thickness
Depth
(feet)
coarse sand
medium sand
fine sand
silt
clay
Description
Interpretation
20
7911
18
7913
16
7915
14
7917
12
7919
10
7921
8
7923
6
7925
4
7927
2
7929
0
7931
Lenticular bedded siltstone
Soft sediment deformed siltstone
Lenticular bedded siltstone
Soft sediment deformed siltstone
Wispy laminated siltstone
Gradational contact
Soft sediment deformed (convoluted bedding) oolitic quartz arenite
Trough cross stratified oolitic quartz arenite
Climbing translatent stratified oolitic quartz arenite
Trough cross stratified oolitic quartz arenite
Sharp erosional contact
Bioturbated (Helminthopsis) dark siltstones
Backbarrier deposits
Eolian dunes on barrier islands
Quiescent deposits on mid ramp

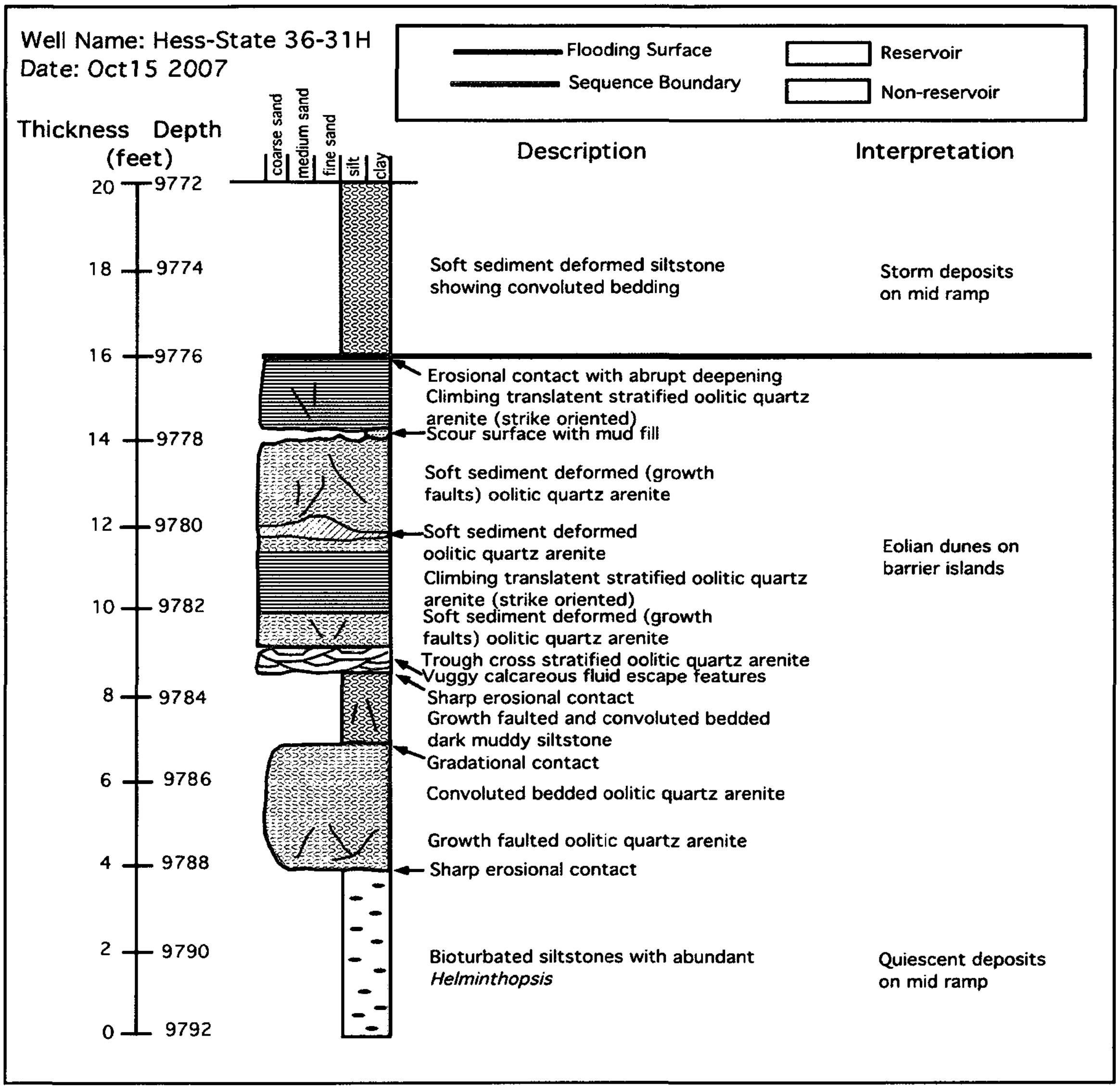
Well Name: Hess-State 36-31H
Date: Oct15 2007
Flooding Surface
Sequence Boundary
Reservoir
Non-reservoir
Thickness Depth
(feet)
coarse sand
medium sand
fine sand
silt
clay
Description
Interpretation
20 9772
18 9774
16 9776
14 9778
12 9780
10 9782
8 9784
6 9786
4 9788
2 9790
0 9792
Soft sediment deformed siltstone showing convoluted bedding
Storm deposits on mid ramp
Erosional contact with abrupt deepening
Climbing translatent stratified oolitic quartz arenite (strike oriented)
Scour surface with mud fill
Soft sediment deformed (growth faults) oolitic quartz arenite
Soft sediment deformed oolitic quartz arenite
Climbing translatent stratified oolitic quartz arenite (strike oriented)
Soft sediment deformed (growth faults) oolitic quartz arenite
Trough cross stratified oolitic quartz arenite
Vuggy calcareous fluid escape features
Sharp erosional contact
Growth faulted and convoluted bedded dark muddy siltstone
Gradational contact
Convoluted bedded oolitic quartz arenite
Growth faulted oolitic quartz arenite
Sharp erosional contact
Eolian dunes on barrier islands
Bioturbated siltstones with abundant *Helminthopsis*
Quiescent deposits on mid ramp

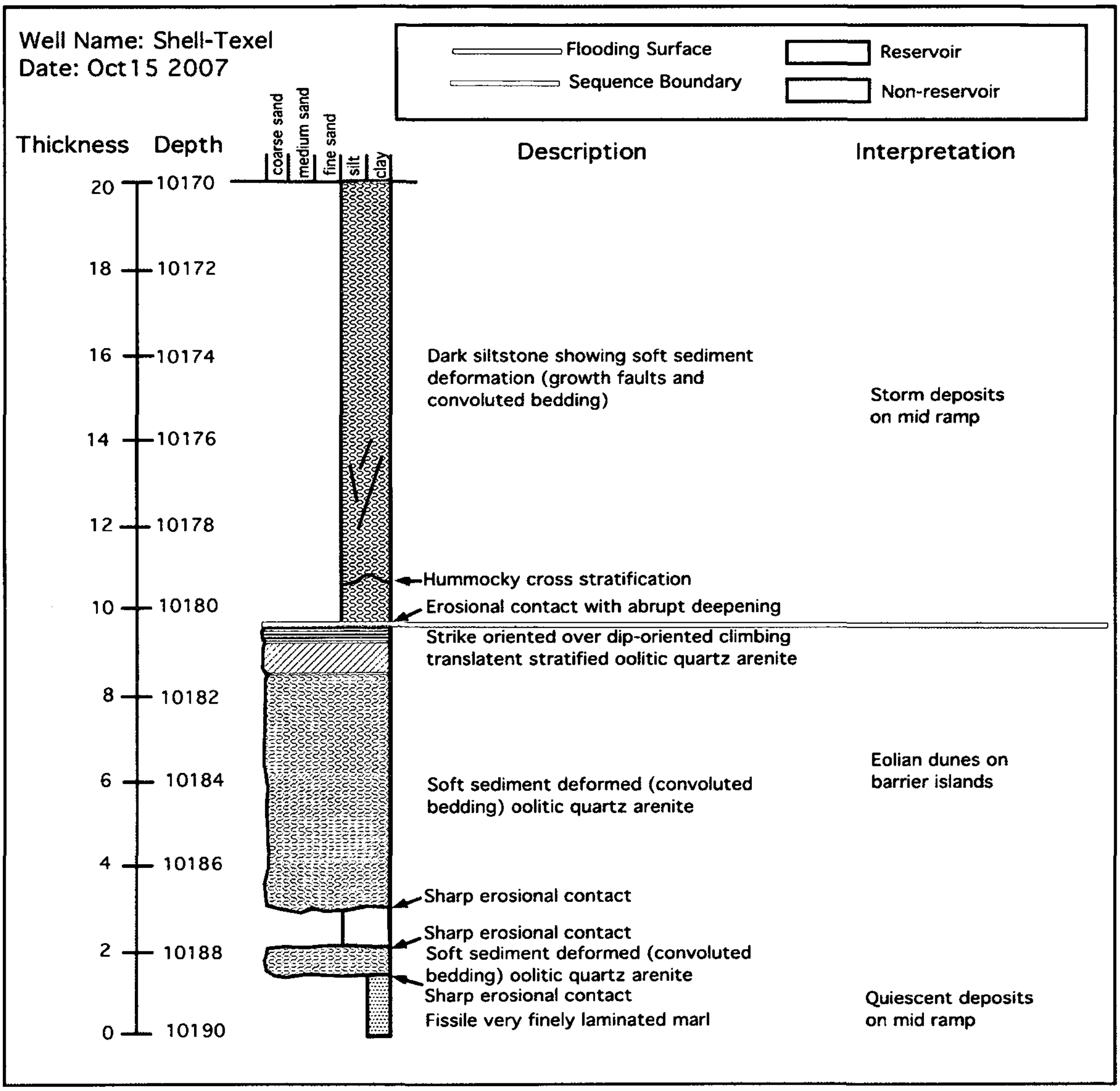
Well Name: Shell-Texel
Date: Oct15 2007
Flooding Surface
Sequence Boundary
Reservoir
Non-reservoir
Thickness
Depth
coarse sand
medium sand
fine sand
silt
clay
Description
Interpretation
20 10170
18 10172
16 10174
14 10176
12 10178
10 10180
8 10182
6 10184
4 10186
2 10188
0 10190
Dark siltstone showing soft sediment deformation (growth faults and convoluted bedding)
Storm deposits on mid ramp
Hummocky cross stratification
Erosional contact with abrupt deepening
Strike oriented over dip-oriented climbing translatent stratified oolitic quartz arenite
Eolian dunes on barrier islands
Soft sediment deformed (convoluted bedding) oolitic quartz arenite
Sharp erosional contact
Sharp erosional contact
Soft sediment deformed (convoluted bedding) oolitic quartz arenite
Sharp erosional contact
Fissile very finely laminated marl
Quiescent deposits on mid ramp

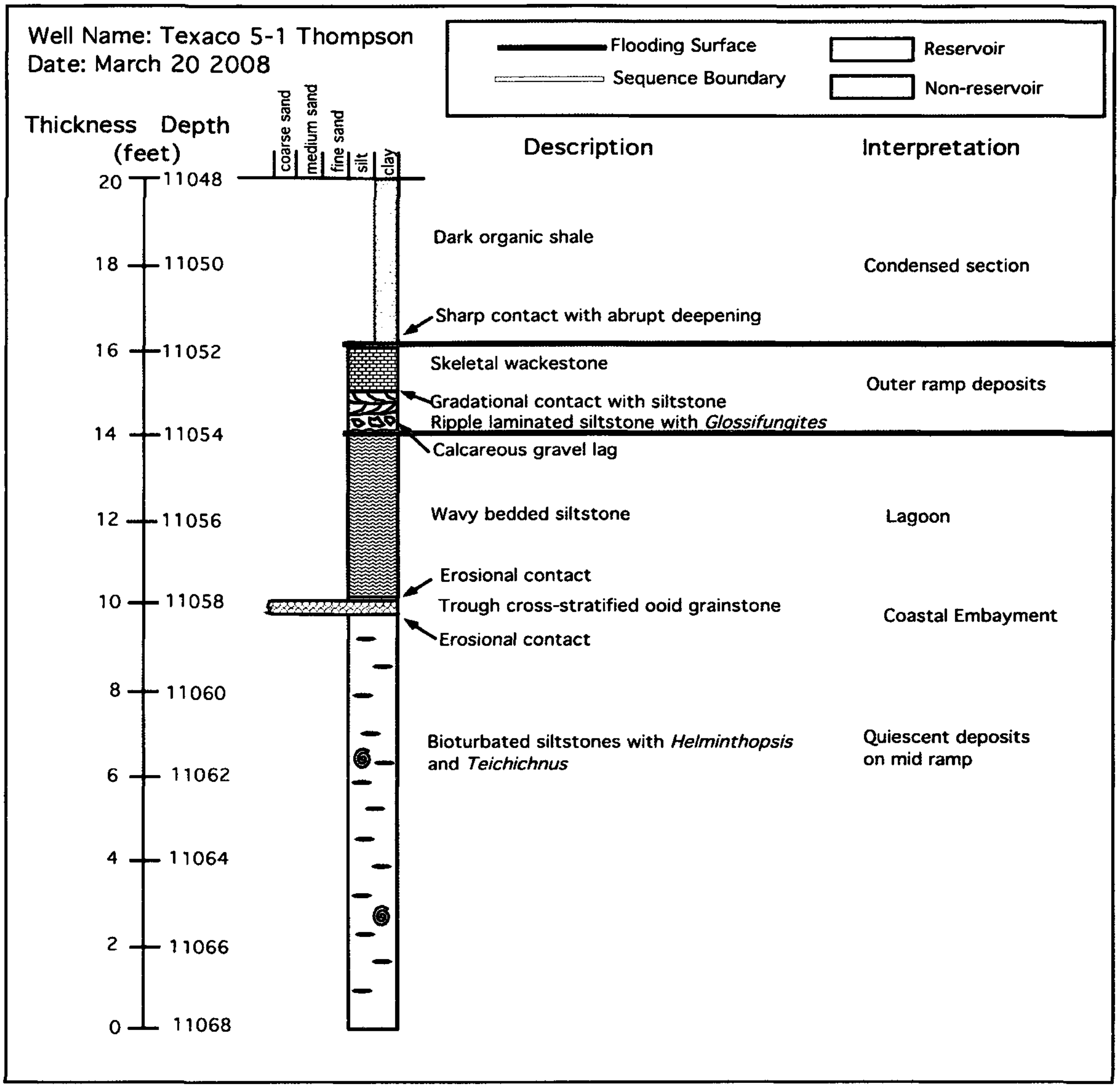
Well Name: Texaco 5-1 Thompson
Date: March 20 2008
Flooding Surface
Sequence Boundary
Reservoir
Non-reservoir
Thickness (feet)
Depth
coarse sand
medium sand
fine sand
silt
clay
Description
Interpretation
20
18
16
14
12
10
8
6
4
2
0
11048
11050
11052
11054
11056
11058
11060
11062
11064
11066
11068
Dark organic shale
Condensed section
Sharp contact with abrupt deepening
Skeletal wackestone
Outer ramp deposits
Gradational contact with siltstone
Ripple laminated siltstone with Glossifungites
Calcareous gravel lag
Wavy bedded siltstone
Lagoon
Erosional contact
Trough cross-stratified ooid grainstone
Coastal Embayment
Erosional contact
Bioturbated siltstones with Helminthopsis and Teichichnus
Quiescent deposits on mid ramp

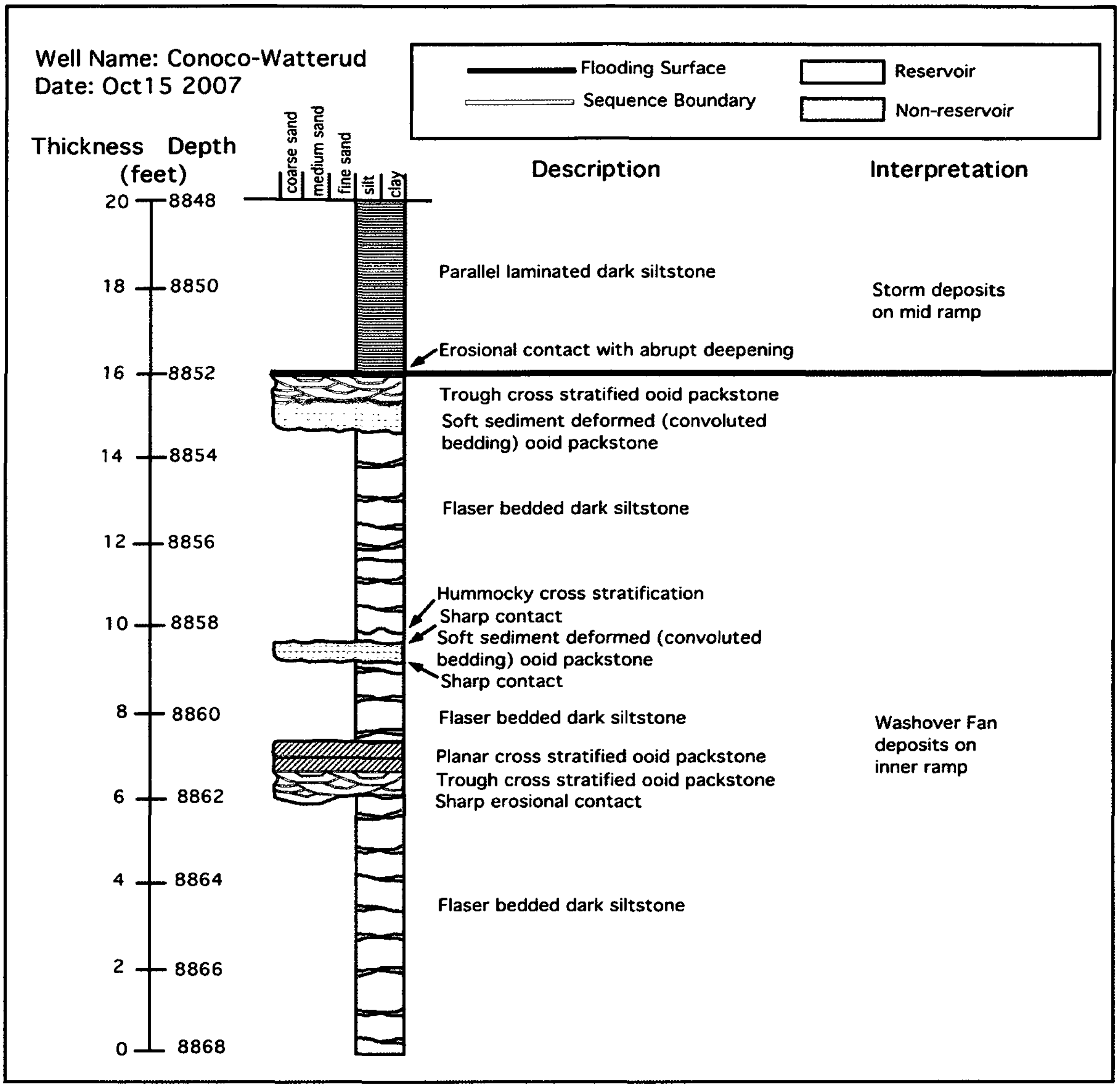
Well Name: Conoco-Watterud
Date: Oct15 2007
Flooding Surface
Sequence Boundary
Reservoir
Non-reservoir
Thickness
Depth
(feet)
coarse sand
medium sand
fine sand
silt
clay
Description
Interpretation
20 8848
18 8850
16 8852
14 8854
12 8856
10 8858
8 8860
6 8862
4 8864
2 8866
0 8868
Parallel laminated dark siltstone
Storm deposits on mid ramp
Erosional contact with abrupt deepening
Trough cross stratified ooid packstone
Soft sediment deformed (convoluted bedding) ooid packstone
Flaser bedded dark siltstone
Hummocky cross stratification
Sharp contact
Soft sediment deformed (convoluted bedding) ooid packstone
Sharp contact
Flaser bedded dark siltstone
Planar cross stratified ooid packstone
Trough cross stratified ooid packstone
Sharp erosional contact
Washover Fan deposits on inner ramp
Flaser bedded dark siltstone

APPENDIX B. DATA FROM MODERN OOLITIC TIDAL CHANNELS IN THE PERSIAN GULF

Data Point	Channel Width (m)	Channel Depth (m)	W/D ratio	Stream Magnitude	Channel Length	Valley Length	Sinuosity
1	11.51	1	11.51	1	185.062	182.39	1.014649926
2	6.76	1	6.76	1			
3	5.59	1	5.59	1	77.12	75.55	1.02078094
4	33.03	1	33.03	1			
5	14.11	1	14.11	1			
6	8.92	1	8.92	1			
7	2.35	1	2.35	1			
8	3.18	1	3.18	1			
9	3.45	1	3.45	1			
10	3.61	1	3.61	1			
11	4.84	1	4.84	1			
12	3.61	1	3.61	1			
13	4.5	1	4.5	1	109.5	93.66	1.169122357
14	4.98	3	1.66	1			
15	21.64	3	7.213333333	10	79.75	79.06	1.008727549
16	28.05	3	9.35	13			
17	42.79	3	14.26333333	14			
18	15.18	1	15.18	1			
19	3.28	1	3.28	1			
20	4.87	1	4.87	1			
21	1.22	1	1.22	1			
22	2.04	1	2.04	1			
23	3.18	1	3.18	1			
24	3.37	1	3.37	1	44.05	43.74	1.007087334
25	3.25	1	3.25	1	45.49	43.7	1.040961098

Table A1. Data from Abu Dhabi Tidal Channels

Data Point	Channel Width (m)	Channel Depth (m)	W/D ratio	Stream Magnitude	Channel Length	Valley Length	Sinuosity
26	3.26	3	1.086666667	1	26.32	26.23	1.003431186
27	20.42	1	20.42	9			
28	3.52	3	1.173333333	1			
29	23.85	1	23.85	10			
30	3.6	3	1.2	1			
31	32.81	1	32.81	11			
32	5.68	1	5.68	1			
33	3.86	2	1.93	1			
34	4.4	1	4.4	1			
35	3.36	1	3.36	1			
36	4.32	1	4.32	1			
37	4.46	1	4.46	1			
38	5.27	1	5.27	2	18.96	18.96	1
39	10.76	2	5.38	3	22.19	22.19	1
40	12.42	2	6.21	4	17.86	17.86	1
41	16.4	1	16.4	6			
42	2.34	1	2.34	1			
43	5.38	1	5.38	1			
44	2.07	1	2.07	1			
45	2.89	1	2.89	1			
46	3	1	3	1			
47	5.87	1	5.87	1			
48	20.37	2	10.185	8			
49	24.97	1	24.97	11			
50	3.4	3	1.133333333	1			

Table A1. Data from Abu Dhabi Tidal Channels

Data Point	Channel Width (m)	Channel Depth (m)	W/D ratio	Stream Magnitude	Channel Length	Valley Length	Sinuosity
51	25.12	3	8.373333333	12			
52	10.29	3	3.43	1			
53	33.34	3	11.11333333	1			
54	14.36	3	4.786666667	2	91.37	91.37	1
55	34.86	3	11.62	14			
56	96.67	3	32.22333333	39	168.35	166.04	1.01391231
57	9.64	3	3.213333333	1			
58	185.19	3	61.73	40	522.37	490.14	1.065756723
59	5.16	3	1.72	1			
60	2.4	3	0.8	1			
61	2.59	1	2.59	1			
62	4.47	1	4.47	1	67.09	66.05	1.015745647
63	6.92	1	6.92	1	36.85	30.22	1.219391132
64	1.82	1	1.82	1			
65	7.22	1	7.22	2	89.12	87.52	1.018281536
66	16.61	1	16.61	5	26.18	26.18	1
67	14.23	1	14.23	6	112.36	110.97	1.012525908
68	6.16	1	6.16	1			
69	2.73	1	2.73	1			
70	6.45	1	6.45	2	91.42	87.94	1.039572436
71	2.6	1	2.6	1			
72	18.28	2	9.14	2			
73	17.85	1	17.85	3	31.26	31.26	1
74	18.28	2	9.14	4	13.01	13.01	1
75	3.64	1	3.64	1			

Table A1. Data from Abu Dhabi Tidal Channels

Data Point	Channel Width (m)	Channel Depth (m)	W/D ratio	Stream Magnitude	Channel Length	Valley Length	Sinuosity
76	2.73	1	2.73	1			
77	3.83	2	1.915	1			
78	18.84	1	18.84	7			
79	4.73	1	4.73	1			
80	21.78	2	10.89	8			
81	3.85	3	1.283333333	1			
82	40.78	3	13.59333333	13			
83	6.38	3	2.126666667	1			
84	45	1	45	14			
85	25.87	1	25.87	1			
86	14.21	1	14.21	1			
87	22.14	1	22.14	2	132.61	130.53	1.015935034
88	17.84	1	17.84	1			
89	43.3	3	14.43333333	1			
90	86.98	5	17.396	4	201.32	201.32	1
91	217.66	5	43.532	58	224.1	224.1	1
92	225.13	5	45.026	59	1589.26	1566.8	1.01433495
93	4.8	1	4.8	1	658.71	604.84	1.089064877
94	6.12	1	6.12	1	712.44	641.99	1.109736912
95	18.54	1	18.54	1			
96	30.49	3	10.16333333	3	270.3	263.1	1.027366021
97	158.09	3	52.69666667	4	1990.79	1891.27	1.052620726
98	27.32	3	9.106666667	1			
99	57.45	3	19.15	1			
100	295.99	3	98.66333333	1			

Table A1. Data from Abu Dhabi Tidal Channels

Data Point	Channel Width (m)	Channel Depth (m)	W/D ratio	Stream Magnitude	Channel Length	Valley Length	Sinuosity
101	133.03	3	44.34333333	2	706.8	705.31	1.00211254 6
102	94.87	3	31.62333333	1			
103	116.88	3	38.96	2	903.64	899.69	1.00439040 1
104	438.61	5	87.722	66	4533.33	4395.8	1.03128668 3

Table A1. Data from Abu Dhabi Tidal Channels

Channel Length (m)	Valley Length(m)	Sinuosity	Width
4912.52	3006.75	1.633831	149.95
			122.23
			193.97
			308.96
			70.7
			155.36

Table A2. Data from Ras al-Khaimah Tidal Channels

Reach	Valley Length (m)	Channel Length (m)	Sinuosity	Channel Width	CBW
R1	606.75	820.77	1.352731768		
1				10.29	
2				7.41	
3				7.75	
4				7.91	
5				6.44	
R3	60.29	118.97	1.973295737		
R4	57.93	80.89	1.396340411		
R2	103.6	175.38	1.692857143		
a			1.603806265	0.5	7.04
b				0.91	14.95
c				0.85	16.63
d				0.94	18.37
e				0.91	7.84
f				0.94	8.44
g				0.84	11.95
h				2.32	14.84
i				2.28	9.13
j				1.91	6.5

Table A3. Data from Qatar Tidal Channels